

Modeling, Analysis, and Control of a Class of Resource Allocation Systems Arising in Concurrent Software

by

Hongwei Liao

A dissertation submitted in partial fulfillment
of the requirements for the degree of
Doctor of Philosophy
(Electrical Engineering: Systems)
in The University of Michigan
2012

Doctoral Committee:

Professor Stéphane Lafortune, Chair
Professor Mingyan Liu
Professor Scott Mahlke
Professor Dawn Tilbury
Professor Spyros Reveliotis, Georgia Institute of Technology
Senior Researcher Terence Kelly, HP Labs
Research Scientist Yin Wang, HP Labs

廖宏微

Liào Hóngwēi



© Hongwei Liao 2012

All Rights Reserved

ACKNOWLEDGEMENTS

I would like to express my deepest gratitude to my advisor, Professor Stéphane Lafortune, for his guidance. Through his advice and support, I have learned how to grow as a professional researcher. He is not only my advisor on research, but also my mentor on my career and many aspects beyond.

My special thanks also go to Professor Spyros Reveliotis, for his invaluable advice and feedback on my work throughout this rigorous process. I would like to thank Professor Scott Mahlke and Dr. Terence Kelly for their continuous encouragement, thank Dr. Yin Wang for his long-term support, as well as give thanks to Professors Dawn Tilbury and Mingyan Liu for accepting to sit on my dissertation committee.

I would like to sincerely thank Hyoun Kyu Cho for many suggestions on program analysis; thank Jason Stanley for his continuous support on experimentation and many inspiring discussions; thank Professors Mark Van Oyen and Ricardo Lüders, as well as my colleague, Hao Zhou, for their support on simulation analysis; and thank Ahmed Nazeem for his comments on control synthesis. Also, I would like to sincerely thank Dr. Sahika Genc, Dr. Weiling Wang, Dr. David VanderVeen, and Guru Umasankar for their invaluable advice on my professional development.

I wish to acknowledge the financial support from NSF, HP Labs, EECS Department Fellowship, and a Rackham Predoctoral Fellowship Award from the Rackham Graduate School at the University of Michigan.

Finally, I would like to extend my deepest gratitude to my family for their constant source of love, support, and encouragement.

TABLE OF CONTENTS

ACKNOWLEDGEMENTS	ii
LIST OF FIGURES	vi
LIST OF TABLES	viii
ABSTRACT	ix
CHAPTER	
I. Introduction	1
1.1 Challenges in the multicore era	1
1.2 Overview of the Gadara project	4
1.3 Discrete Event Systems Theory	5
1.4 Main contributions	7
II. Modeling: The Class of Gadara Nets	10
2.1 Introduction	10
2.2 Modeling of multithreaded software	11
2.3 Petri net preliminaries	13
2.3.1 Standard definitions	14
2.3.2 Control synthesis for Petri nets	15
2.4 Gadara nets	16
2.5 Controlled Gadara nets	20
2.6 Uncontrollability in modeling	22
2.7 Discussion of related classes of Petri nets	23
III. Analysis: Properties of Gadara Nets	25
3.1 Introduction	25
3.2 Petri net liveness and reversibility	26
3.3 Resource-induced deadly marked siphons and modified markings	27

3.4	The multithreaded program and its Gadara net model	29
3.5	Liveness of Gadara nets	31
3.6	Reversibility of Gadara nets	35
3.7	Linear separability and optimal control of Gadara nets	36
3.8	Verification of liveness using mathematical programming	39
3.8.1	Key properties	42
3.8.2	Verification of liveness of \mathcal{N}_G	42
3.8.3	Verification of liveness of \mathcal{N}_{G1}^c	45
3.8.4	Verification of liveness of \mathcal{N}_G^c	47
3.8.5	Experimental results	50
3.9	Case study: A deadlock bug in the Linux kernel	54
IV. Control I: Optimal Control of Gadara Nets – General Theory		58
4.1	Introduction	58
4.2	Problem statement and motivation	59
4.3	Overall strategy: Iterative control of Gadara nets	62
4.4	Fundamentals of the UCCOR Algorithm	64
4.4.1	Definitions and partial-marking analysis	64
4.4.2	Notion of covering	67
4.4.3	Feasibility of maximally permissive control	68
4.5	UCCOR Algorithm	69
4.5.1	Unsafe Covering Construction Algorithm	71
4.5.2	Unsafe Covering Generalization	72
4.5.3	Inter-Iteration Coverability Check	75
4.5.4	Monitor Place Synthesis Algorithm	76
4.6	Properties	82
4.6.1	Correctness and maximal permissiveness	82
4.6.2	Ordinariness of monitor places synthesized by UCCOR	86
4.7	Discussion of related approaches	88
V. Control II: Optimal Control of Gadara Nets – Customization for Ordinary Case		90
5.1	Introduction	90
5.2	Foundation for control synthesis	91
5.3	Overall strategy: Iterative control of ordinary Gadara nets	93
5.4	Optimal control algorithm based on RI empty siphons	95
5.4.1	UCCOR-O Algorithm: Overview	95
5.4.2	Unsafe Covering Generation	96
5.4.3	Unsafe Covering Generalization	97
5.4.4	Monitor Place Synthesis Algorithm	98
5.5	Properties	103
5.5.1	Properties of the UCCOR-O Algorithm	104
5.5.2	Properties of the ICOG-O Methodology	106

5.6	Experimental evaluation	108
5.6.1	Objective and setup of the experiments	109
5.6.2	Comparative analysis of ICOG-O and ICOG-O-ES	110
5.6.3	Scalability study of ICOG-O	113
5.7	Discussion of applications	113
VI. Evaluation: Analysis of Program Models Using Discrete Event Simulation		116
6.1	Introduction	116
6.2	Stochastic timed Gadara net model	117
6.3	The discrete event simulation model	118
6.4	Performance metrics	120
6.4.1	Measure of safety	120
6.4.2	Measure of efficiency	121
6.4.3	Measure of activity level	121
6.5	Case studies	122
6.5.1	Case study 1: A deadlock scenario in OpenLDAP	122
6.5.2	Case study 2: Two threads sharing three resources	125
6.6	Discussion of related work and applications	129
VII. Conclusion		133
7.1	Summary of main contributions	133
7.2	Future work	135
BIBLIOGRAPHY		137

LIST OF FIGURES

<u>Figure</u>		
1.1	The Gadara project architecture	4
2.1	A deadlock example in BIND: (a) Simplified code; (b) Gadara net model	13
3.1	Example: $S = \{p_{c_1}, p_{c_2}, p_{12}, p_{13}, p_{22}, p_{23}\}$ is a nonempty RIDM siphon at the marking shown in the figure	28
3.2	A deadlock example in BIND: Controlled Gadara net model	40
3.3	Sample statistics: (a) MIP- $\mathcal{N}_{G_1}^c$ vs. MIP-ES; (b) MIP- \mathcal{N}_G^c vs. MIP-RS	51
3.4	Normalized Cumulative Frequency (NCF): (a) MIP- $\mathcal{N}_{G_1}^c$ vs. MIP-ES; (b) MIP- \mathcal{N}_G^c vs. MIP-RS	52
3.5	A deadlock example in the Linux kernel: Simplified code	56
3.6	A deadlock example in the Linux kernel: Gadara net model	57
4.1	A running example of control synthesis using ICOG	61
4.2	Iterative control of Gadara nets (ICOG)	63
4.3	UCCOR Algorithm	70
4.4	The constraint transformation technique used in Stage 2 of the Monitor Place Synthesis Algorithm	78
4.5	Gadara net model of a deadlock example in the OpenLDAP software	80
4.6	A simple example of UCCOR	81

4.7	Illustration of the rearranged order of rows in a marking, covering, and incidence matrix	87
5.1	Iterative control of Gadara nets: Ordinary case (ICOG-O)	93
5.2	Flowchart of the UCCOR-O Algorithm	96
5.3	A deadlock example in the Linux kernel: Controlled Gadara net model	100
5.4	The constraint transformation technique used in Stage 2 of the Monitor Place Synthesis Algorithm	101
5.5	Cases considered in the proof: (a) Case 1; (b) Case 2; (c) Case 3; (d) Case 4	105
5.6	(a) TTC of ICOG-O and ICOG-O-ES: Normalized cumulative frequency; (b) TTC of ICOG-O and ICOG-O-ES: Estimated probability density function; (c) Difference of the number of iterations of ICOG-O-ES and ICOG-O	111
6.1	Enhanced event list	119
6.2	P_d of uncontrolled program model under various values of (π_4, π_6) .	124
6.3	MTTF under various values of (π_4, π_6) : (a) Before control; (b) After control; (c) Overhead	124
6.4	β under various values of (π_4, π_6) : (a) Before control; (b) After control; (c) Overhead	125
6.5	A Gadara net model of two threads sharing three resources	127
6.6	Sensitivity analysis results for Strategy 2: (a) P_d ; (b) MTTF; (c) β .	128
6.7	Deadlock probability reduction rate of Strategy 2	129
6.8	Control Strategy Maps: (a) Tradeoff between P_d and MTTF; (b) Tradeoff between P_d and β	130

LIST OF TABLES

Table

3.1	Experimental results of comparative analysis on liveness verification algorithms	54
5.1	Experimental results of comparative analysis between ICOG-O and ICOG-O-ES	114
5.2	Experimental results of scalability study of ICOG-O	115
6.1	Definition of control strategies	128

ABSTRACT

Modeling, Analysis, and Control of a Class of Resource Allocation Systems
Arising in Concurrent Software

by

Hongwei Liao

Chair: Stéphane Lafortune

In the past decade, computer hardware has undergone a true revolution, moving from uniprocessor architectures to multiprocessor architectures, or multicore. In order to exploit the full potential of multicore hardware, there is an unprecedented interest in parallelizing the applications that were previously conducted in sequential order. This trend forces parallel programming upon the average programmer. However, reasoning about concurrency is challenging for human programmers. Significant effort has been spent to eliminate several types of concurrency bugs.

In this dissertation, we study the modeling, analysis, control, and evaluation of a class of resource allocation systems arising in concurrent software using Petri nets, a commonly used modeling formalism in Discrete Event Systems. We formally define a new class of Petri nets, called Gadara nets, to systematically model multithreaded programs with lock allocation and release operations, a widely used programming paradigm for concurrent software with shared data. We focus on an important class of concurrency bugs, known as circular-mutex-wait deadlocks, or simply deadlocks. Deadlock-freeness of a program corresponds to liveness of its Gadara net model. We

establish necessary and sufficient conditions for liveness and reversibility properties of Gadara nets, which lay the foundations for their control synthesis. We propose a new liveness-enforcing control synthesis methodology for general Gadara nets that need not be ordinary. The method is based on structural analysis and converges in finite iterations. It is shown to be correct and maximally permissive with respect to the goal of liveness enforcement. We further customize this control synthesis methodology for ordinary Gadara nets and establish a set of important properties. Performance evaluations are conducted for comparing the original and controlled program models, using Discrete Event Simulation. Our results are applied to the analysis of large-scale multithreaded program models, showing that our approach is scalable to real-world software. Finally, we discuss potential directions for future work.

CHAPTER I

Introduction

1.1 Challenges in the multicore era

A fundamental revolution has taken place in the computer industry in the past decade. The mainstream computer CPUs used to have only a single processor core capable of executing a single task at a time. CPU speeds doubled roughly every 18 months according to Moore's law. Processor core speed cannot increase indefinitely, however, because faster cores generate excessive heat. Successive CPU generations therefore now provide more processor cores rather than a faster single core and can execute several tasks at once.

The revolution of computer hardware from uniprocessor architectures to multiprocessor architectures also leads to some challenges. One problem is that only parallel software can exploit the full performance potential of multicore architectures, and parallel software is far harder to write than conventional serial software. Choreographing a productive and harmonious interplay among concurrent tasks is very difficult because reasoning about concurrency is very challenging for human programmers. Multicore architectures are making parallel programming unavoidable but concurrency bugs are making it costly and error-prone. Significant effort has been spent to eliminate several types of concurrency bugs; see, e.g., [84, 77, 78, 79, 72, 82].

In this dissertation, we are interested in shared-memory multithreaded software,

a very common computing paradigm in which concurrent tasks share access to a pool of computer memory. Mutual exclusion locks (or “mutexes”) prevent tasks from accessing the same memory concurrently, thus allowing tasks to update shared memory in an orderly way, because a given lock may be held by at most one task at any moment. However, it is easy for situations to arise in which, e.g., task 1 has acquired lock A and needs lock B, while task 2 holds B but requires A; these tasks are deadlocked and neither can perform useful work. Such deadlocks are called *circular-mutex-wait (CMW) deadlocks* in the literature, where a set of threads is waiting indefinitely and no thread can proceed. In this dissertation, we focus on CMW deadlocks, an important class of failures arising in concurrent software.

Development of highly reliable and robust software is a very active research area in the software and operating systems communities. The “Rx” system proposed in [84] responds to failures by rolling back execution state to a previous checkpoint and re-executing after heuristically perturbing the execution environment in an attempt to prevent recurrence of the failure. For example, replacing default memory allocation mechanisms with safer and more conservative alternatives may prevent recurrence of failures attributed to memory corruption. Rx repeats the rollback/perturbation/re-execution cycle until the software successfully executes beyond the failure or a timeout occurs; the latter indicates that Rx’s heuristic approach cannot address the failure. “Bouncer” [13] generates filters to prevent potential exploits of software vulnerabilities, based on heuristics and learning from practice. “ASSURE” [94] uses a self-healing method, called rescue points, to recover software from faults in server applications. In case of a fault, the system restores to the closest rescue point and attempts to recover by employing the existing error-handling facilities. “Exterminator” [78, 79] detects, isolates, and corrects certain classes of memory errors. After pinpointing the cause of an error, Exterminator automatically generates patches to correct the software that experienced it. These patches may be shared

among users of the same software, thus enabling automated collaborative bug remediation. The works above address various types of failures and reliability issues in software and operating systems.

When it comes to the specific issue of program deadlock, many approaches have been proposed for deadlock analysis and resolution. Variants of the Banker’s Algorithm [15, 16] provide a principled approach to dynamic deadlock avoidance for concurrent software. The algorithm, however, requires a central controller that can potentially impose a global serial bottleneck on the software it governs. Deadlock “Healing” [77] addresses potential deadlocks by adding “gate locks” that prevent out-of-order lock acquisitions from causing deadlocks. At runtime, actual deadlocks are detected and remedied by adding further gate locks, gradually eliminating deadlocks from programs. Healing is more practical than the Banker’s Algorithm because its runtime checks are efficient and because it does not introduce a global serialization point into the software that it controls. Another deadlock avoidance approach is “Dimmunix” [44, 45], which equips the software system with an “immune system”. The deadlock immunity can resist future occurrences of similar deadlocks, and it is obtained by learning from the control flows that led to deadlocks. Reference [111] employs Just-in-time compilation techniques and exploits deadlock patterns at runtime, so that deadlocks of the same patterns can be avoided in the future. A randomized dynamic technique is presented in [43] for deadlock detection in multithreaded programs. This technique uses a random scheduler to create real deadlocks with high probability in a two-stage process, and it does not report any false positives. References [24, 25] propose a type and effect system to dynamically avoid deadlocks, by using the information of lock operations that is computed statically. A key feature of this system is that it does not assume block-structured locking or a strict order of lock allocation.

In spite of the above approaches toward software reliability and robustness, there

is an emerging need for systematic methodologies that will enable programmers to characterize, analyze, and resolve software failures, such as deadlocks.

1.2 Overview of the Gadara project

The broad context for the research work reported in this dissertation is the Gadara project [98, 48, 108]. The objective of the Gadara project is to develop a software tool that takes as input a deadlock-prone multithreaded C program and outputs a modified version of the program that is guaranteed to run deadlock-free without affecting any of the functionalities of the program. The system architecture of the Gadara project is shown in Figure 1.1, which includes four stages [104].

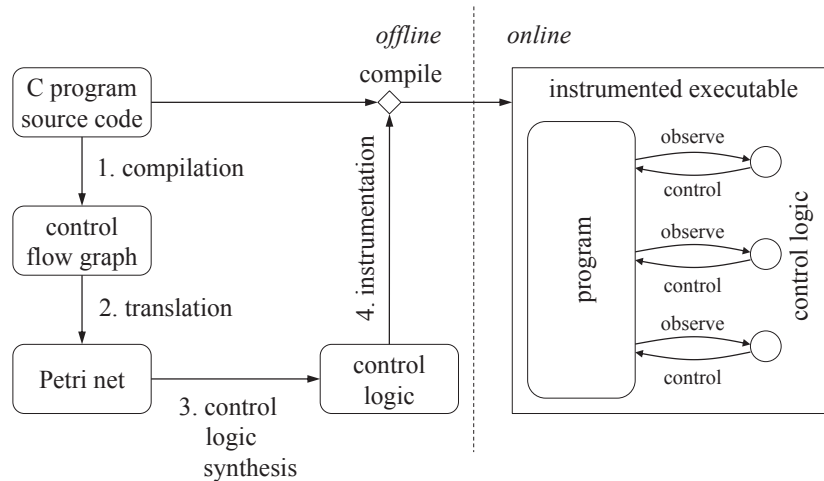


Figure 1.1: The Gadara project architecture

1. The C program source code is converted into a Control Flow Graph (CFG) by compiler techniques. A CFG is a high-level graphical representation of all code execution paths that might be traversed by the program. The CFG is augmented with additional information about lock variables and lock functions. The enhanced CFG is a directed graph.
2. The enhanced CFG is translated into a Petri net model of the program, formally

defined as a Gadara net, based on which potential deadlocks in the program can be mapped to structural features in the net.

3. Optimal control logic is synthesized for the Gadara net. The output of this step is a controlled Gadara net, augmented with *monitor* (a.k.a. *control*) places, which corresponds to a CMW-deadlock-free program.
4. The synthesized control logic captured by the monitor places is incorporated into the program by instrumenting the original code.

The four steps described above are all conducted off-line. During program execution, the only on-line overhead is due to the additional lines of code pertaining to checking and updating the contents of the monitor places. In this dissertation, we focus on Steps 2 and 3, and we systematically model, analyze, and control multithreaded software for the purpose of deadlock avoidance. The details on Steps 1 and 4 are reported in [103, 104, 105].

1.3 Discrete Event Systems Theory

In view of the event-driven nature of program dynamics and the logical control specification of deadlock avoidance, we adopt a model-based approach by employing the techniques from Discrete Event Systems (DES) Theory [8]. Discrete event systems are a class of dynamic systems that have discrete state spaces and event-driven dynamics. While classical control theory, which focuses on time-driven systems, has been successfully applied to computer systems [34], the application of DES to computer systems is more recent; see, e.g., [101, 83, 65, 17, 3, 22, 40, 14, 49]. Concurrent software is a typical example of a DES.

Finite state automata and Petri nets are the two most popular modeling formalisms for DES. We chose Petri nets as our modeling formalism, because there are at least three advantages of using Petri nets in this application context: (i) Petri

nets provide a compact, graphical representation of a concurrent program's inherent dynamics, without explicitly enumerating its state space; (ii) the Petri net models enable formal analysis and verification of important properties of their associated programs via efficient structural analysis; (iii) the models also make possible the synthesis of *provably* correct and optimal control logic that can be instrumented in the original programs for deadlock avoidance at run-time.

Deadlock analysis based on Petri nets has been widely studied for flexible manufacturing systems and other technological applications involving a resource allocation function [56, 88]. Various special classes of Petri nets have been proposed to analyze manufacturing systems [56]. Recently, there has also been a growing interest in the application of DES to software systems and embedded systems. A review of the application of Petri nets to computer programming is presented in [39]. Modeling thread creation/termination and mutex lock/unlock operations is in fact a classical application of Petri nets [70]; in particular, Petri nets were used in the static analysis and deadlock analysis of Ada programs [92, 71, 93]. In the case of the popular Pthread library for C/C++ programs, Petri nets have also been employed to model multithreaded synchronization primitives [47].

The results presented in this dissertation allow us to specialize the existing theory of Petri net-based deadlock analysis and avoidance for sequential resource allocation systems. We can then apply this theory to lock allocations in shared-memory multithreaded software. At the same time, the results take advantage of the additional structure that is present in the considered resource allocation function in order to substantially strengthen and extend the existing theory. A more detailed discussion of the main contributions of this dissertation is provided in the next section. Furthermore, additional reviews of related work will be presented throughout the dissertation.

1.4 Main contributions

The main contributions and organization of this dissertation are summarized as follows.

- *Chapter II: Modeling ([64, 107])*. We formally define a new class of Petri nets, called Gadara nets, to systematically model multithreaded programs with lock allocation and release operations. The class of Gadara nets explicitly models the locking behavior of multithreaded programs and enables the efficient characterization of the CMW deadlocks of programs through structural analysis. Gadara nets also capture some special features of programs, e.g., in general, these nets are cyclic due to the modeling of loops, and they contain uncontrollable transitions due to the modeling of branch selections.
- *Chapter III: Analysis ([64, 61, 107])*. We investigate a set of important properties of Gadara nets, such as liveness, reversibility, and linear separability. Based on these properties, deadlock-freeness – a *behavioral* property – of the program corresponds to liveness of its Gadara net model, which can in turn be analyzed via the *structural* properties of the net in terms of siphons. For the verification of the liveness property, we propose a set of mathematical programming formulations, which are customized for Gadara nets.
- *Chapter IV: Control – General theory ([60, 59])* and *Chapter V: Control – Customization ([62, 61])*. We propose a new liveness-enforcing control synthesis methodology for general Gadara nets that need not be ordinary. The method is based on structural analysis and converges in a finite number of iterations. It is shown to be correct and maximally permissive with respect to the goal of liveness enforcement. We further customize this control synthesis methodology for the particular application of concurrent software, where we always have an ordinary Gadara net as the initial condition. We show that the customized

method will never synthesize redundant control logic throughout the control iterations.

- *Chapter VI: Evaluation ([63]).* We extend the class of untimed Gadara nets to the class of stochastic timed Gadara nets and propose a customized discrete event simulation methodology for the extended class. We conduct simulation analysis on the Gadara net models of programs before and after control, where the performance metrics related to safety, efficiency, and activity level are studied via output data analysis. We further conduct sensitivity analysis on these Gadara net models and investigate the effect of key parameters on the programs. We also discuss the implication of the simulation results for deadlock-avoidance control.
- *Chapter VII: Conclusion.* We summarize the main contributions of this dissertation and discuss the potential directions for future work.

The property of the proposed control synthesis methodology discussed above, namely the maximally-permissive liveness-enforcing (MPLE) property, is also called “*optimal*” in this dissertation. In the context of program deadlock avoidance, optimality refers to the elimination of deadlocks in the program with minimally restrictive control logic.

As a technical note, the two terminologies, “deadlock” and “deadlock avoidance”, have different meanings in the software engineering and control engineering communities. We make the following remarks for the sake of clarity.

Remark I.1. The notion of “deadlock” we discussed above refers to the CMW-deadlock of a program; in the Petri net literature, “deadlock” usually refers to the case where all the transitions in the net are disabled. To avoid any confusion, in the rest of this dissertation, we refer to these two types of deadlocks as *CMW-deadlock* (Definition II.1) and *total-deadlock* (Definition III.4), respectively. When the context

provides no confusion, we sometimes refer to “CMW-deadlock” as “deadlock” for the sake of simplicity. Moreover, as we will show in Chapter III, in order to avoid the CMW-deadlocks of a program, we require *liveness* of its corresponding Petri net model. Therefore, the key Petri net property under study in this dissertation is liveness, rather than total-deadlock-freeness. \square

Remark I.2. Our strategy corresponds to what is termed “deadlock avoidance” in computer systems [96]; in the Petri net literature, such strategies are usually classified as “deadlock prevention” [56]. \square

CHAPTER II

Modeling: The Class of Gadara Nets

2.1 Introduction

As discussed in Chapter I, various special classes of Petri nets have been proposed to analyze resource allocations of manufacturing systems [56]. We discovered that the existing special classes of Petri nets in the literature do not exactly match the specific features of Petri nets that arise when modeling the locking behavior of multithreaded programs. Therefore, we propose a new class of Petri nets, called Gadara nets, that systematically models multithreaded programs with lock allocation and release operations. With the class of Gadara nets formally defined, we can efficiently analyze program deadlocks via formal models and synthesize deadlock avoidance control policies, which can in turn be instrumented in the underlying programs.

This chapter is organized as follows. We present some background about the modeling of multithreaded software in Section 2.2, and we introduce the Petri net preliminaries in Section 2.3. The class of Gadara nets is formally defined in Section 2.4, and the class of controlled Gadara nets is further defined in Section 2.5. We discuss the issue of uncontrollability in modeling in Section 2.6, and we review the related classes of Petri nets in Section 2.7. Some of the results in this chapter also appear in [64, 107].

2.2 Modeling of multithreaded software

We first introduce the definition of a CMW-deadlock.

Definition II.1. A program is said to be in a *CMW-deadlock* if there exists a circular chain of two or more threads in the program, where each thread in the chain waits for a mutex that is held by the next thread in the chain, and none of the threads can proceed.

Determining if a program is deadlock-free, for any type of deadlock, is undecidable, as it is a special instance of the halting problem for Turing machines [35]. We overcome this obstacle by focusing on CMW-deadlocks and by making modeling assumptions. A key challenge is scalability. Real-world large-scale software contains thousands of functions and millions of lines of code. Inlining the whole program, which is required for CMW-deadlock analysis, is not an option. We first prune functions and code regions that are irrelevant to deadlock analysis. We apply lock graph analysis [18, 7] to isolate the code regions that are subject to CMW-deadlock, and inline only the tail of the whole call stack that fully contains the CMW-deadlock. After pruning and lock graph analysis, we obtain a manageable model that is tractable for the analysis of mutex interactions and CMW deadlocks. In addition to scalability, language features also pose difficulties, e.g., recursion, function pointers, and dynamic locks. When in doubt about what particular lock a given call refers to, we model the lock in a conservative way [104]. Finally, there are Operating System, C language, and Pthread library specific features that we do not currently model, e.g., UNIX Inter-Process Communication calls that can result in other types of deadlocks, and `setjump`, `longjump` functions in C. Using all of the above techniques and under the above restrictions, we are able to capture all CMW-deadlocks in multithreaded programs using Petri nets.

As discussed above, a wide range of sub-classes of Petri nets have been proposed

in the literature, most of them motivated by applications in flexible manufacturing systems. Similarly, the class of Gadara nets formally defined in this chapter is motivated by the application domain of concurrent software, with a focus on the analysis of CMW-deadlocks. A Petri net model is obtained in Step 2 of the Gadara architecture in Figure 1.1 by translating the enhanced CFG of the program. We create a place to represent each node (i.e., *basic block*) in the enhanced CFG. Moreover, a directed arc connecting two nodes in the enhanced CFG is represented by a transition and associated arcs in the Petri net. For example, if there is an arc \overrightarrow{AB} in the enhanced CFG that connects node A to node B , then in the corresponding Petri net model, the two nodes A and B are represented by two places p_A and p_B , respectively; further, \overrightarrow{AB} is represented by three components in the Petri net: a transition t , an arc from p_A to t , and another arc from t to p_B . Lock variables are also modeled by places, whose connectivity to the transitions is determined by the actions of lock acquisitions or releases of the program. If a transition represents a lock acquisition call, we add an arc from the place modeling the lock to the transition; if a transition represents a lock release call, we add an arc from the transition to the place modeling the lock. A token in a place that represents a basic block models a thread executing in this basic block; a token in a place that represents a lock models the availability of this lock. The final Petri net model is called a Gadara net.

To facilitate our discussion, we will use a deadlock bug in the BIND software as a running example, which is shown in Figure 2.1. The acronym BIND stands for “Berkeley Internet Name Daemon,” which is a popular Domain Name System (DNS) on the Internet. Figure 2.1(a) shows the lines of code that are related to the deadlock under consideration; the corresponding Gadara net model is shown in Figure 2.1(b). The deadlock occurs if there is one token in p_1 , which represents one thread holding lock A while waiting for lock B , and there is one token in p_4 , which represents another thread holding lock B while waiting for lock A . This deadlock bug occurred in the

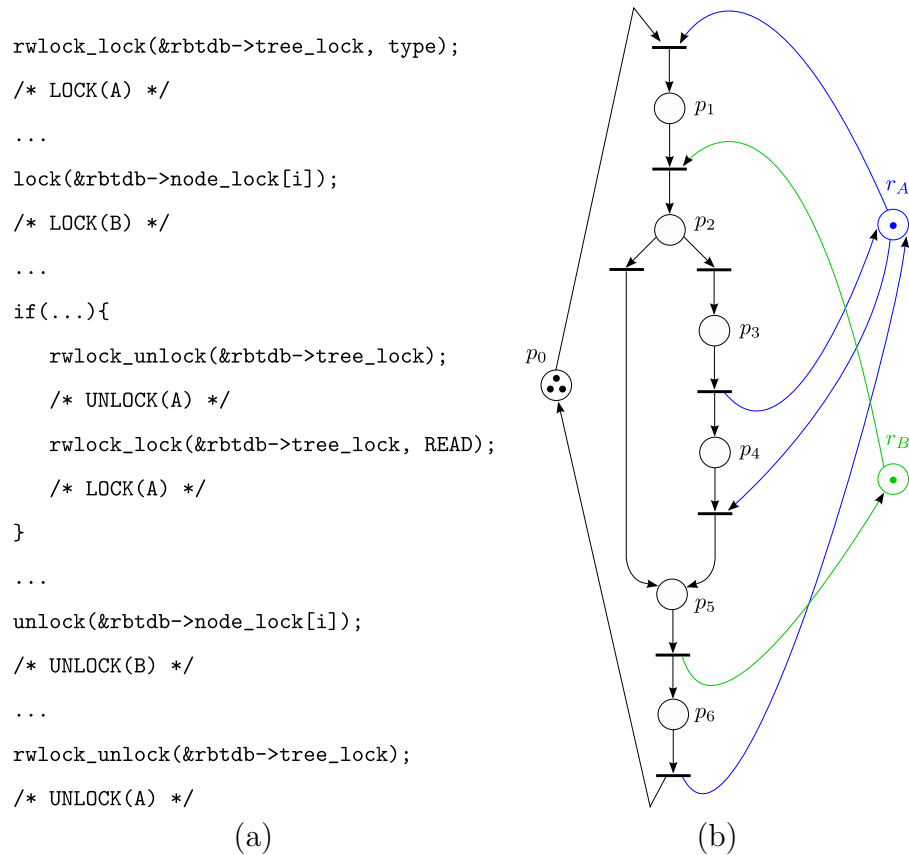


Figure 2.1: A deadlock example in BIND: (a) Simplified code; (b) Gadara net model final release version 9.2.2, and was fixed in the release candidate version 9.2.3rc1. As the bug database of BIND is not open to the public, we confirmed the bug by the change log of 9.2.3rc1, as well as using source code comparison. The bug resided in the `rdb.c` file, which is a red black tree data structure that stores domain names and IP addresses. For the sake of discussion, the Gadara net model has been simplified; in particular, we model the Reader/Writer lock in this example as a mutex.

2.3 Petri net preliminaries

Before introducing the formal definition of Gadara nets, we first briefly review some Petri net preliminaries; see [70, 8] for a detailed discussion.

2.3.1 Standard definitions

Definition II.2. A *Petri net dynamic system* $\mathcal{N} = (P, T, A, W, M_0)$ is a bipartite graph (P, T, A, W) with an initial number of tokens. Specifically, $P = \{p_1, p_2, \dots, p_n\}$ is the set of places, $T = \{t_1, t_2, \dots, t_m\}$ is the set of transitions, $A \subseteq (P \times T) \cup (T \times P)$ is the set of arcs, $W : A \rightarrow \{1, 2, \dots\}$ is the arc weight function, and for each $p \in P$, $M_0(p)$ is the initial number of tokens in p .

The *marking* (a.k.a. *state*) of a Petri net \mathcal{N} is a column vector M of n entries corresponding to the n places. As defined above, M_0 is the initial marking. We use $M(p)$ to denote the (partial) marking on a place p , which is a scalar; we use $M(Q)$ to denote the (partial) marking on a set of places Q , which is a $|Q| \times 1$ column vector. The notation $\bullet p$ denotes the set of input transitions of place p : $\bullet p = \{t \mid (t, p) \in A\}$. Similarly, $p\bullet$ denotes the set of output transitions of p . The sets of input and output places of transition t are similarly defined by $\bullet t$ and $t\bullet$. This notation is extended to sets of places or transitions in a natural way.

A transition t is *enabled* or *fireable* at M , if $\forall p \in \bullet t, M(p) \geq W(p, t)$. When an enabled transition t *fires*, for each $p \in \bullet t$, it removes $W(p, t)$ tokens from p ; and for each $q \in t\bullet$, it adds $W(t, q)$ tokens to q . The *reachable state space* $R(\mathcal{N}, M_0)$ of \mathcal{N} is the set of all markings reachable by transition firing sequences starting from M_0 .

A pair (p, t) is called a *self-loop* if p is both an input and output place of t . We consider only *self-loop-free* Petri nets in this dissertation. A Petri net is called *ordinary* if all the arcs in the net have unit arc weights, i.e., $W(a) = 1, \forall a \in A$; otherwise, it is called *non-ordinary*. Without any confusion, we can drop W in the definition of any Petri net \mathcal{N} that is ordinary.

Definition II.3. The *incidence matrix* D of a Petri net is an integer matrix $D \in \mathbb{Z}^{n \times m}$, where $D_{ij} = W(t_j, p_i) - W(p_i, t_j)$ represents the net change in the number of tokens in place p_i when transition t_j fires.

Definition II.4. A *state machine* is an ordinary Petri net such that each transition t has exactly one input place and exactly one output place, i.e., $\forall t \in T, |\bullet t| = |t \bullet| = 1$.

Definition II.5. Let D be the incidence matrix of a Petri net \mathcal{N} . Any non-zero integer vector y such that $D^T y = 0$ is called a *P-invariant* of \mathcal{N} . Further, P-invariant y is called a *P-semiflow* if all the elements of y are non-negative.

By definition, P-semiflow is a special case of P-invariant. A straightforward property of P-invariants is given by the following well-known result [70]: If a vector y is a P-invariant of Petri net $\mathcal{N} = (P, T, A, M_0)$, then we have $M^T y = M_0^T y$ for any reachable marking $M \in R(\mathcal{N}, M_0)$. The *support* of P-semiflow y , denoted as $\|y\|$, is defined to be the set of places that correspond to nonzero entries in y . A support $\|y\|$ is said to be *minimal* if there does not exist another nonempty support $\|y'\|$, for some other P-semiflow y' , such that $\|y'\| \subset \|y\|$. A P-semiflow y is said to be *minimal* if there does not exist another P-semiflow y' such that $y'(p) \leq y(p), \forall p$. For a given minimal support of a P-semiflow, there exists a unique minimal P-semiflow, which we call the *minimal-support P-semiflow* [70].

2.3.2 Control synthesis for Petri nets

Supervision Based on Place Invariants (SBPI) [28, 27, 110, 68, 38] provides an efficient algebraic technique for control logic synthesis by introducing a monitor place, which essentially enforces a P-invariant so as to achieve a given linear inequality constraint of the following form

$$l^T M \leq b \tag{2.1}$$

where M is the marking vector of the net under control, l is a weight (column) vector, and b is a scalar. All entries of l and b are integers. The main result of SBPI is as follows.

Theorem II.1. [38] Consider a Petri net \mathcal{N} , with incidence matrix D and initial marking M_0 . If $b - l^T M_0 \geq 0$, then a monitor place, p_c , with incidence matrix $D_{p_c} = -l^T D$, and initial marking $M_0(p_c) = b - l^T M_0$, enforces the constraint $l^T M \leq b$ upon the net marking. This supervision is maximally permissive.

The property of maximal permissiveness stated in the above theorem implies that a transition in the net is disabled by the monitor place only if its firing leads to a marking where the linear constraint in (2.1) is violated.

2.4 Gadara nets

Gadara nets, first introduced in [107, 64], are a special class of Petri nets that models multithreaded C programs with lock allocation and release operations, for the purpose of CMW-deadlock avoidance. In this section, we formally define the class of Gadara nets.

As discussed in Section 2.2, Gadara nets are translated from the enhanced CFG of multithreaded programs. They provide a formal foundation to model the locking behavior (case of mutexes) of the program. Gadara nets share features with classes of Petri nets that arise in the modeling of manufacturing systems [88, 56]. More specifically, they consist of a set of *process subnets* that correspond to thread entry points in the program, and resource places that model the locks through which threads interact.

Definition II.6. Let $I_{\mathcal{N}} = \{1, 2, \dots, m\}$ be a finite set of process subnet indices. A *Gadara net* is an ordinary, self-loop-free Petri net $\mathcal{N}_G = (P, T, A, M_0)$ where

1. $P = P_0 \cup P_S \cup P_R$ is a partition such that: a) $P_S = \bigcup_{i \in I_{\mathcal{N}}} P_{S_i}$, $P_{S_i} \neq \emptyset$, and $P_{S_i} \cap P_{S_j} = \emptyset$, for all $i \neq j$; b) $P_0 = \bigcup_{i \in I_{\mathcal{N}}} P_{0_i}$, where $P_{0_i} = \{p_{0_i}\}$; and c) $P_R = \{r_1, r_2, \dots, r_k\}$, $k > 0$.
2. $T = \bigcup_{i \in I_{\mathcal{N}}} T_i$, $T_i \neq \emptyset$, $T_i \cap T_j = \emptyset$, for all $i \neq j$.

3. For all $i \in I_{\mathcal{N}}$, the subnet \mathcal{N}_i generated by $P_{S_i} \cup \{p_{0_i}\} \cup T_i$ is a strongly connected state machine. There are no direct connections between the elements of $P_{S_i} \cup \{p_{0_i}\}$ and T_j for any pair (i, j) with $i \neq j$.
4. $\forall p \in P_S$, if $|p \bullet| > 1$, then $\forall t \in p \bullet, \bullet t \cap P_R = \emptyset$.
5. For each $r \in P_R$, there exists a unique minimal-support P-semiflow, Y_r , such that $\{r\} = \|Y_r\| \cap P_R$, $(\forall p \in \|Y_r\|)(Y_r(p) = 1)$, $P_0 \cap \|Y_r\| = \emptyset$, and $P_S \cap \|Y_r\| \neq \emptyset$.
6. $\forall r \in P_R, M_0(r) = 1, \forall p \in P_S, M_0(p) = 0$, and $\forall p_0 \in P_0, M_0(p_0) \geq 1$.
7. $P_S = \bigcup_{r \in P_R} (\|Y_r\| \setminus \{r\})$.

A Gadara net \mathcal{N}_G is defined to be an ordinary Petri net, because it models programs with mutex locks. **Condition 1** classifies the set of places in \mathcal{N}_G into three types: (i) The *idle place* $p_{0_i} \in P_0$ is an artificial place added to facilitate the discussion of liveness and other properties. The tokens in an idle place represent the threads that “wait” for future execution. (ii) P_S is the set of *operation places*. Each operation place models a *basic block* of the program. A token in an operation place represents one instance of thread that is executing in the current basic block. (iii) P_R is the set of *resource places* that model mutex locks. A token in a resource place represents the availability of the mutex lock. For example, in the Gadara net shown in Figure 2.1(b), place p_0 is an idle place, places r_A and r_B are resource places, and the other places in the net are operation places.

Condition 2 defines the set of transitions in \mathcal{N}_G . Each subnet of \mathcal{N}_G has its own set of transitions, which is not shared by any other subnet. A transition in \mathcal{N}_G models the action of lock acquisition or release by the program; a transition can also model branches in the program, such as *if/else*. \mathcal{N}_G consists of a set of subnets \mathcal{N}_i that define work processes, called process subnets in the literature. Based on process subnet \mathcal{N}_i , if we further consider the resource places (and monitor places

to be introduced in the next section) associated with it, then the resulting net is called a *resource-augmented process subnet*, denoted as \mathcal{N}_i^{aug} . Unlike most prior work in manufacturing applications, our process subnets need not be acyclic, due to the modeling of loops in programs. We observe from Figure 2.1(b) that the concurrent execution of multiple threads can even be modeled by one process subnet with multiple tokens in different operation places.

In **Condition 3**, the restriction of the process subnets \mathcal{N}_i to the class of state machines implies that there is no “forking” or “joining” in these subnets. The state machine structure of a process subnet is a natural result of the translation of the enhanced CFG as described in Section 2.2. On the other hand, the strong connectivity of the subnets \mathcal{N}_i , which is also stipulated by Condition 3, ensures that in the dynamics of these subnets, a token starting from the idle place will always be able to come back to the idle place after processing. In more natural terms, this requirement for strong connectivity implies that the only reason that might prevent the completion of the considered processes is their contest for the locks that govern their access to their critical sections and not any other potential errors in the underlying program logic. Further, the process subnets are interconnected only by resource places, i.e., any operation place or idle place in \mathcal{N}_i does not connect to any transition in \mathcal{N}_j , for $i \neq j$.

Condition 4 models the requirement that a transition representing a branch selection should not be engaged in any resource allocation. Conditions 5 and 6 characterize a distinct and crucial property of Gadara nets. First, the semiflow requirement in **Condition 5** guarantees that a resource acquired by a process will always be returned later. A process subnet cannot “generate” or “destroy” resources. We further require all coefficients of these semiflows Y_r to be equal to one. This requirement implies that the total number of tokens in $\|Y_r\|$, the support places of any such semiflow Y_r , is constant at any reachable marking M . Condition 6 defines

the initial token content, and therefore this constant is exactly equal to one. Hence, we have the following proposition:

Proposition II.1. *For any $r \in P_R$, at any reachable marking M in \mathcal{N}_G , there is exactly one token in the support places of P-semiflow Y_r .*

We can also express this proposition in terms of the semiflow equation as follows:

Property II.1. *For any $r \in P_R$, and its associated Y_r , we have the following semiflow equation:*

$$\sum_{p \in \|Y_r\| \cap P_S} M(p) + M(r) = 1 \quad (2.2)$$

To illustrate the concept of P-semiflow, let us consider the Gadara net shown in Figure 2.1(b) that has two resource places r_A and r_B . The minimal-support P-semiflows associated with r_A and r_B are $\|Y_{r_A}\| = \{r_A, p_1, p_2, p_3, p_5, p_6\}$ and $\|Y_{r_B}\| = \{r_B, p_2, p_3, p_4, p_5\}$, respectively.

As we discussed above, if the token is in resource place r , the mutex lock corresponding to r is available. Otherwise, it is in a place $p \in \|Y_r\| \cap P_{S_i}$ of some process subnet \mathcal{N}_i , which means that the thread in p is holding the lock. **Condition 6** specifies the initial markings of the three types of places. At the initial state, all the mutex locks are available; there is no thread executing in the process subnets; and, the number of threads waiting for future execution can be any positive integer.

Condition 7 states that any operation place models a basic block, which requires the acquisition of at least one lock for its execution. A multithreaded program contains sections executed with at least one lock held by the executing thread, called *critical sections* in operating systems terms, and sections executed without holding any lock. Condition 7 implies that the process subnets only model the critical sections of the programs. Since the sections executed without involving any lock are irrelevant to CMW-deadlock analysis, in practice, we prune the Petri nets translated from CFGs

so that our obtained Gadara nets only model the critical sections. This pruning process is automated; see [103] for details.

2.5 Controlled Gadara nets

Based on the Gadara net model of the program, we want to synthesize control logic to be enforced on the net so that the controlled net corresponds to a CMW-deadlock-free program. As introduced in Section 2.3, SBPI is a common control technique for Petri nets [28, 27, 110, 68, 38, 37]. Control specifications implemented by SBPI are represented by a set of linear inequalities on the net markings. Each linear inequality is enforced via a *monitor* place with its associated arcs that augment the original net. The added monitor place establishes a new invariant in the net dynamics and guarantees that the specified linear inequality is always satisfied in the controlled net. This invariant has a structure that is similar to that introduced by Condition 5 of Definition II.6, with the monitor place playing the role of a new (generalized) resource place. When we use SBPI on the Gadara net, we obtain a controlled Gadara net, as defined below. Note that one need not associate a controlled Gadara net with any specific control policy. It is a structural definition that does not refer explicitly to the content of the linear inequalities that are enforced by SBPI.

Definition II.7. Let $\mathcal{N}_G = (P, T, A, M_0)$ be a Gadara net. A *controlled Gadara net* $\mathcal{N}_G^c = (P \cup P_C, T, A \cup A_C, W^c, M_0^c)$ is a self-loop-free Petri net such that, in addition to all conditions in Definition II.6 for \mathcal{N}_G , we have

8. For each $p_c \in P_C$, there exists a unique minimal-support P-semiflow, Y_{p_c} , such that $\{p_c\} = \|Y_{p_c}\| \cap P_C$, $P_0 \cap \|Y_{p_c}\| = \emptyset$, $P_R \cap \|Y_{p_c}\| = \emptyset$, $P_S \cap \|Y_{p_c}\| \neq \emptyset$, and $Y_{p_c}(p_c) = 1$.
9. For each $p_c \in P_C$, $M_0^c(p_c) \geq \max_{p \in P_S} Y_{p_c}(p)$.

Definition II.7 indicates that the introduction of the monitor places into \mathcal{N}_G^c preserves the net structure of \mathcal{N}_G as specified by Definition II.6. **Condition 8** states that the monitor places P_C share similar structural properties with the resource places P_R in terms of the place invariants imposed on the net, which is inspired by the SBPI technique. But they have weaker constraints. More specifically, monitor places may have multiple initial tokens and non-unit arc weights. Thus, \mathcal{N}_G^c does not necessarily have to be an ordinary net, due to the arcs with non-unit weights that can be potentially introduced by a monitor place. A monitor place in \mathcal{N}_G^c can be considered as a *generalized* resource place, which preserves the conservative nature of resources in \mathcal{N}_G and has the following property.

Property II.2. *For any $p_c \in P_C$, and its associated Y_{p_c} , we have the following semiflow equation:*

$$Y_{p_c}^T M = M_0(p_c) \quad (2.3)$$

Due to the similarity between the original resource places and the synthesized monitor places, we will use the term “*generalized resource place*” to refer to any place $p \in P_R \cup P_C$.

Condition 9 implies that the initial marking of a monitor place provides a number of tokens that is able to cover, in isolation, the token request posed by any stage in the support of the semiflow of that monitor place.

As a special case of \mathcal{N}_G^c , if all the arcs in the net have unit arc weights (or, more specifically, all the arcs associated with monitor places in the net have unit arc weights), then \mathcal{N}_{G1}^c , the class of controlled Gadara nets that remain ordinary, can be defined as follows.

Definition II.8. Let $\mathcal{N}_G = (P, T, A, M_0)$ be a Gadara net. An *ordinary controlled Gadara net* $\mathcal{N}_{G1}^c = (P \cup P_C, T, A \cup A_C, M_0^c)$ is an *ordinary*, self-loop-free Petri net that satisfies Conditions 1 to 7 in Definition II.6 and Conditions 8 and 9 in Definition

II.7.

Remark II.1. From Definitions II.6, II.7, and II.8, we observe that \mathcal{N}_G is a special subclass of both \mathcal{N}_{G1}^c and \mathcal{N}_G^c , where $P_C = \emptyset$ and $A_C = \emptyset$. Furthermore, \mathcal{N}_{G1}^c is a special subclass of \mathcal{N}_G^c , where $W^c(a) = 1, \forall a \in A \cup A_C$. Therefore, any property that we derive for \mathcal{N}_G^c holds for both \mathcal{N}_{G1}^c and \mathcal{N}_G . Also, any property that we derive for \mathcal{N}_{G1}^c holds for \mathcal{N}_G . In the following, for the sake of simplicity, we refer to \mathcal{N}_G^c as a “Gadara net” (unless special mention is made). \square

Conditions 5, 6, and 7 of Definition II.6 together lead to the following important property of Gadara nets.

Proposition II.2. *Given a Gadara net \mathcal{N}_G^c , for any reachable marking $M, \forall p \in P_S, M(p)$ is either 0 or 1. In other words, all operation places in \mathcal{N}_G^c are 1-bounded.*

Proof. Proposition II.1 states that for any $r \in P_R$, there is exactly one token in the support places, $\|Y_r\|$, of its P-semiflow Y_r . This result, when considered together with Condition 7 of Definition II.6, implies that for any operation place in \mathcal{N}_G^c , its marking is either 0 or 1. \square

2.6 Uncontrollability in modeling

We see that \mathcal{N}_G^c is obtained by augmenting the original net with monitor places that will control the firing of transitions. In this regard, we partition the transitions in the net T into two disjoint subsets: $T = T_c \cup T_{uc}$, where T_c is the set of controllable transitions (which can be disabled by a monitor place), and T_{uc} is the set of uncontrollable transitions (which cannot be disabled by a monitor place). Then, \mathcal{N}_G^c is said to be *admissible* if $P_C \bullet \cap T_{uc} = \emptyset$. In the remainder of this dissertation, we make the following assumption:

Assumption II.1. \mathcal{N}_G^c is admissible.

According to the semantics of the program represented by Gadara nets, branching transitions are uncontrollable; this is why the branching transitions must satisfy Condition 4 of Definition II.6. On the other hand, lock acquisition transitions are controllable so that we can avoid CMW-deadlocks. The rest of the transitions can be classified either way, representing the “upper bound” and the “lower bound” of T_{uc} , respectively.

Assumption II.2. $\{t \in T : (\exists p \in P_S), (|p \bullet| > 1) \wedge (t \in p \bullet)\} \subseteq T_{uc} \subseteq T \setminus (P_R \bullet)$

The development of results in this dissertation *only* requires that T_{uc} contains all the branch selection transitions (i.e., the lower bound in Assumption II.2); these results also extend to any other choice of T_{uc} that satisfies Assumption II.2.

2.7 Discussion of related classes of Petri nets

Petri nets have been extensively applied to the modeling and analysis of flexible manufacturing systems and other technological applications involving a resource allocation function [56, 88]. In this application domain, the class of S^3PR nets is one of the most widely studied sub-classes of Petri nets; it consists of process-oriented nets that possess an acyclicity property [19]. Many sub-classes of Petri nets have been developed to extend the formulation of S^3PR in order to model special features of specific systems. Recently, a new class of Petri nets, called $STPR$, has been proposed for anomaly detection in manufacturing systems [1, 2]. A unique characteristic of $STPR$ nets is that the system allows resource creation and negated resources; these features are not suitable for our needs in this dissertation.

Multithreaded software systems share some similarities with manufacturing systems, e.g., the operation of both systems requires acquisition and release of resources (i.e., locks). However, loops, such as `for` and `while`, are very common in programs, and they result in internal cycles in the process subnets of their Petri

net models. Thus, there is a need to relax the acyclicity constraint of S^3PR nets. The resulting superclass is called S^*PR . Deadlock analysis is known to be difficult when the process subnets in process-oriented nets contain internal cycles [81, 41]. In [41], the authors study the class of RCN* merged nets, which arises in semiconductor manufacturing systems. The potentially degraded behaviors (e.g., reworks and failures) in this manufacturing setting necessitate the internal cycles in the model. In [81], liveness-enforcing supervision is investigated for a broad class of resource allocation systems, in the presence of uncontrollable behavior that can also lead to cyclic behavior. Reference [80] extends the results on liveness analysis and control of ordinary nets to the class of non-ordinary process-resource nets. There are few results on deadlock analysis in S^*PR [20]. Gadara nets \mathcal{N}_G fall within the S^*PR class, but they possess features, such as unit arc weight and 1-bounded operation places, which render deadlock analysis more tractable and enable the synthesis of optimal control logic through monitor places.

CHAPTER III

Analysis: Properties of Gadara Nets

3.1 Introduction

With the class of Gadara nets formally defined, our next task is to establish the relevant properties of Gadara nets, such that the goal of CMW-deadlock-free execution of a program can be mapped to an equivalent objective in terms of its corresponding Gadara net model.

We briefly overview this chapter as follows. We introduce some standard definitions of Petri net behavioral properties in Section 3.2, and some definitions of Petri net structural properties in Section 3.3. Then, we carry out our analysis in three steps. (i) We establish in Section 3.4 that the goal of CMW-deadlock-free execution of a program is equivalent to the reversibility of its corresponding Gadara net model, which is a *behavioral* property. (ii) We prove in Section 3.5 that for a Gadara net, liveness, which is another *behavioral* property, is equivalent to the absence of certain types of siphons in the net, which is a *structural* feature. (iii) We show in Section 3.6 that for a Gadara net, liveness is equivalent to reversibility. As a result of the above three steps of analysis, the *behavioral* property of CMW-deadlock-free execution of a program is mapped to an equivalent objective in terms of a *structural* property of the Gadara net. This mapping has important implications for efficient optimal control synthesis.

In Section 3.7, we discuss an additional property of Gadara nets that is known as the linear separability of their state space and facilitates the optimal control of these nets through monitor places. In Section 3.8, we propose a set of mathematical programming formulations for the verification of liveness of Gadara nets. In Section 3.9, we present a case study of a deadlock bug in the Linux kernel. Some of the results in this chapter also appear in [64, 107, 61].

3.2 Petri net liveness and reversibility

First, let us provide a series of definitions that formalize the Petri net concepts of liveness and reversibility and some additional concepts related to them; see [70, 88] for a detailed discussion. For the sake of simplicity, in the following discussion we use $R(\mathcal{N}, M)$ to denote the set of reachable markings of net \mathcal{N} starting from marking M .

Definition III.1. A marking M is *live* if $\forall t \in T$, there exists $M' \in R(\mathcal{N}, M)$, such that t is enabled at M' . A Petri net (\mathcal{N}, M_0) is *live* if $\forall M \in R(\mathcal{N}, M_0)$, M is live.

Definition III.2. Petri net \mathcal{N} is said to be *quasi-live* if, for all $t \in T$, there exists $M \in R(\mathcal{N}, M_0)$, such that t is enabled at M .

Definition III.3. Petri net \mathcal{N} is said to be *reversible* if $M_0 \in R(\mathcal{N}, M)$, for all $M \in R(\mathcal{N}, M_0)$.

Definition III.4. A Petri net is in a *total-deadlock* if all the transitions in the net are disabled.

Clearly, the state machine structure of subnets and the initial marking of idle places (as specified by Conditions 3 and 6 of Definition II.6, respectively) imply that all subnets \mathcal{N}_i in a Gadara net \mathcal{N}_G are quasi-live. Furthermore, the resource requirement of operation places and the initial marking of resource places (as specified by Conditions 5 and 6 of Definition II.6, respectively) imply that quasi-liveness is

preserved, when each subnet \mathcal{N}_i is augmented with the corresponding resource places in P_R . Similarly, Conditions 8 and 9 of Definition II.7 imply the preservation of quasi-liveness for the subnets \mathcal{N}_i of \mathcal{N}_G^c when augmented with the monitor places $p_c \in P_C$. Finally, the combination of Condition 3 of Definition II.6 with the quasi-liveness of the resource and monitor-place-augmented subnets \mathcal{N}_i established above, further implies the reversibility of the latter, when executing in isolation, i.e., when $M_0(p_{0_i}) = 1$.

3.3 Resource-induced deadly marked siphons and modified markings

We introduce some further definitions to facilitate our structural analysis of Gadara nets; see [70, 88] for a detailed discussion.

Definition III.5. A nonempty set of places S is said to be a *siphon* if $\bullet S \subseteq S \bullet$.

Siphon is a well-defined structural construct in Petri nets. In Figure 2.1(b), the set of places $S_{AB} = \{r_A, r_B, p_2, p_3, p_5, p_6\}$ is a siphon.

The following concepts pertain to the process-resource net structure of Gadara nets, and they play a very important role in the characterization of the liveness and reversibility of Gadara nets that is provided in the rest of this chapter.

Definition III.6. Place p is said to be a *disabling place* at marking M if there exists $t \in p \bullet$, s.t. $M(p) < W(p, t)$.

Definition III.7. A siphon S of a Gadara net \mathcal{N}_G^c is said to be a *resource-induced deadly marked (RIDM) siphon* [88] at marking M , if it satisfies the following conditions:

1. every transition $t \in \bullet S$ is disabled by some place $p \in S$ at marking M ;
2. $S \cap (P_R \cup P_C) \neq \emptyset$;

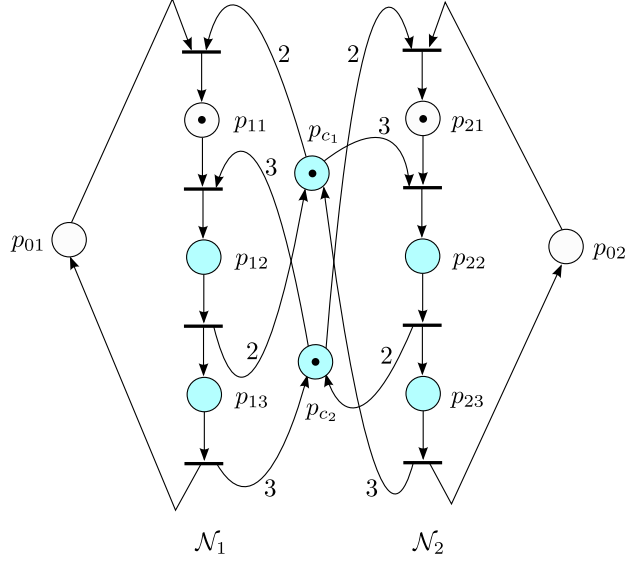


Figure 3.1: Example: $S = \{p_{c_1}, p_{c_2}, p_{12}, p_{13}, p_{22}, p_{23}\}$ is a nonempty RIDM siphon at the marking shown in the figure

3. $\forall p \in S \cap (P_R \cup P_C)$, p is a disabling place at marking M .

From Definition III.7, a RIDM siphon is defined by a siphon S , together with a partial marking on S . Thus, whenever we refer to a RIDM siphon S , it means the set of places that constitute S as well as the partial marking on S . To illustrate the notion of RIDM siphon, again, refer to the example in Figure 2.1(b), and consider the reachable marking M , where there is one token in p_0 , one in p_1 , and one in p_4 , while all other places are empty. The siphon $S_{AB} = \{r_A, r_B, p_2, p_3, p_5, p_6\}$ discussed above is a RIDM siphon at marking M . Further, S_{AB} is an *empty* siphon at marking M . The notion of RIDM siphon can also be used in a non-ordinary net. In general, a RIDM siphon can be nonempty. Figure 3.1 shows an example of a nonempty RIDM siphon in a non-ordinary net: $S = \{p_{c_1}, p_{c_2}, p_{12}, p_{13}, p_{22}, p_{23}\}$ with its associated marking.

Definition III.8. Given a Gadara net \mathcal{N}_G^c and a marking $M \in R(\mathcal{N}_G^c, M_0^c)$, the *modified marking* \overline{M} is defined by

$$\overline{M}(p) = \begin{cases} M(p), & \text{if } p \notin P_0; \\ 0, & \text{if } p \in P_0. \end{cases} \quad (3.1)$$

Modified markings essentially “erase” the tokens in idle places. The set of modified markings induced by the set of reachable markings is defined by $\overline{R}(\mathcal{N}_G^c, M_0^c) = \{\overline{M} \mid M \in R(\mathcal{N}_G^c, M_0^c)\}$. Note that the number of tokens in idle places P_0 can always be uniquely recovered from the invariant implied by the strongly-connected state-machine structure of the subnet \mathcal{N}_i . Therefore, we have the following property.

Property III.1. *There is a one-to-one mapping between the original marking and the modified marking, i.e., $M_1 = M_2$ if and only if $\overline{M}_1 = \overline{M}_2$, where M_1 and M_2 are reachable.*

Condition 7 of Definition II.6 indicates that the set of idle places do not directly interact with any resource place, and therefore they are irrelevant to the analysis of CMW-deadlocks. The notion of modified markings enables us to associate the non-liveness of the net to RIDM siphons.

3.4 The multithreaded program and its Gadara net model

The following result provides a bridge between a program and its corresponding Gadara net model, under the assumptions discussed in Section 2.2, in terms of two relevant behavioral properties.

Proposition III.1. *A multithreaded program that can be modeled as a Gadara net \mathcal{N}_G^c is CMW-deadlock-free iff \mathcal{N}_G^c is reversible.*

Proof. First we show the “ \Rightarrow ” direction.

If a program is free from any CMW-deadlocks, then for any stage the program is executing, all instances of threads in the program can always complete the rest of their executions, and terminate the processes. This corresponds to the case in the Gadara net model, where starting from any marking of the net, the tokens in the operation places can eventually return to the idle places, which leads the net back to the initial marking. Thus, the net is reversible.

Next we show the “ \Leftarrow ” direction.

(Proof by contra-positive proposition) Suppose there exist at least two threads involved in a CMW-deadlock of the program; then these instances of threads are unable to complete their executions. In the corresponding Gadara net model of the program, these deadlocked threads are modeled as tokens in operation places. The fact that these threads are unable to terminate implies that the aforementioned tokens will never return to the idle places. In other words, starting from this state, the net will never return to the initial marking. Thus, the net is not reversible. \square

Remark III.1. When it is not possible to build an exact Gadara net model of a program due to modeling constraints such as those discussed in Section 2.2, it is preferable to build a “conservative” model that is certain to include all possible execution paths of the program (and possibly some infeasible paths as well). In this case, the reversibility property of the Gadara net model is a sufficient (but possibly not necessary) condition for CMW-deadlock-freeness of the program; the rest of the discussion in this dissertation still applies for the conservative model. \square

Remark III.2. From Remark I.1 and the above discussion, we know that a Gadara net model being total-deadlock-free does *not* guarantee that its corresponding program is free from any CMW-deadlocks. For example, let us consider a Gadara net model containing N process subnets. Assume that at some marking of the net: (i) there exist two process subnets, say \mathcal{N}_1 and \mathcal{N}_2 , such that all the transitions in these two process subnets are disabled; and (ii) for the remaining $N - 2$ process subnets, there exists at least one enabled transition in each of them. The Gadara net at this marking is total-deadlock-free by Definition III.4. However, the underlying program has a CMW-deadlock, which involves the threads modeled by \mathcal{N}_1 and \mathcal{N}_2 . \square

It is well known that if an ordinary Petri net cannot reach an empty siphon, then the net is total-deadlock-free [87]. But, Remark III.2 implies that for the purpose of CMW-deadlock avoidance in a multithreaded program, requiring its Gadara net

model to be total-deadlock-free is not sufficient. This motivates our investigation of the liveness property of Gadara nets in the next section, where we establish *necessary and sufficient* conditions for liveness (of \mathcal{N}_G^c , \mathcal{N}_G , and $\mathcal{N}_{G_1}^c$) in terms of the absence of certain types of siphons.

3.5 Liveness of Gadara nets

Liveness and reversibility are closely related properties of Gadara nets. In fact, they are shown to be equivalent in Section 3.6. In this section, we first establish some results about the liveness of Gadara nets, which connect this *behavioral* property to a certain *structural* property in terms of siphons. Similar results exist in the literature (see Theorem 5.3 and Corollary 3 on p. 132 of [88]) for a class of process-resource nets that are structurally similar but model processes with no internal cycles. Despite the presence of cycles and other technical differences in our process subnets, the above results in [88] can be extended to Gadara nets.

Theorem III.1. *Gadara net \mathcal{N}_G^c is live iff there does not exist a modified marking $\overline{M} \in \overline{R}(\mathcal{N}_G^c, M_0^c)$ and a siphon S such that S is a RIDM siphon at \overline{M} .*

Proof. First we show the “ \Rightarrow ” direction.

(Proof by contra-positive proposition) Suppose that there exists a marking M such that the corresponding modified marking \overline{M} contains a RIDM siphon S . From the definition of the RIDM siphon, there exists a place $q \in S \cap (P_R \cup P_C)$, and a transition $t \in q\bullet$ that is disabled due to the lack of enough tokens in q . On the other hand, since $q \in S$, by the definition of RIDM siphons, the transitions in $\bullet q$ are all disabled. Therefore, place q will never get replenished in $R(\mathcal{N}_G^c, \overline{M})$, and the disabled transition t will remain non-live in $R(\mathcal{N}_G^c, \overline{M})$. Furthermore, Condition 5 of Definition II.6 and Condition 8 of Definition II.7 imply that $P_0 \cap \|Y_q\| = \emptyset$, and $q \notin T_I\bullet$, where $T_I = P_0\bullet$. So, when we move from the modified markings to the original markings

in \mathcal{N}_G^c by re-introducing the tokens in P_0 , place q will not gain new tokens, and the disabled transition t will remain non-live. Therefore, the liveness of \mathcal{N}_G^c implies that $\overline{R}(\mathcal{N}_G^c, M_0)$ contains no RIDM siphons.

Next we show the “ \Leftarrow ” direction.

(Proof by contra-positive proposition) Suppose that \mathcal{N}_G^c is not live. We want to show that $\overline{R}(\mathcal{N}_G^c, M_0)$ contains at least one RIDM siphon. By the non-liveness assumption, we know that there exists a marking $M' \in R(\mathcal{N}_G^c, M_0)$ such that at least one transition $t' \in T$ is never enabled in $R(\mathcal{N}_G^c, M')$.

In view of the structural assumptions made in defining \mathcal{N}_G^c , there also exists a marking $M \in R(\mathcal{N}_G^c, M')$, that satisfies the following two conditions: (i) There exists at least one process subnet \mathcal{N}_i such that $M(p_{0_i}) < M_0(p_{0_i})$. Namely, an instantiation of the thread modeled by \mathcal{N}_i is “half-way” in execution at marking M . Furthermore, the dead transition t' must belong to one of these thread subnets. (ii) Every transition $t \notin P_{0\bullet}$ is disabled at M . From the definition of the modified marking, this fact further implies that all the transitions are disabled at \overline{M} . That is, \overline{M} is a total-deadlock.

We claim that (i) must be satisfied, because otherwise M_0 is reachable from M' . In this case, the quasi-liveness property of \mathcal{N}_i , discussed in Section 3.2, implies that t' is not dead at M' , which contradicts our assumption. We claim that (ii) must also be satisfied. Although a process subnet of \mathcal{N}_G^c may contain an internal cycle, Condition 4 of Definition II.6 and Assumption II.1 guarantee that the entering/leaving of any cycle will not be constrained by any generalized resource, and thus a token will never be “trapped” in a cycle where it loops indefinitely. Therefore, the remaining process subnets, which are not involved in the CMW-deadlock, can eventually complete the execution of all their active thread instances and return all their tokens back to their idle places. Hence, the only enabled transitions of these subnets at M are the output transitions of their idle places, which further implies that they are in a total-deadlock at \overline{M} . In other words, a marking $M \neq M_0^c$, whose modified marking \overline{M} corresponds

to a total-deadlock, is always reachable from M' .

We are left to show that \overline{M} contains a RIDM siphon. Let S denote the set of disabling places at \overline{M} . Since \overline{M} is a total-deadlock, $S\bullet = T$, where T is the set of all transitions in the net. Thus, we have the relationship: $\bullet S \subseteq S\bullet = T$. By definition, S is a siphon. Obviously, S also satisfies Conditions 1 and 3 of Definition III.7. Furthermore, Condition (i) that characterizes marking M , when combined with the state machine structure of net \mathcal{N}_i (cf. Condition 3 of Definition II.6), implies that there exists at least one transition $t \in T_i$ with $\bullet t \cap P_S = \{p\} \neq \emptyset$ and with $M(p) = \overline{M}(p) = 1$. Therefore, the total-deadlock at \overline{M} must involve some place $q \in P_R \cup P_C$, and Condition 2 of Definition III.7 is satisfied. Hence, S is a RIDM siphon in \mathcal{N}_G^c . \square

When a Gadara net is ordinary (i.e., \mathcal{N}_G or $\mathcal{N}_{G_1}^c$), we can characterize liveness in terms of empty siphons, which is a special case of RIDM siphons.

Theorem III.2. (1) *Gadara net \mathcal{N}_G is live iff there does not exist a marking $M \in R(\mathcal{N}_G, M_0)$ and a siphon S such that S is an empty siphon at M .*

(2) *Gadara net $\mathcal{N}_{G_1}^c$ is live iff there does not exist a marking $M \in R(\mathcal{N}_{G_1}^c, M_0^c)$ and a siphon S such that S is an empty siphon at M .*

The proof of this theorem is similar to the proof of Corollary 3 on p. 132 of [88]. It is presented below for the sake of completeness.

Proof. From Theorem III.1, \mathcal{N}_G^c is not live if and only if there exists a marking $M \in R(\mathcal{N}_G^c, M_0)$ and $M \neq M_0$, such that its modified marking \overline{M} contains a RIDM siphon S . From the proof of Theorem III.1, we further know that S is constructed by the set of disabling places at \overline{M} . For an ordinary net, a disabling place is essentially a place with no tokens. Since every place $p \in S$ is a disabling place, $\overline{M}(p) = 0, \forall p \in S$. Hence, S is an empty siphon at \overline{M} .

Next we show that the presence of the resource-induced empty siphon S at \overline{M} implies the presence of an empty siphon S' at the original marking M . Let

$$S' = \{w : w \in S \cap (P_R \cup P_C)\} \cup \{p \in P_S : M(p) = \overline{M}(p) = 0 \wedge \exists w \text{ s.t. } w \in S \cap (P_R \cup P_C) \wedge y_w(p) > 0\}$$

where, $y_w(p) > 0$ iff the operation place p needs the allocation of tokens from w . Note that $S' \neq \emptyset$, since S is a resource-induced empty siphon. Furthermore, $M(p) = 0, \forall p \in S$. Next we show that S' is also a siphon, by considering the following two main cases:

Case 1: Consider $t \in \bullet w$ for some place $w \in S \cap (P_R \cup P_C)$. Then, by the definition of siphon, $\exists q \in S$ such that $t \in q \bullet$. If $q \in P_R \cup P_C$, then $q \in \{w : w \in S \cap (P_R \cup P_C)\} \subset S'$. On the other hand, if $q \notin P_R \cup P_C$, then $q \in P_S$. Furthermore, $y_w(q) > 0$, and $M(q) = 0$ (since $q \in S$). Therefore, $q \in \{p \in P_S : M(p) = \overline{M}(p) = 0 \wedge \exists w \text{ s.t. } w \in S \cap (P_R \cup P_C) \wedge y_w(p) > 0\} \subset S'$. So, $t \in S' \bullet$.

Case 2: Consider $t \in \bullet q$ for some $q \in P_S$ with $M(p) = \overline{M}(p) = 0 \wedge \exists w \text{ s.t. } w \in S \cap (P_R \cup P_C) \wedge y_w(p) > 0$. Let us consider to the following two subcases.

(i) If $\exists w \text{ s.t. } w \in S \cap (P_R \cup P_C) \wedge t \in w \bullet$, then, $t \in \{w : w \in S \cap (P_R \cup P_C)\} \bullet \subseteq S' \bullet$.

(ii) Otherwise, $\exists q' \in P_S \cap \bullet t$ with $\overline{M}(q') = 0$. Furthermore, since $y_w(q) > 0$, it must be that $y_w(q') > 0$ (i.e., the operation of place q needs some tokens from w in order to be executed, but since $w \notin \bullet(\bullet q)$, by the assumption of this subcase, there must exist an upstream operation place q' which will “pass” these tokens to q). It needs to be pointed out that such an upstream operation place $q' \notin P_0$, because idle places do not hold any tokens from w , by the definition of \mathcal{N}_G^c . Therefore, $t \in \{p \in P_S : M(p) = \overline{M}(p) = 0 \wedge \exists w \text{ s.t. } w \in S \cap (P_R \cup P_C) \wedge y_w(p) > 0\} \bullet \subseteq S' \bullet$.

In both cases, $\forall t \in \bullet S', t \in S' \bullet$. Thus, S' is a siphon. \square

As discussed in Section 3.3, the siphon $S_{AB} = \{r_A, r_B, p_2, p_3, p_5, p_6\}$ in the Gadara

net shown in Figure 2.1(b) becomes an empty siphon at the reachable marking M , where there is one token in p_0 , one in p_1 , and one in p_4 , while all other places are empty. Thus, from Theorem III.2, the Gadara net depicted in Figure 2.1(b) is not live. Alternatively, we can also verify that S_{AB} is a RIDM siphon at \overline{M} ; hence, from Theorem III.1, we arrive at the same conclusion that the Gadara net in Figure 2.1(b) is not live.

3.6 Reversibility of Gadara nets

In this section, we establish the equivalence between liveness and reversibility in Gadara nets. This result “links” Proposition III.1 with Theorems III.1 and III.2, such that the goal of CMW-deadlock-free execution of the program can be mapped to the absence of certain types of siphons in the Gadara net.

Theorem III.3. *Gadara net \mathcal{N}_G^c is live iff it is reversible.*

Proof. First we show the “ \Rightarrow ” direction.

Given a marking $M \in R(\mathcal{N}_G^c, M_0)$ with $M \neq M_0$, consider a non-empty place $p \in P_S$ and its corresponding process subnet \mathcal{N}_i . The strong connectivity of \mathcal{N}_i implies that there is a path (i.e., a sequence of feasible transitions) from p to p_{0_i} . Let t' denote the transition in that path with $t' \in \bullet p_{0_i}$. The assumed liveness of the net implies that starting from M , we shall eventually be able to fire t' . Furthermore, the activation of the aforementioned sequence of feasible transitions does not have to involve any of the tokens in $M(p_{0_i})$. Thus, the token in p at marking M can eventually be collected into p_{0_i} . Since the above argument holds for any non-empty operation place at any marking $M \in R(\mathcal{N}_G^c, M_0)$, and the total number of tokens in P_S at M is finite, we shall eventually be able to collect all the tokens in P_S at marking M into P_0 . Denote this last marking as M' . Combined with Condition 5 of Definition II.6, it follows that $M' = M_0$.

Next we show the “ \Leftarrow ” direction.

We discussed in Section 3.2 that the resource and monitor-place-augmented subnets in \mathcal{N}_G^c are quasi-live. This property, together with the assumed reversibility of the net, implies that \mathcal{N}_G^c is live. \square

3.7 Linear separability and optimal control of Gadara nets

We summarize the properties we have shown so far with the following important results.

Theorem III.4. (1) *If a multithreaded program can be modeled as Gadara net \mathcal{N}_G^c , then the program is CMW-deadlock-free iff \mathcal{N}_G^c cannot reach a modified marking \bar{M} such that there exists at least one RIDM siphon at \bar{M} .*

(2) *If a multithreaded program can be modeled as Gadara net \mathcal{N}_G (or $\mathcal{N}_{G_1}^c$), then the program is CMW-deadlock-free iff \mathcal{N}_G (or $\mathcal{N}_{G_1}^c$) cannot reach a marking M such that there exists at least one empty siphon at M .*

Theorem III.4 implies that the problem of CMW-deadlock avoidance in a multithreaded program is *equivalent* to the problem of preventing any RIDM siphon (resp., empty siphon) from becoming reachable in the modified reachability space (resp., original reachability space) of its Gadara net model \mathcal{N}_G^c (resp., \mathcal{N}_G or $\mathcal{N}_{G_1}^c$). The results established in this section serve as the foundations for the development of optimal control policies for Gadara nets based on structural analysis [60, 59, 106]. They also provide a formal method for efficiently verifying the liveness of a Gadara net (and the CMW-deadlock-freeness of its underlying program), as we will see in Section 3.8.

Optimal control synthesis is an important class of problems in supervisory control of Petri nets. Next we show that optimal control through monitor places is always feasible in Gadara nets. Note that such a property does not always hold in general

for other classes of nets; see [107] for a counter-example. We first establish a general property that in Gadara nets, any set of reachable markings can always be separated from the rest through a set of linear inequalities, so that the SBPI technique can be used to synthesize monitor places to enforce such a separation. The property is referred to as the *linear separability* of the state space of Gadara nets.

For the sake of discussion, let us denote the control specifications in SBPI as a set of linear constraints $\{(l_k, b_k), k = 1, 2, \dots\}$ of the form

$$l_k^T M \leq b_k \quad (3.2)$$

that are enforced on the net markings, where for any k , l_k is a weight vector and b_k is a scalar. Similarly to the notion of modified marking, we define the notion of P_S -marking to facilitate the ensuing discussion.

Definition III.9. Given a Gadara net \mathcal{N}_G^c and a marking $M \in R(\mathcal{N}_G^c, M_0^c)$, the P_S -marking $\overline{\overline{M}}$ is defined by

$$\overline{\overline{M}}(p) = \begin{cases} M(p), & \text{if } p \in P_S; \\ 0, & \text{if } p \notin P_S. \end{cases} \quad (3.3)$$

P_S -markings essentially “erase” the tokens in idle places and generalized resource places, retaining only tokens in operation places. As in the case of modified markings, the P_S -marking does not introduce any ambiguity. More specifically, given the P_S -marking $\overline{\overline{M}}$ corresponding to the original marking M , the number of tokens in places P_R and P_C under M can be uniquely recovered by solving the equations given in Properties II.1 and II.2, respectively. Combining this result with Property III.1 of the modified markings, we have the following property.

Property III.2. *There is a one-to-one mapping between the original marking and the P_S -marking, i.e., $M_1 = M_2$ if and only if $\overline{\overline{M}}_1 = \overline{\overline{M}}_2$, where M_1 and M_2 are*

reachable.

Therefore, we consider linear constraints for P_S -markings only, i.e., the coefficients corresponding to places in sets P_0 , P_R , and P_C are all zero. From Proposition II.2, we know that $\overline{\overline{M}}$ is a binary vector, which is a key result to establish the desired linear separability property.

Theorem III.5. *Given a Gadara net \mathcal{N}_G^c and a set of markings $V \subseteq R(\mathcal{N}_G^c, M_0^c)$, there exists a finite set of linear constraints $LC(V) = \{(l_1, b_1), (l_2, b_2), \dots\}$ such that $M \in V$ iff $\forall (l_i, b_i) \in LC(V)$, $l_i^T M \leq b_i$.*

Proof. We prove by construction. According to Definition III.9, any marking is uniquely characterized by its corresponding P_S -marking. Thus, for any marking $M' \notin V$, we can focus our attention on the associated P_S -marking $\overline{\overline{M'}}$. We construct the linear constraint associated with M' based on $\overline{\overline{M'}}$ as follows.

$$l(p) := \begin{cases} -1, & \text{if } \overline{\overline{M'}}(p) = 0 \\ 1, & \text{if } \overline{\overline{M'}}(p) = 1 \\ 0, & \text{if } p \notin P_S \end{cases} ; \quad b := \sum_{p \in P_S} \overline{\overline{M'}}(p) - 1 \quad (3.4)$$

Observe that the coefficient vector l and the scalar b specified in (3.4) satisfy: $l^T M' = b+1 > b$. We know that any P_S -marking is a binary vector, i.e., its component is either 0 or 1. Thus, the choice of l and b guarantees that if we change any component in $\overline{\overline{M'}}$, then the value of $l^T M'$ will decrease by 1 after the change. Any reachable marking $M \neq M'$ can be considered as being obtained by changing a set of components of $\overline{\overline{M'}}$. As a result, any reachable marking $M \neq M'$ satisfies the linear inequality $l^T M \leq b$; and, M' is the only marking that does not satisfy this linear inequality. In other words, if we enforce the constraint $l^T M \leq b$ on the net, then we *only* prevent one single marking M' from being reachable and nothing else.

We can construct such a linear constraint for every marking in $R(\mathcal{N}_G^c, M_0^c) \setminus V$. Since $R(\mathcal{N}_G^c, M_0^c)$ is finite, containing no more than $2^{|P_S|}$ states, $R(\mathcal{N}_G^c, M_0^c) \setminus V$ is

finite as well, and there is a finite set of linear constraints that separates V from its complement in $R(\mathcal{N}_G^e, M_0^e)$. \square

Separating the set of desirable markings from the set of undesirable markings, with respect to the goal of liveness enforcement, is a special case of this general result. Therefore, we have established the feasibility of optimal control for Gadara nets through monitor places.

This result provides the foundation for the optimal control synthesis of Gadara nets, which will be presented in Chapters IV and V, and are reported in [60, 59, 61]. We make the following brief comments. In [60, 59, 61], we presented an efficient siphon-based optimal control synthesis algorithm for Gadara nets, while in [75, 76], an alternative approach based on state space expansion and classification theory was proposed. When applied to the BIND example in Figure 2.1(b), both methodologies synthesize the same control specification: $p_1 + p_4 \leq 1$. Using SBPI, we obtain the monitor place p_c that enforces this specification, as shown in Figure 3.2.

3.8 Verification of liveness using mathematical programming

According to Theorems III.1 and III.2, liveness in Gadara nets can be verified by detecting certain types of siphons that may be reachable in the nets. The problem of siphon detection in Petri nets has been extensively studied in the literature. In [6], a basis siphon generation algorithm is presented using the sign incidence matrix derived from the original incidence matrix of the net. In the Gadara project, an efficient siphon detection algorithm using the so-called *lock dependency graph* is reported in [103]. Recently, a similar method of siphon detection using graph theory has been applied to the class of S^4PR nets [7]. In contrast to the above explicit siphon generation approaches, a generic Mixed Integer Programming (MIP) formulation is presented in [11] for the detection of *maximal empty siphons* in *ordinary, structurally*

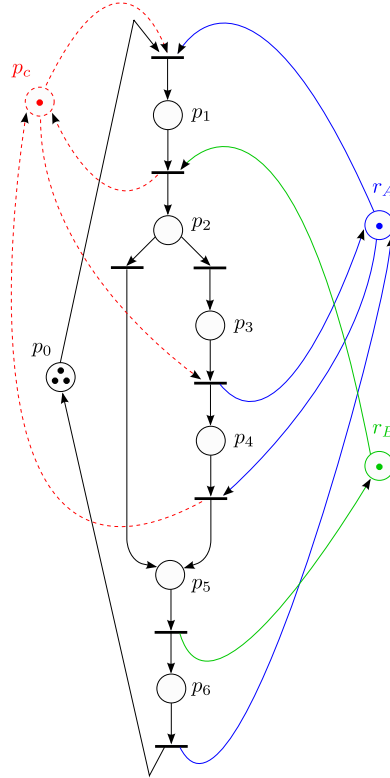


Figure 3.2: A deadlock example in BIND: Controlled Gadara net model

bounded Petri nets; we refer to this formulation as MIP-ES hereafter. Furthermore, MIP has also been employed to detect *maximal RIDM siphons* in general process-resource nets that are not necessarily ordinary [88]; we refer to this general MIP formulation stated on pp. 139-140 of [88] as MIP-RS hereafter.

From the development of Theorem III.1, we know that if a Gadara net is not live, then the net will eventually reach a so-called “total-deadlock modified-marking”, where all the transitions in the net are disabled. This result is formally stated as Corollary III.1 in Section 3.8.1 below. This corollary also provides us with an efficient methodology to verify the liveness of a Gadara net through mathematical programming formulations by detecting total-deadlock modified-markings. Similar in spirit to the aforementioned mathematical programming formulations, our formulations search for a total-deadlock modified-marking over the broader set of markings defined by the state equation of the net. Thus, any total-deadlock modified-marking

identified by these formulations might or might not be reachable in the actual net. More specifically, *if the proposed formulations do not have a solution, then the net is live*; otherwise, the net may or may not be live. A “byproduct” of these formulations is a RIDM siphon (or an empty siphon in the case of ordinary nets) that is constructed from the identified total-deadlock modified-marking through Corollary III.2 in Section 3.8.1 below. The constructed siphon can then be used for optimal control synthesis, as we do in [62, 61].¹

A more detailed description of the technical developments of this section is as follows. Exploiting the special properties of Gadara nets, we propose in Section 3.8.2, an efficient MIP formulation for liveness verification of \mathcal{N}_G . This MIP formulation is then generalized for liveness verification of $\mathcal{N}_{G_1}^c$ in Section 3.8.3. In Section 3.8.4, we propose another MIP formulation for liveness verification of \mathcal{N}_G^c . In the following discussion, we denote the above three formulations as MIP- \mathcal{N}_G , MIP- $\mathcal{N}_{G_1}^c$, and MIP- \mathcal{N}_G^c , respectively, which are self-explanatory from their names. The formulations MIP- \mathcal{N}_G and MIP- $\mathcal{N}_{G_1}^c$ customize the generic formulation MIP-ES; the formulation MIP- \mathcal{N}_G^c customizes the generic formulation MIP-RS. The development of the customized MIP formulations was motivated by the need of efficient control synthesis for large-scale concurrent software, and it exploits the special structure of Gadara net models of multithreaded programs. These customized formulations enhance the efficiency and scalability of liveness verification of Gadara nets, which is important for CMW-deadlock analysis of large-scale software. They are also employed in the optimal control synthesis of Gadara nets [62, 61]. In Section 3.8.5, we report experimental results that compare the performance of liveness verification of $\mathcal{N}_{G_1}^c$ using MIP- $\mathcal{N}_{G_1}^c$ with that of using MIP-ES; we also compare the performance of liveness verification of \mathcal{N}_G^c using MIP- \mathcal{N}_G^c with that of using MIP-RS. Although the formulations considered

¹It should also be noticed that, in the particular case that the identified RIDM siphon is actually unreachable, the monitor places resulting from the optimal synthesis do not compromise the maximal permissiveness of the synthesized control logic.

in our comparative study use different objective functions and produce, in general, different siphons, they all have the same implication for the purpose of liveness verification: a special property of the optimal solution or, in certain cases, the absence of such a solution itself, is a sufficient condition for the liveness of the Gadara net.

3.8.1 Key properties

We first present some properties of Gadara nets that are relevant to the development of the formulation of liveness verification. Based on Theorem III.1, we have the following results. Both Corollaries III.1 and III.2 follow from the “ \Leftarrow ” direction of the proof of Theorem III.1.

Corollary III.1. *If \mathcal{N}_G^c is not live, then \mathcal{N}_G^c will reach a modified marking $\overline{M} \in \overline{R}(\mathcal{N}_G^c, M_0^c)$ and $M \neq M_0^c$, such that \mathcal{N}_G^c is in a total-deadlock at the modified marking \overline{M} .*

Corollary III.2. *In \mathcal{N}_G^c , given a total-deadlock modified-marking $\overline{M} \in \overline{R}(\mathcal{N}_G^c, M_0^c)$ and $M \neq M_0^c$, let S be the set of disabling places at \overline{M} . Then, S is a RIDM siphon at \overline{M} .*

Given a total-deadlock modified-marking $\overline{M} \neq \overline{M}_0^c$, we can easily construct a RIDM siphon at \overline{M} using Corollary III.2. Note that the modified initial marking is always a total-deadlock modified-marking. But for liveness verification, we are interested in detecting a total-deadlock modified-marking that is different from the modified initial marking. Therefore, instead of repeating the above statement, we impose this qualification on any sought total-deadlock modified-marking considered in the rest of this section.

3.8.2 Verification of liveness of \mathcal{N}_G

Recall that a place p is said to be a disabling place at marking M if p disables at least one of its output transitions at M . Further, in an ordinary net, if a place

p is a disabling place at marking M , then we have $M(p) = 0$ and p disables *all* of its output transitions. By Definition III.8, we know that for any place $p \in P_0$, its modified marking $\overline{M}(p) = 0$. Moreover, from Definition II.6 and Proposition II.2, we know that \mathcal{N}_G is an ordinary net, and the modified marking of any place $p \in P_S \cup P_R$ is either 0 or 1. Therefore, in \mathcal{N}_G , the modified marking of a place p , $\overline{M}(p)$, can be used as a *binary indicator variable* associated with p , as described in the following remark.

Remark III.3. For any place $p \in P_0 \cup P_S \cup P_R$, we have: (i) $\overline{M}(p) = 0$ *iff* at \overline{M} , place p is a disabling place and p disables all of its output transitions; (ii) $\overline{M}(p) = 1$ *iff* at \overline{M} , place p is not a disabling place and p enables all of its output transitions. \square

According to Corollary III.1, if \mathcal{N}_G^c is not live, then we know *a priori* that the net will reach a total-deadlock at some modified marking \overline{M} . Moreover, once \overline{M} is reached, we know *a priori* from Corollary III.2 that there exists a RIDM siphon S at \overline{M} , which contains the set of all disabling places at \overline{M} . In particular, we know from Remark III.3 that in the case of \mathcal{N}_G , this RIDM siphon S is an empty siphon at \overline{M} .

The above discussion implies that we can verify the liveness of \mathcal{N}_G very efficiently, by detecting a total-deadlock modified-marking \overline{M} , i.e., a modified marking \overline{M} where all the net transitions are disabled. Based on the special structure of \mathcal{N}_G , any transition t in the net can be categorized into one of the following three types. (i) Transition t is an output transition of an idle place. We know that under the notion of modified marking, t is always disabled. (ii) Transition t has only one input place, and this input place is an operation place. For t to be disabled, its input place must be a disabling place. (iii) Transition t has more than one input place. For t to be disabled, at least one of its input places must be a disabling place.

Therefore, in order to detect a total-deadlock modified-marking \overline{M} , we need to enforce the above three types of transitions to be disabled at \overline{M} , which is addressed by Constraints (3.7)–(3.9) of the MIP formulation presented below. If \overline{M} is detected,

then we can use Corollary III.2 to construct an empty siphon, which will be used in optimal control synthesis; otherwise, we know that the net is live. In other words, the problem of liveness verification of \mathcal{N}_G can be mapped to the problem of finding a total-deadlock modified-marking in the modified reachability space of \mathcal{N}_G . The latter problem can be solved by the following MIP formulation, MIP- \mathcal{N}_G , which customizes the generic MIP-ES formulation presented in [11] for maximal empty siphon detection in structurally bounded ordinary nets.

$$\mathbf{MIP}\text{-}\mathcal{N}_G: \min \sum_{p \in P_S} \bar{M}(p) \quad (3.5)$$

$$s.t. M = M_0 + D\sigma \quad (3.6)$$

$$\bar{M}(p) = M(p), \forall p \in P_S \cup P_R; \bar{M}(p) = 0, \forall p \in P_0 \quad (3.7)$$

$$\bar{M}(p) = 0, \forall p \in Q, \text{ where} \quad (3.8)$$

$$Q = \{q \in P : (\exists t \in T), (\bullet t = \{q\}) \wedge (q \in P_S)\}$$

$$\sum_{p \in \bullet t} \bar{M}(p) - |\bullet t| + 1 \leq 0, \forall t \text{ s.t. } |\bullet t| > 1 \quad (3.9)$$

$$\sum_{p \in P_S} \bar{M}(p) \geq 2 \quad (3.10)$$

$$\sum_{p \in P_R} \bar{M}(p) \leq |P_R| - 2 \quad (3.11)$$

$$M \geq 0; \sigma \in \mathbb{Z}_0^+ \quad (3.12)$$

We explain the MIP- \mathcal{N}_G formulation presented in (3.5)–(3.12) as follows. In the objective function (3.5), we want to minimize the number of marked operation places in the detected total-deadlock modified-marking. The selection of such an objective function will produce siphons that are efficient for optimal control synthesis [62, 61]; the further details will be presented in Chapter V.

Constraint (3.6) is the state equation of the net, which is a necessary condition for the set of reachable markings. Constraint (3.7) connects an original marking with its

associated modified marking based on Definition III.8. From the above discussion, we want to verify liveness by finding a total-deadlock modified-marking \overline{M} . Constraints (3.7), (3.8), and (3.9) enforce that the three types of transitions, discussed above, are all disabled at \overline{M} . Constraint (3.10) follows from the fact that at least two threads must be involved in a CMW-deadlock. In the context of the Gadara net model, this implies that at least two operation places are marked in a CMW-deadlock. As a result, it follows from Constraint (3.10), and Conditions 6 and 7 of Definition II.6, that at least two resource places must be empty, and hence become disabling places in a CMW-deadlock; this leads to Constraint (3.11). Constraint (3.12) specifies the bounds of the variables.

The solution of $\text{MIP-}\mathcal{N}_G$, if it exists, is a total-deadlock modified-marking \overline{M} , based on which we can construct an empty siphon using Corollary III.2. The correctness of the MIP formulation follows as a result of Proposition II.2 and Corollary III.1, together with the preceding discussion. The number of variables and constraints used by $\text{MIP-}\mathcal{N}_G$ is $O(|P| + |T|)$; in particular, the formulation involves $2|P|$ non-negative real variables and $|T|$ non-negative integer variables.

3.8.3 Verification of liveness of $\mathcal{N}_{G_1}^c$

The class of Gadara nets $\mathcal{N}_{G_1}^c$ shares all the features of \mathcal{N}_G . The only difference between $\mathcal{N}_{G_1}^c$ and \mathcal{N}_G is that $\mathcal{N}_{G_1}^c$ has a set of monitor places P_C , whose initial markings may be greater than 1. Observing this difference, the $\text{MIP-}\mathcal{N}_G$ formulation presented in (3.5)–(3.12) in Section 3.8.2 can be immediately extended to liveness verification of $\mathcal{N}_{G_1}^c$. Although Remark III.3 remains true in $\mathcal{N}_{G_1}^c$ for any $p \in P_0 \cup P_S \cup P_R$, it generally does not hold for the modified markings of monitor places. Thus, we need to introduce a new constraint on the binary indicator variables associated with the monitor places. For the sake of simplicity, with a slight abuse of notation, we also use the notation $\overline{M}(p)$ to denote the *binary indicator variable* for any $p \in P_C$ in the

formulation $\text{MIP-}\mathcal{N}_{G_1}^c$ presented below. That is, $\overline{M}(p)$ is not necessarily the modified marking for any $p \in P_C$ in $\text{MIP-}\mathcal{N}_{G_1}^c$. $\overline{M}(p)$ is used as an indicator variable such that if p is not a disabling place at \overline{M} , then $\overline{M}(p) = 1$; otherwise, $\overline{M}(p) = 0$.

Define $SB(p)$ to be a *structural bound* of place p . In Gadara nets, we can set: $SB(p) = M_0^c(p)$, $\forall p \in P_0 \cup P_C$, and $SB(p) = 1$, $\forall p \in P_S \cup P_R$.

The liveness of $\mathcal{N}_{G_1}^c$ can be verified by detecting a total-deadlock modified-marking in the modified reachability space of $\mathcal{N}_{G_1}^c$, which can be solved by the following MIP formulation:

MIP- $\mathcal{N}_{G_1}^c$: In addition to the $\text{MIP-}\mathcal{N}_G$ formulation (3.5)–(3.12)², we also need Constraints (3.13) and (3.14) on $\overline{M}(p)$ for any $p \in P_C$.

$$\overline{M}(p) \in \{0, 1\}, \forall p \in P_C \quad (3.13)$$

$$M(p) \geq \overline{M}(p) \geq \frac{M(p)}{SB(p)}, \forall p \in P_C \quad (3.14)$$

Constraint (3.13) specifies that $\overline{M}(p)$ is a binary indicator variable associated with any $p \in P_C$. Constraint (3.14) characterizes the enabling/disabling feature of a monitor place $p \in P_C$ in terms of the binary indicator variable $\overline{M}(p)$. The intuition is explained as follows. Since $\mathcal{N}_{G_1}^c$ is an ordinary net, if a monitor place $p \in P_C$ is a disabling place at marking M , then $M(p) = 0$, which, together with Constraint (3.14), forces the corresponding $\overline{M}(p)$ to be 0. On the other hand, if a monitor place $p \in P_C$ in $\mathcal{N}_{G_1}^c$ is not a disabling place at marking M , then $M(p) \geq 1$, which, together with Constraints (3.13) and (3.14), forces the corresponding $\overline{M}(p)$ to be 1.

Remark III.4. A controlled Gadara net ($\mathcal{N}_{G_1}^c$ or \mathcal{N}_G^c) is obtained by augmenting an original Gadara net \mathcal{N}_G . Thus, Constraints (3.10) and (3.11) used in $\text{MIP-}\mathcal{N}_G$, which are derived based on the definition of \mathcal{N}_G , remain true in $\text{MIP-}\mathcal{N}_{G_1}^c$, presented above, and in $\text{MIP-}\mathcal{N}_G^c$, to be presented in the next section. \square

²Technically, the notation M_0 in (3.6) should be substituted by M_0^c .

Similarly to the case of \mathcal{N}_G , if $\mathcal{N}_{G_1}^c$ is not live, then the solution of MIP- $\mathcal{N}_{G_1}^c$ corresponds to a total-deadlock modified-marking, based on which we can construct an empty siphon using Corollary III.2. The number of variables and constraints used by MIP- $\mathcal{N}_{G_1}^c$ is $O(|P| + |T|)$; in particular, the formulation involves $2|P| - |P_C|$ non-negative real variables, $|P_C|$ binary variables, and $|T|$ non-negative integer variables.

3.8.4 Verification of liveness of \mathcal{N}_G^c

We know from Definition II.7 that \mathcal{N}_G^c is not necessarily ordinary. The potential non-ordinariness makes the liveness verification formulation for \mathcal{N}_G^c more complicated than those for \mathcal{N}_G and $\mathcal{N}_{G_1}^c$. In MIP- \mathcal{N}_G^c , we need to further introduce a new binary indicator variable, defined as follows.

Let $A(p, t)$ be an indicator variable associated with the directed arc from place p to transition t at \bar{M} . The dependency of $A(p, t)$ on \bar{M} is suppressed in the notation for the sake of simplicity. The value of $A(p, t)$ is defined as:

$$A(p, t) = \begin{cases} 1, & \text{if place } p \text{ enables transition } t \text{ at } \bar{M}; \\ 0, & \text{if place } p \text{ disables transition } t \text{ at } \bar{M}. \end{cases} \quad (3.15)$$

If $A(p, t) = 1$, then the arc (p, t) is said to be an *enabled arc*; otherwise, it is said to be a *disabled arc*. Note that the potential non-ordinariness in \mathcal{N}_G^c , which motivates the introduction of the indicator variable $A(p, t)$, can only be caused by the associated arcs of the monitor places. Therefore, we only need to introduce the indicator variable $A(p, t)$ for place-transition pairs (p, t) such that $p \in P_C$ and $t \in p\bullet$.

Similar to MIP- $\mathcal{N}_{G_1}^c$, we use $\bar{M}(p)$ as a binary indicator variable associated with $p \in P$ in the MIP- \mathcal{N}_G^c formulation. That is, if p is not a disabling place at \bar{M} , then $\bar{M}(p) = 1$; otherwise, $\bar{M}(p) = 0$. In the formulation, for any $p \in P_0 \cup P_S \cup P_R$, $\bar{M}(p)$ represents *both* the indicator variable associated with p and the modified marking of p (according to Remark III.3); for any $p \in P_C$, $\bar{M}(p)$ *only* represents the indicator

variable associated with p (a slight abuse of notation as discussed in Section 3.8.3).

The liveness of \mathcal{N}_G^c can also be verified by detecting a total-deadlock modified-marking in the modified reachability space of \mathcal{N}_G^c . This can be solved by the following MIP formulation, $\text{MIP-}\mathcal{N}_G^c$, which customizes the generic MIP-RS formulation presented in [88] for maximal RIDM siphon detection in general process-resource nets.

$$\text{MIP-}\mathcal{N}_G^c: \min \sum_{p \in P_S} \bar{M}(p) \quad (3.16)$$

$$\text{s.t. } M = M_0^c + D\sigma \quad (3.17)$$

$$\bar{M}(p) = M(p), \forall p \in P_S \cup P_R; \bar{M}(p) = 0, \forall p \in P_0 \quad (3.18)$$

$$\bar{M}(p) = 0, \forall p \in Q, \text{ where} \quad (3.19)$$

$$Q = \{q \in P : (\exists t \in T), (\bullet t = \{q\}) \wedge (q \in P_S)\}$$

$$\sum_{p \in \bullet t \cap P_C} A(p, t) + \sum_{p \in \bullet t \cap (P \setminus P_C)} \bar{M}(p) - |\bullet t| + 1 \leq 0, \quad (3.20)$$

$$\forall t \text{ s.t. } |\bullet t| > 1$$

$$A(p, t) \geq \frac{M(p) - W(p, t) + 1}{SB(p)}, \quad (3.21)$$

$$\forall W(p, t) > 0 \text{ s.t. } p \in P_C$$

$$A(p, t) \geq \bar{M}(p), \forall W(p, t) > 0 \text{ s.t. } p \in P_C \quad (3.22)$$

$$\sum_{t \in p\bullet} A(p, t) - |p\bullet| + 1 \leq \bar{M}(p), \forall p \in P_C \quad (3.23)$$

$$\sum_{p \in P_S} \bar{M}(p) \geq 2 \quad (3.24)$$

$$\sum_{p \in P_R} \bar{M}(p) \leq |P_R| - 2 \quad (3.25)$$

$$M \geq 0; \sigma \in \mathbb{Z}_0^+; \bar{M}(p) \in \{0, 1\}, \forall p \in P_C; \quad (3.26)$$

$$A(p, t) \in \{0, 1\}, \forall p \in P_C, \forall t \in p\bullet$$

We explain the MIP- \mathcal{N}_G^c formulation presented in (3.16)–(3.26) as follows. The objective function (3.16) and Constraints (3.17)–(3.19), (3.24), and (3.25) are the same as their counterparts in MIP- \mathcal{N}_G and MIP- $\mathcal{N}_{G_1}^c$. Similar to MIP- \mathcal{N}_G and MIP- $\mathcal{N}_{G_1}^c$, the MIP- \mathcal{N}_G^c formulation aims to verify the liveness of \mathcal{N}_G^c by detecting a total-deadlock modified-marking \overline{M} . Constraint (3.19) enforces that the set of transitions, which have only one input place, must be disabled. Moreover, for the set of transitions that have more than one input place, Constraint (3.20) enforces that at least one input place must be a disabling place. On the other hand, Constraint (3.21)³ ensures that the value of $A(p, t)$, which is associated with an enabled arc (p, t) with $p \in P_C$, must be 1. Hence, all variables $A(p, t)$ that are forced to zero by Constraint (3.20) are indeed variables that correspond to disabled arcs. Constraint (3.22) recognizes any monitor place, which disables at least one of its outgoing arcs and hence is a disabling place. Constraint (3.23) recognizes any monitor place, which enables all of its outgoing arcs and hence is not a disabling place. Constraint (3.26) specifies the bounds of the variables.

If \mathcal{N}_G^c is not live, then the solution of MIP- \mathcal{N}_G^c corresponds to a total-deadlock modified-marking, based on which we can construct a RIDM siphon using Corollary III.2. Compared to MIP- \mathcal{N}_G and MIP- $\mathcal{N}_{G_1}^c$, the additional complexity in MIP- \mathcal{N}_G^c arises from the variables and constraints associated with the arcs (p, t) , where $p \in P_C$. The number of variables and constraints used by MIP- \mathcal{N}_G^c is $O(|P| + |T| + |P_C||T|)$ in the worst case. In practice, we observe that $|P_C| \ll |P|$ in controlled Gadara net models of real-world software.

³Constraint (3.21) does not completely characterize the correct pricing of $A(p, t)$ for all arcs. But what we need for liveness verification (and RIDM siphon construction) is the correct pricing of $\overline{M}(p)$, which is guaranteed by the nature and role of the objective function (3.16).

3.8.5 Experimental results

In this section, we report the experimental results from a comparative analysis between the performance of the customized algorithms MIP- $\mathcal{N}_{G_1}^c$ and MIP- \mathcal{N}_G^c with that of the generic siphon detection algorithms MIP-ES and MIP-RS, respectively, for liveness verification of Gadara nets. The experiments were completed on a Mac OS X laptop with a 2.4 GHz Intel Core2Duo processor and 2 GB of RAM. The mathematical programming formulations are solved using Gurobi 3.0.1 [30].

We first compare the performance of MIP- $\mathcal{N}_{G_1}^c$ with that of MIP-ES presented in [11]. Random Gadara nets for these experiments are generated by a random-walk-style algorithm. At each step, the program randomly decides either to grab a lock or to release one already held; the number of steps is specified as an input parameter. Additional logic is applied to ensure valid behavior. The random Gadara net generator (available at <http://gadara.eecs.umich.edu/software.html>) is based on our experience in modeling real concurrent programs [103]. Furthermore, we apply the optimal control techniques proposed in [60, 59] to synthesize control logic for these random Gadara nets. Monitor places are added to the original Gadara nets by running a random number of control iterations for each net.⁴ The resulting controlled Gadara nets, which belong to the class $\mathcal{N}_{G_1}^c$, are input to MIP- $\mathcal{N}_{G_1}^c$ and MIP-ES, for the purpose of liveness verification. Their execution times on these nets are recorded as sample data.

Figure 3.3(a) shows the sample statistics of the execution times of the two algorithms, where the y -axis is on a log scale. We group the samples according to the pair of parameters (a, s) that is used in generating the random Gadara nets, where a is the number of resource acquisitions per subnet, and s is the number of process subnets in the Gadara net. The x -axis of the figure shows the nine different

⁴For a given Gadara net, if the iterative control technique converges before the pre-selected random number of iterations are completed, we output the converged net and disregard the remaining iterations.

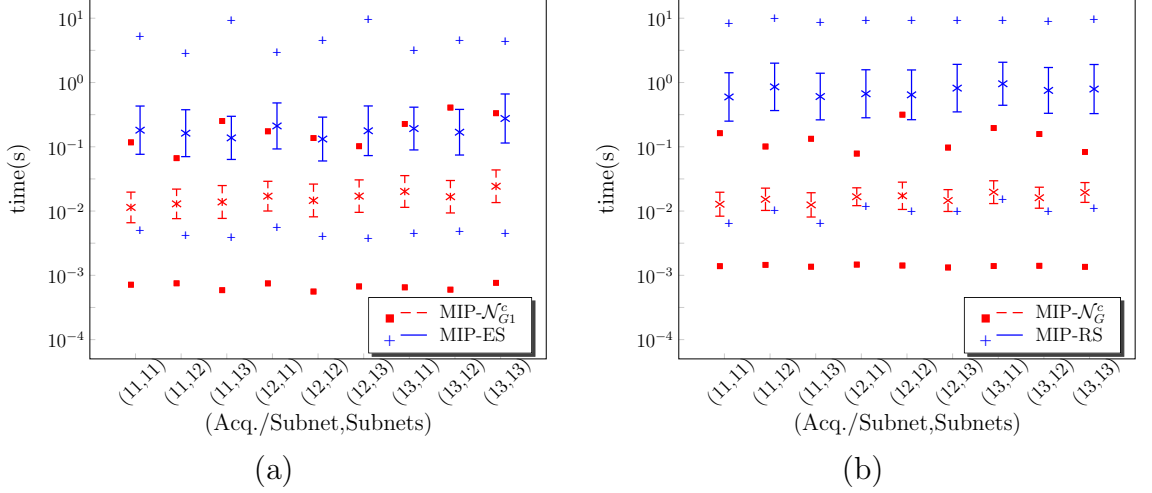


Figure 3.3: Sample statistics: (a) MIP- $\mathcal{N}_{G_1}^c$ vs. MIP-ES; (b) MIP- \mathcal{N}_G^c vs. MIP-RS

groups we studied. The number of monitor places is suppressed, because it varies within a group. We report the average number of monitor places for each group in Table 3.1. In Figure 3.3, the crosses represent the means, the segments represent the half-standard-deviation confidence intervals, and the solid squares and plus signs represent the maxima or minima.⁵

Next, we analyze the performance of the two algorithms using the Normalized Cumulative Frequency (NCF), which is defined as follows.

$$NCF(x) = \frac{\sum_{i=1}^n J_i(x)}{n} \quad (3.27)$$

where n is the sample size of a group, and $J_i(x)$ is an indicator variable associated with the i -th sample and is a function of x ($x \geq 0$), such that

$$J_i(x) = \begin{cases} 1, & \text{if the value of the } i\text{-th sample} \leq x; \\ 0, & \text{otherwise.} \end{cases} \quad (3.28)$$

The NCFs of our experiments on MIP- $\mathcal{N}_{G_1}^c$ and MIP-ES are shown in Figure 3.4(a),

⁵Sample statistics are based on log-scale data.

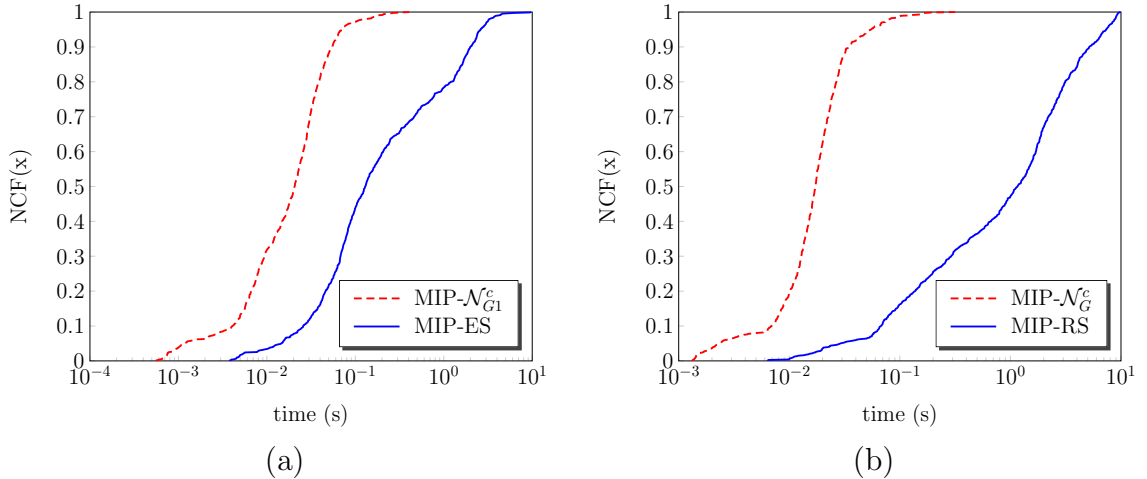


Figure 3.4: Normalized Cumulative Frequency (NCF): (a) MIP- \mathcal{N}_{G1}^c vs. MIP-ES; (b) MIP- \mathcal{N}_G^c vs. MIP-RS

where the x -axis is on a log scale.

We also compare the performance of MIP- \mathcal{N}_G^c with that of MIP-RS presented in [88]. In this case, we apply the Empty-Siphon-Based Control Algorithm, described in Section IV-A.1 of [59], to the Gadara nets, and choose the controlled Gadara nets that are non-ordinary and belong to the class of \mathcal{N}_G^c . These nets are input to the two algorithms, for the purpose of liveness verification. Similarly, the sample statistics are shown in Figure 3.3(b) and the NCFs are shown in Figure 3.4(b).

From the above analysis, we observe in Figure 3.3 that the proposed customized algorithms are more efficient for liveness verification of Gadara nets than the generic siphon detection algorithms in all the nine groups in terms of means, standard deviations, and ranges. From Figure 3.4, we find that for MIP- \mathcal{N}_{G1}^c , 98% of the samples are smaller than 0.1 second, while for MIP-ES, only 40% of the samples are; further, for MIP- \mathcal{N}_G^c , 99% of the samples are smaller than 0.1 second, while for MIP-RS, only 15% of the samples are.

Table 3.1 presents a summary of the experimental results. For each set of parameters (each row in the table), over 100 samples of random Gadara nets are generated. Consider the comparison between the performance of MIP- \mathcal{N}_{G1}^c and that

of MIP-ES. We set a time-out threshold of 10 seconds. A net times out if its liveness cannot be determined by either MIP- $\mathcal{N}_{G_1}^c$ or MIP-ES in less than 10 seconds. The proportion of sample nets that timed out is reported in the last column (TLE) of the table. All the other statistical data in this table are calculated over only sample nets where both MIP- $\mathcal{N}_{G_1}^c$ and MIP-ES did not time out. The comparison between the performance of MIP- \mathcal{N}_G^c and that of MIP-RS is carried out in a similar way. The first column lists the four algorithms under consideration. The second (a) and third (s) columns are the number of resource acquisitions per subnet and the number of process subnets, which are input parameters to the random program generator. In generating the random nets, the number of resources (locks) in the original Gadara net is set to be 12, and the probability of acquiring a new resource before releasing one already held is 0.5. The fourth (P), fifth (T), and sixth (C) columns correspond to the average number of places, transitions, and monitor places in the sample Gadara nets. The seventh (SS) and eighth (US) columns describe the state space complexity, i.e., the average numbers of safe and unsafe states that are reachable in the nets. Note that the solution of the mathematical programming formulations does *not* require the construction of the state space; the numbers of safe and unsafe states were generated separately for the sake of scalability assessment. The last column (TLE) is the proportion of sample nets that did time out.

From Table 3.1, we see that the proposed customized algorithms seldom timed out, while the generic algorithms timed out more often. Moreover, for the nets where the proposed customized algorithms timed out, the generic algorithms also timed out. Since MIP- $\mathcal{N}_{G_1}^c$ and MIP- \mathcal{N}_G^c were formulated to exploit the structural properties of Gadara nets, it is not surprising that they outperform MIP-ES and MIP-RS, respectively. What is encouraging is that the results in Figs. 3.3 and 3.4 and in Table 3.1 demonstrate that MIP- $\mathcal{N}_{G_1}^c$ and MIP- \mathcal{N}_G^c are scalable to large nets, which make them attractive for analyzing CMW-deadlock-freeness in large software

programs.

Table 3.1: Experimental results of comparative analysis on liveness verification algorithms

Method	a	s	P	T	C	SS	US	TLE
MIP- $\mathcal{N}_{G_1}^c$	11	11	87.25	68.65	7.12	230581	91889	0.01
MIP-ES								0.06
MIP- \mathcal{N}_G^c			85.86	66.55	7.88	218741	85157	0.00
MIP-RS								0.22
MIP- $\mathcal{N}_{G_1}^c$	11	12	94.84	76.08	7.15	496055	221560	0.01
MIP-ES								0.11
MIP- \mathcal{N}_G^c			93.66	73.64	8.46	444871	202773	0.00
MIP-RS								0.19
MIP- $\mathcal{N}_{G_1}^c$	11	13	101.34	82.02	7.62	614988	235364	0.01
MIP-ES								0.10
MIP- \mathcal{N}_G^c			99.61	79.68	8.26	653032	274092	0.00
MIP-RS								0.24
MIP- $\mathcal{N}_{G_1}^c$	12	11	89.63	71.52	6.64	291166	104067	0.01
MIP-ES								0.06
MIP- \mathcal{N}_G^c			87.45	68.48	7.51	286145	125343	0.00
MIP-RS								0.16
MIP- $\mathcal{N}_{G_1}^c$	12	12	96.01	77.58	6.87	523258	203359	0.01
MIP-ES								0.10
MIP- \mathcal{N}_G^c			95.06	75.64	7.81	535029	241084	0.00
MIP-RS								0.18
MIP- $\mathcal{N}_{G_1}^c$	12	13	103.89	84.79	7.49	862689	324566	0.01
MIP-ES								0.06
MIP- \mathcal{N}_G^c			103.14	83.05	8.41	745614	310375	0.00
MIP-RS								0.18
MIP- $\mathcal{N}_{G_1}^c$	13	11	93.09	73.84	7.71	254733	101207	0.01
MIP-ES								0.13
MIP- \mathcal{N}_G^c			91.24	71.50	8.26	235609	95000	0.00
MIP-RS								0.22
MIP- $\mathcal{N}_{G_1}^c$	13	12	98.50	79.62	7.28	394573	155436	0.02
MIP-ES								0.08
MIP- \mathcal{N}_G^c			97.25	77.62	8.06	398204	160820	0.00
MIP-RS								0.18
MIP- $\mathcal{N}_{G_1}^c$	13	13	105.34	85.62	7.99	716595	314641	0.01
MIP-ES								0.04
MIP- \mathcal{N}_G^c			104.28	83.66	8.87	703018	298153	0.00
MIP-RS								0.17

3.9 Case study: A deadlock bug in the Linux kernel

In addition to BIND, whose deadlock bug is used as a running example in our discussion, we have used our model-based approach to perform deadlock analysis of several open-source programs so far in the Gadara project [108, 104, 105]. These

case studies demonstrate the benefits of a formal, model-based approach in providing an accurate and compact characterization of a deadlock scenario and in enabling systematic deadlock analysis using the techniques we presented.

In this section, we discuss in detail a deadlock bug in version 2.5.62 of the Linux kernel that is captured in its Gadara net model. The deadlock example is inspired by the study conducted in [18]. Figure 3.5 shows this deadlock example. We annotated the lines of code that are related to lock allocations and releases. Each annotation explains the specifics of the corresponding line of code using four components: lock/unlock action, file name, function name, and line number in the code. The deadlock involves three threads and three locks. Further, Thread 1 involves a six-level call chain, and Thread 2 calls two functions. We have inlined the chains of function calls and simplified the control flows, so that only the code that is relevant to the deadlock is presented in Figure 3.5.

The Gadara net model of the considered lines of code is shown in Figure 3.6. Analysis of this model using the techniques presented in this chapter reveals two total-deadlock markings that are reachable from the initial marking as depicted in the figure: (i) The first total-deadlock marking is M_1 , where there is one token in p_{12} , one in p_{22} , and one in p_{33} , while all other places are empty. At marking M_1 , all three threads are involved in the deadlock. (ii) The second total-deadlock marking is M_2 , where there is one token in p_{14} , one in p_{22} , and one in p_{03} , while all other places are empty. At marking M_2 , only Threads 1 and 2 are involved in the deadlock. As we can see, the original deadlock bug in the program, which involves chains of function calls and complicated branchings, is clearly captured in this Gadara net model, which lays the groundwork for formal deadlock analysis.

```

/** Thread 1 */
spin_lock(&im->lock);          /* LOCK(A), igmp.c, igmp_timer_expire(), 268 */
...
if (!fl.fl4_src){
    ...
    read_lock(&inetdev_lock);  /* LOCK(B), devinet.c, inet_select_addr(), 786 */

    for (...){
        ...
        read_lock(&in_dev->lock); /* LOCK(C), devinet.c, inet_select_addr(), 791 */
        ...
        if (...){
            read_unlock(&in_dev->lock); /* UNLOCK(C), devinet.c, inet_select_addr(), 795 */
            ...
            break;
        }
        ...
        read_unlock(&in_dev->lock); /* UNLOCK(C), devinet.c, inet_select_addr(), 800 */
    }
    ...
    read_unlock(&inetdev_lock); /* UNLOCK(B), devinet.c, inet_select_addr(), 803 */
    ...
}
...
spin_unlock(&im->lock);        /* UNLOCK(A), igmp.c, igmp_timer_expire(), 289 */

/** Thread 2 */
read_lock(&in_dev->lock);      /* LOCK(C), igmp.c, igmp_heard_query(), 338 */
for (...){
    ...
    spin_lock_bh(&im->lock);    /* LOCK(A), igmp.c, igmp_mod_timer(), 165 */
    ...
    spin_unlock_bh(&im->lock); /* UNLOCK(A), igmp.c, igmp_mod_timer(), 171 & 177 */
}
read_unlock(&in_dev->lock);    /* UNLOCK(C), igmp.c, igmp_heard_query(), 346 */

/** Thread 3 */
read_lock(&inetdev_lock);      /* LOCK(B), devinet.c, inet_select_addr(), 759 */
...
if (!in_dev){
    read_unlock(&inetdev_lock); /* UNLOCK(B), devinet.c, inet_select_addr(), 808 */
    return addr;
}
read_lock(&in_dev->lock);      /* LOCK(C), devinet.c, inet_select_addr(), 764 */
...
read_unlock(&in_dev->lock);    /* UNLOCK(C), devinet.c, inet_select_addr(), 775 */
read_unlock(&inetdev_lock);    /* UNLOCK(B), devinet.c, inet_select_addr(), 776 */

```

Figure 3.5: A deadlock example in the Linux kernel: Simplified code

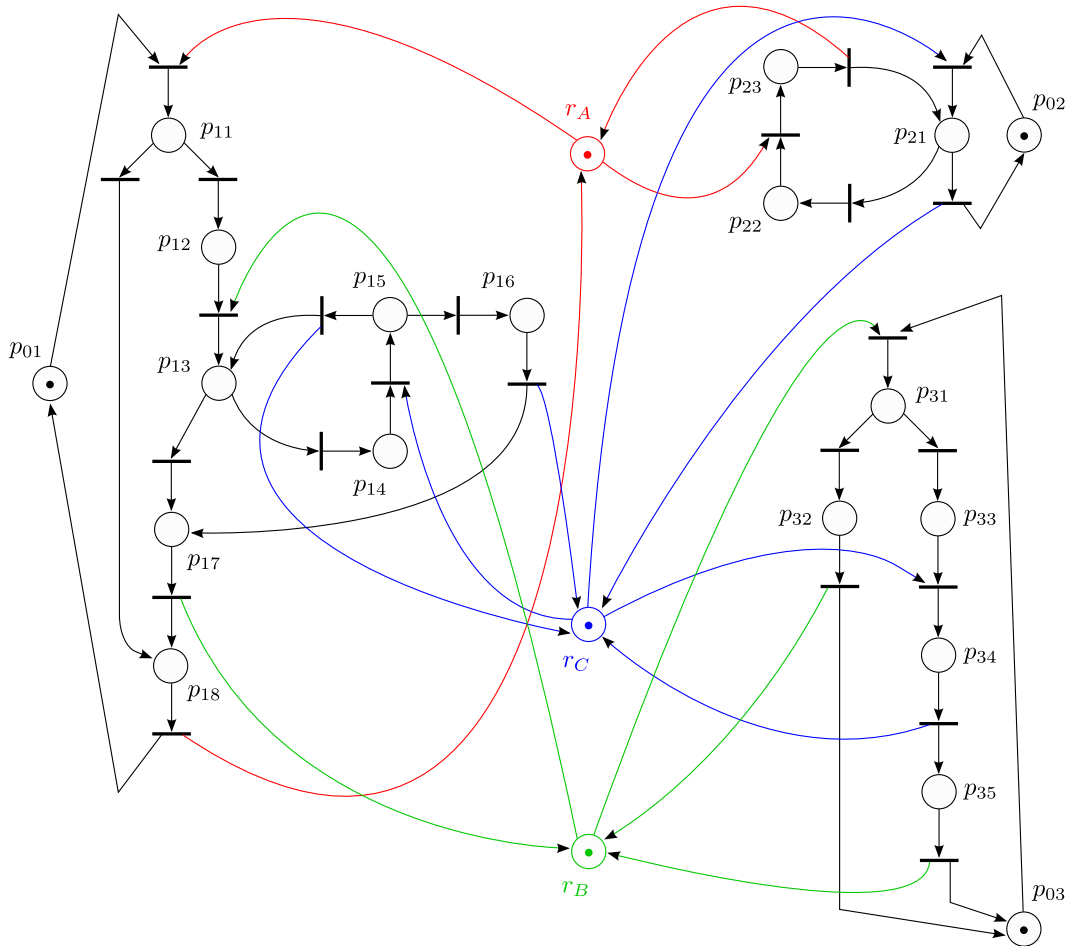


Figure 3.6: A deadlock example in the Linux kernel: Gadara net model

CHAPTER IV

Control I: Optimal Control of Gadara Nets – General Theory

4.1 Introduction

In Chapter III, we formally established that a multithreaded program that can be modeled as a Gadara net is CMW-deadlock-free if and only if its associated Gadara net is *live* (cf. Proposition III.1 and Theorem III.3). This correspondence motivates our study of *liveness-enforcing* control of Gadara nets. In addition to liveness, another important property desired in control synthesis is *maximal permissiveness*, so that the control logic will provably eliminate deadlocks while otherwise minimally constraining program behavior. Therefore, the main focus of this chapter is on the synthesis of *maximally-permissive liveness-enforcing (MPLE)* control policies for Gadara nets.

By definition, an original Gadara net model of a concurrent program is ordinary (i.e., all its arc weights are equal to one), while a controlled Gadara net may no longer be ordinary due to the structure (new *monitor* places and arcs) added as a result of a control synthesis step. Such a step can be carried out prior to the type of control synthesis presented in this chapter. In this step, users may enforce properties other than liveness on the net, or they may attempt to enforce liveness by using other methods. In either case, ordinariness of the resulting Gadara net is not guaranteed

in general. This motivates our development of an MPLE control synthesis strategy for the *general* class of non-ordinary controlled Gadara nets that may arise from various applications. An MPLE control policy is often called an optimal liveness-enforcing control policy [54], or simply an *optimal* control policy. We employ the same terminology in this dissertation.

This chapter is organized as follows. We first present the problem statement and motivation in Section 4.2. Then we overview the proposed iterative control methodology in Section 4.3. The UCCOR Algorithm is an important component of this methodology. The fundamentals of UCCOR are introduced in Section 4.4, and the development of UCCOR is presented in Section 4.5. In Section 4.6, we formally prove a set of important properties of the proposed control synthesis algorithms. We discuss the related approaches in Section 4.7. Some of the results in this chapter also appear in [60, 59].

4.2 Problem statement and motivation

Since \mathcal{N}_G^c represents the most general subclass of Gadara nets, we will focus on optimal control synthesis for \mathcal{N}_G^c in this chapter; the derived results can also be applied to \mathcal{N}_G and \mathcal{N}_{G1}^c . We formally state our problem as follows.

Problem statement: Given a controlled Gadara net, find a monitor-based control policy such that the resulting controlled Gadara net is admissible, live, and maximally permissive with respect to the goal of liveness enforcement.

Remark IV.1. We briefly discuss the existence of a solution to the aforementioned problem. From the viewpoint of an automaton model, if we construct the reachability graph (i.e., an automaton model) of a Gadara net and only mark its initial state, then the coaccessible part of this automaton [8] will not be empty. This is because a single instance from any given process subnet can always execute to completion, in isolation. On the other hand, according to Theorem III.3, if a Gadara net can always return to

its initial marking, then it is live. Therefore, the simple control policy that executes all threads sequentially is necessarily live, thereby proving that a liveness-enforcing control policy always exists. This control policy is also admissible because it can be realized by connecting an outgoing arc of a monitor place, with one initial token, to the first lock acquisition transition of each process subnet (which is not an uncontrollable transition by Assumption II.2), and returning this token to the monitor place only at the last transition of each process subnet. Further, in Section 3.7 we have shown that a *maximally permissive* control policy using monitor places always exists in Gadara nets. \square

In this chapter, we present a new MPLE control synthesis methodology, called the *ICOG Methodology*, for general controlled Gadara nets that need not be ordinary. According to Theorem III.1, the proposed methodology exploits the structural properties of Gadara nets and enforces liveness by preventing RIDM siphons from being reachable.

We will use a running example, as shown in Figure 4.1, to facilitate our discussion. The net structure shown in solid lines is the original Gadara net before control; the net structure shown in dashed lines represents the monitor places that are synthesized using the algorithms to be presented next. For the sake of discussion, we denote the original Gadara net in solid lines as \mathcal{N}_G . We define three controlled Gadara nets of interest: (i) $\mathcal{N}_G^{c(1)}$ consists of \mathcal{N}_G and p_{c1} ; (ii) $\mathcal{N}_G^{c(2)}$ consists of \mathcal{N}_G , p_{c1} , and p_{c2} ; and (iii) $\mathcal{N}_G^{c(3)}$ consists of \mathcal{N}_G , p_{c1} , p_{c2} , and p_{c3} .

We briefly discuss the motivation of our investigation of the MPLE control of \mathcal{N}_G^c as follows.

A non-ordinary \mathcal{N}_G^c can arise from various reasons in applications. For example, a non-ordinary Gadara net may be the result of enforcing other properties on multithreaded programs, like *atomicity* [42], prior to the control synthesis presented in this chapter, where more general types of specifications expressible as linear

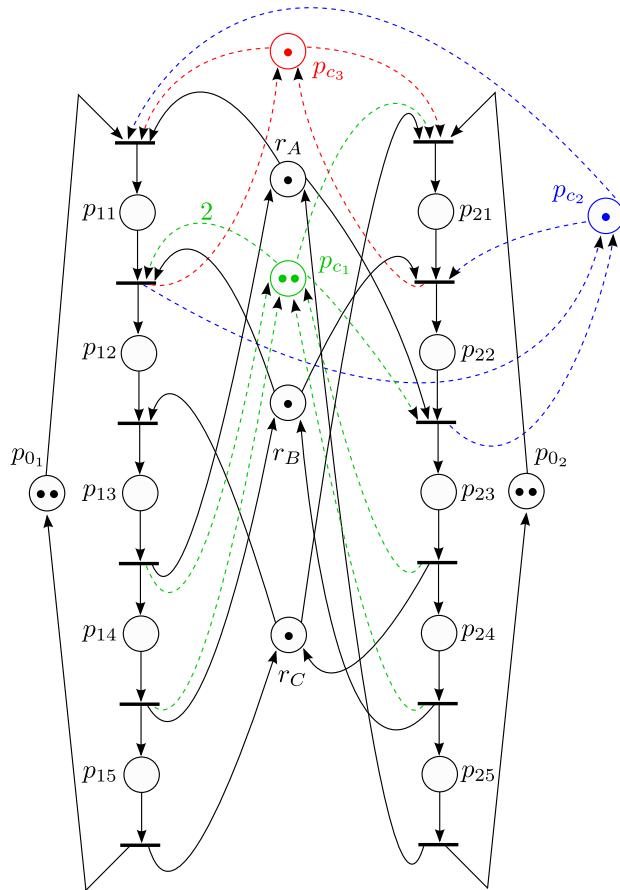


Figure 4.1: A running example of control synthesis using ICOG

inequalities may be enforced upon the net. In general, the enforcement of such linear inequalities (e.g., by the SBPI technique) may result in monitor places that have non-unit arc weights.

Example IV.1. Consider the running example as shown in Figure 4.1. The original Gadara net, denoted as \mathcal{N}_G , is shown in solid lines. Prior to ICOG, the following specification¹ was enforced upon \mathcal{N}_G by using SBPI:

$$r_A + r_B + r_C + p_{11} + p_{13} + p_{14} + p_{15} + p_{22} + p_{23} + p_{24} + p_{25} \geq 1 \quad (4.1)$$

The synthesized monitor place is denoted as p_{c1} and shown in dashed lines. The resulting net, which consists of \mathcal{N}_G , p_{c1} , and its associated arcs, is a controlled Gadara net, denoted as $\mathcal{N}_G^{c(1)}$. Note that $\mathcal{N}_G^{c(1)}$ is non-ordinary, due to the introduction of p_{c1} . Therefore, to fully resolve liveness enforcement in a maximally permissive manner for $\mathcal{N}_G^{c(1)}$, a general MPLE control synthesis methodology that works for non-ordinary Gadara nets is required. \square

4.3 Overall strategy: Iterative control of Gadara nets

We propose an Iterative Control Of Gadara nets (ICOG) Methodology, with a net in the class of \mathcal{N}_G^c as the initial condition. The flowchart of ICOG is shown in Figure 4.2. Given a controlled Gadara net, we first see if there is any new RIDM siphon under the modified markings of the net. If no RIDM siphon is detected, then, according to Theorem III.1, the net is live and ICOG terminates. Otherwise, we synthesize control logic to prevent the detected RIDM siphon from becoming reachable, by using an algorithm, called UCCOR, to be presented next. The UCCOR algorithm outputs a set of monitor places, which are added to the net. After UCCOR,

¹The set of places involved in the left-hand-side of (4.1) consists of a maximal empty siphon, obtained from the siphon detection algorithm presented in [11]. The rationale of (4.1) was to attempt to address liveness enforcement by preventing this maximal empty siphon from being reachable.

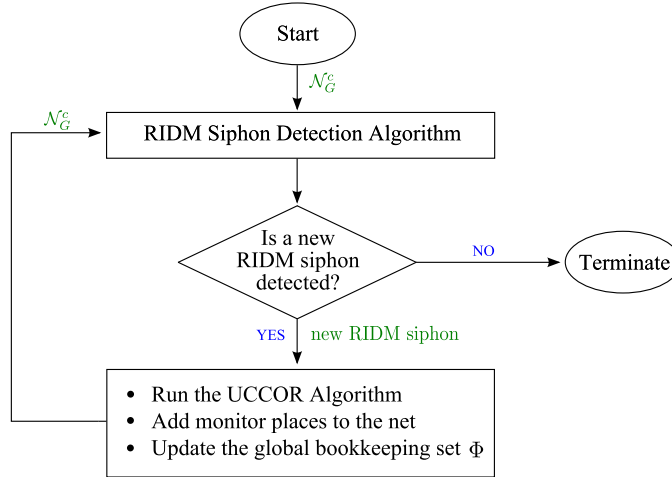


Figure 4.2: Iterative control of Gadara nets (ICOG)

we go back to the first step of ICOG and determine if there are any remaining or *new* RIDM siphons. One important feature of the proposed ICOG is that we maintain a “global bookkeeping set”, denoted by Φ , throughout the iterations. The set Φ records all the control syntheses that have been carried out in terms of prevented unsafe coverings, which will be introduced shortly.

ICOG is an iterative process in general, because there may be some siphons that have not been identified in the previous iterations and need further consideration. Moreover, we explained above that the added monitor place can be considered as a generalized resource place, and may introduce new potential deadlocks.

Note that the ICOG Methodology is fully modular so that the detection of RIDM siphons is not associated with any specific algorithm. This can be done, for instance, by using an MIP based approach that finds a maximal RIDM siphon in the net [88]. In the case of an ordinary net, the MIP technique has also been employed to detect a maximal empty siphon in the net [11]. We have developed a set of customized and efficient MIP formulations for RIDM siphon detection in general Gadara nets and empty siphon detection in ordinary Gadara nets [61, 64]. Moreover, siphons can also be detected via structural analysis; a recent result on siphon detection in S^4PR nets using graph theory is presented in [7].

We emphasize that the RIDM siphon detection is carried out under the *modified markings*, due to Theorem III.1. The detected RIDM siphon, say S , will be characterized by the set of places S , and an associated partial modified marking on S .

4.4 Fundamentals of the UCCOR Algorithm

We propose a new algorithm, used as a module of ICOG, for preventing RIDM siphons in \mathcal{N}_G^c . We call it the *UCCOR Algorithm*, where UCCOR is short for “Unsafe-Covering-based Control Of RIDM siphons”. (The notion of unsafe covering induced by a RIDM siphon will be introduced in Section 4.4.2.)

4.4.1 Definitions and partial-marking analysis

As revealed by Properties III.1 and III.2, there is a one-to-one mapping among the original marking, modified marking, and P_S -marking. Thus, in the UCCOR Algorithm, when synthesizing linear inequality specifications for monitor-based control, we can focus our attention on $\overline{\overline{M}}$ only, and the coefficients in linear inequalities corresponding to places P_0 , P_R and P_C are all zero, i.e., they are “don’t care” terms in the linear inequalities. We observe that Conditions 5, 6, and 7 of Definition II.6 imply that $\overline{\overline{M}}$ is always a *binary* vector. It is this property that motivates us to focus on $\overline{\overline{M}}$.

Through the UCCOR Algorithm, essentially we want to synthesize control logic that can prevent the net from reaching any unsafe marking with respect to RIDM siphons. The next definition concretizes this concept.

Definition IV.1. A marking M is said to be a *RIDM-unsafe marking* if there exists at least one RIDM siphon at the corresponding modified marking $\overline{\overline{M}}$. Given a siphon S , a marking M is said to be a RIDM-unsafe marking *with respect to S* , if S is a RIDM siphon at marking $\overline{\overline{M}}$.

From Definition IV.1 and Theorem III.1, we immediately have:

Corollary IV.1. \mathcal{N}_G^c is live iff it cannot reach a marking that is a RIDM-unsafe marking.

Example IV.2. Let us refer to the controlled Gadara net $\mathcal{N}_G^{c(1)}$ in Figure 4.1, and consider the following two markings (for the sake of simplicity, we only specify the marked places; the unspecified places are empty by default): (i) M_{u1} , where p_{01} , p_{02} , p_{11} , and p_{22} each have one token, and (ii) M_{u2} , where p_{01} , p_{02} , p_{11} , and p_{21} each have one token. In this example, the marking M_{u1} is RIDM-unsafe; the marking M_{u2} is not RIDM-unsafe, but starting from M_{u2} , the net cannot go back to the initial marking and can only go to a RIDM-unsafe marking. Therefore, both M_{u1} and M_{u2} should be prevented by control synthesis.

As we will see in the following discussion, the latter type of markings (such as M_{u2} in this example) will be eventually exposed as RIDM-unsafe markings as the iterations evolve. Thus, in the rest of this chapter, we can focus our attention on RIDM-unsafe markings. \square

From the above discussion, for any given RIDM-unsafe marking M_u , it is the *partial modified marking* $\overline{M}_u(S)$ on the RIDM siphon S that is critical to the lack of safety. Here, $\overline{M}_u(S)$ is a column vector with $|S|$ entries corresponding to the places in S , and the subscript “ u ” denotes “RIDM-unsafe”. In other words, if we know that S is a RIDM siphon, and an associated partial modified marking is $\overline{M}_u(S)$, then *any* (full) marking M , such that $\overline{M}(S) = \overline{M}_u(S)$, must also be a RIDM-unsafe marking with respect to S . This leads to the following result.

Proposition IV.1. *Given a RIDM siphon S , and an associated partial modified marking $\overline{M}_u(S)$, any marking M such that $\overline{M}(S) = \overline{M}_u(S)$, is RIDM-unsafe with respect to S .*

Thus, in the control synthesis, we want to prevent *any* marking M such that

$\overline{M}(S) = \overline{M}_u(S)$. This is achieved by considering RIDM-unsafe *partial* markings in a way that each synthesized monitor place can prevent more than one RIDM-unsafe marking. As we mentioned, the control will be implemented on P_S -markings. From Proposition IV.1, we observe that the partial modified marking $\overline{M}_u(S)$ is sufficient to characterize the corresponding RIDM-unsafe markings with respect to S . However, this is not true for partial P_S -marking $\overline{\overline{M}}_u(S)$. Consider the siphon $S = \{p_{c_1}, p_{c_2}, p_{12}, p_{13}, p_{22}, p_{23}\}$ in Figure 3.1 that we discussed earlier. Since S is a RIDM siphon, in this case we know that the current marking of the net, say M , is RIDM-unsafe with respect to S . On the other hand, Figure 4.6 (without considering the dashed lines) shows the same net under its initial marking M_0 . M_0 is not RIDM-unsafe by assumption.² But, we observe that $\overline{\overline{M}}(S) = \overline{\overline{M}}_0(S)$. This is because from the partial P_S -marking $\overline{\overline{M}}_u(S)$, one cannot tell the “status” of the resources (namely, tokens) in $S \cap (P_R \cup P_C)$. Intuitively, we want to consider more places under the partial P_S -marking. This deficiency can be made up by further considering the partial P_S -marking on the supports of minimal semiflows associated with $S \cap (P_R \cup P_C)$, which are introduced as follows.

As we introduced in Section 2.3, the minimal-support P-semiflow for any generalized resource place is a well-defined concept in Petri nets. This concept can be extended for any resource-induced siphon; for the sake of discussion, we introduce the notation, $\|\tilde{Y}_S\|$, as follows:

$$\|\tilde{Y}_S\| = \bigcup_{p \in S \cap (P_R \cup P_C)} \|Y_p\|$$

where, Y_p is the minimal-support P-semiflow of p .

Property IV.1. *For any resource-induced siphon S , the corresponding $\|\tilde{Y}_S\|$ is unique.*

²More specifically, this statement is true since no place in $P_R \cup P_C$ can be a disabling place at M_0 .

Based on Properties II.1 and II.2, starting from a partial P_S -marking on $\|\tilde{Y}_S\|$, one can uniquely recover the tokens in $S \cap (P_R \cup P_C)$. This observation, together with Proposition IV.1, implies that the partial P_S -marking $\overline{\overline{M}}_u(S \cup \|\tilde{Y}_S\|)$ (or, equivalently, $\overline{\overline{M}}_u((S \cup \|\tilde{Y}_S\|) \cap P_S)$ since the P_S -marking only considers tokens in P_S), is sufficient to characterize the RIDM-unsafe markings with respect to S . For simplicity, we define $\Theta_S := (S \cup \|\tilde{Y}_S\|) \cap P_S$. This leads to our next result.

Proposition IV.2. *Given a RIDM siphon S , and an associated partial modified marking $\overline{\overline{M}}_u(\Theta_S)$, any marking M such that $\overline{\overline{M}}(\Theta_S) = \overline{\overline{M}}_u(\Theta_S)$, is RIDM-unsafe with respect to S .*

Remark IV.2. Proposition IV.2 bridges the notion of partial *modified marking* on S , which is obtained in the RIDM siphon detection, and the notion of partial P_S -marking on S , which is used in the control synthesis. It also implies that the P_S -marking of any $p \notin \Theta_S$ is a “don’t care” term in the control synthesis, i.e., the coefficient associated with it in the linear inequality that will prevent siphon S is 0. The partial P_S -marking analysis is further facilitated by the notion of covering, which is introduced next. \square

4.4.2 Notion of covering

We introduce the notation “ χ ” for the value of a P_S -marking component, where “ χ ” stands for “0 or 1”.

Definition IV.2. In \mathcal{N}_G^c , a *covering* C is a generalized P_S -marking, whose components can be 0, 1, or χ .

For any place $p \in P_S$, $C(p)$ represents the covering component value on p . This notation can be extended to a set of places $Q \subseteq P_S$ in a natural way. Furthermore, we extend the notion of covering so that it encompasses any place $p \in P$ by setting $C(p) = \chi, \forall p \in P_0 \cup P_R \cup P_C$.

Given two coverings C_1 and C_2 , we say that C_1 *covers* C_2 , denoted as $C_1 \succeq C_2$, if $\forall p \in P_S$ such that $C_1(p) \neq C_2(p)$, $C_1(p) = \chi$. As a special case, if $C_1 = C_2$, then we have $C_1 \succeq C_2$ and $C_2 \succeq C_1$. The “cover” relationship between a covering and a P_S -marking, which have the same dimensions, is defined in a similar way. For example, for a binary marking vector $[p_1, p_2, p_3]^T$, $C = [1, \chi, 1]^T$ *covers* the P_S -markings $\overline{\overline{M}}_1 = [1, 0, 1]^T$ and $\overline{\overline{M}}_2 = [1, 1, 1]^T$.

Definition IV.3. A covering C is said to be a *RIDM-unsafe covering* if for all P_S -markings $\overline{\overline{M}}$ it covers, the corresponding M is RIDM-unsafe.

Remark IV.3. As a result of Proposition IV.2 and the notion of covering, for any RIDM siphon S to be prevented, the control synthesis *only* needs to consider the set of places Θ_S , and the associated RIDM-unsafe covering, $C(\Theta_S)$, and $C(p) = \chi$, $\forall p \notin \Theta_S$. \square

Remark IV.4. By Definition IV.2, a covering is a generalized P_S -marking. So the component values in a covering can only be 0, 1, or χ . In the context of control synthesis, χ is a “*don't care*” term, and the coefficient associated with it in the corresponding linear inequality will always be 0. \square

4.4.3 Feasibility of maximally permissive control

In Section 3.7, we have established the linear separability property of the state space of Gadara nets. This property is based on the *binary* nature of the P_S -markings and it states that, in Gadara nets, any set of reachable markings can be separated from the rest through a set of linear inequalities, which are provided in the constructive proof of Theorem III.5. These linear inequalities can be subsequently enforced upon the original net through monitor places. Following Remarks IV.3 and IV.4, this property can be generalized to any set of RIDM-unsafe coverings with respect to some given RIDM siphon S .

Theorem IV.1. *In \mathcal{N}_G^c , for any RIDM siphon S , the set of all RIDM-unsafe coverings with respect to S can be separated by a finite set of linear inequality constraints $\Lambda = \{(l_1, b_1), (l_2, b_2), \dots\}$ such that a covering C is RIDM-unsafe with respect to S iff $\exists (l_i, b_i) \in \Lambda, l_i^T C > b_i$.*

Theorem IV.1 implies that it is feasible to implement maximally permissive control using monitor-based control in terms of RIDM-unsafe coverings. More specifically, using SBPI, for a given covering C we want to prevent, its associated linear inequality can be specified as: $l_C(p) = 1$, if $C(p) = 1$; $l_C(p) = -1$, if $C(p) = 0$; $l_C(p) = 0$, if $C(p) = \chi$; and, $b_C = \sum_{p: p \in \Theta_S \text{ and } C(p)=1} C(p) - 1$.

4.5 UCCOR Algorithm

We now formally present the UCCOR Algorithm. Our presentation is organized in a top-down manner. We first give the overall procedure of the UCCOR Algorithm in Figure 4.3, and then explain the embedded modules in subsequent sections. We will apply the UCCOR Algorithm to $\mathcal{N}_G^{c(1)}$, which is the controlled Gadara net with the monitor place p_{c1} shown in Figure 4.1, to illustrate the steps of UCCOR.

The input to the algorithm is \mathcal{N}_G^c , a RIDM siphon S , and an associated partial modified marking $\overline{M}_u(S)$. In Step 1, the Unsafe Covering Construction Algorithm is used to solve for a set of possible RIDM-unsafe coverings with respect to S , denoted as \mathcal{C}_u . As a result of Step 1 and Propositions IV.1 and IV.2, any RIDM-unsafe marking M with respect to S , such that $\overline{M}(S) = \overline{M}_u(S)$, is captured by \mathcal{C}_u . In Step 2, \mathcal{C}_u is taken as the input to the Unsafe Covering Generalization. This step further generalizes the RIDM-unsafe coverings obtained from Step 1, by utilizing a certain type of monotonicity property of Gadara nets. It outputs a modified set of coverings, $\mathcal{C}_u^{(1)}$, which is taken as the input to the Inter-Iteration Coverability Check carried out in Step 3. In Step 3, the coverings that have already been controlled are removed

Algorithm: UCCOR Algorithm**Input:** \mathcal{N}_G^c , RIDM siphon S , and an associated partial modified marking on S **Output:** A set of monitor place(s) to prevent S **Method:**

1. Take the RIDM siphon S and the provided partial modified marking on S as the input to the *Unsafe Covering Construction Algorithm*, and obtain a set of RIDM-unsafe coverings with respect to S , denoted as \mathcal{C}_u .
2. Take \mathcal{C}_u as the input to the *Unsafe Covering Generalization*, and obtain the output, denoted as $\mathcal{C}_u^{(1)}$.
3. Take $\mathcal{C}_u^{(1)}$ as the input to the *Inter-Iteration Coverability Check*, and obtain the output, denoted as $\mathcal{C}_u^{(2)}$.
- 4a. If $\mathcal{C}_u^{(2)} = \emptyset$, then output the empty set \emptyset and terminate.
- 4b. If $\mathcal{C}_u^{(2)} \neq \emptyset$, then take $\mathcal{C}_u^{(2)}$ as the input to the *Monitor Place Synthesis Algorithm*, which will synthesize a monitor place for each element in $\mathcal{C}_u^{(2)}$.

Figure 4.3: UCCOR Algorithm

from consideration. The output of this step is a further modified set of coverings, $\mathcal{C}_u^{(2)}$. In Step 4, if $\mathcal{C}_u^{(2)}$ is an empty set, then the algorithm terminates; otherwise, control synthesis using SBPI is carried out. One monitor place will be synthesized for each covering in $\mathcal{C}_u^{(2)}$.

Define Φ to be the set of coverings that have already been prevented in the previous iterations. One can think of Φ as a global “bookkeeping set” in the control synthesis process, which records all the coverings that have been prevented so far. The set Φ helps us to determine the convergence of ICOG. Since Φ only needs to record a relatively *small* number of *coverings* to keep track of a potentially much *larger* number of *markings* that need to be prevented, the complexity of the bookkeeping process is greatly reduced – a saving on both time and space. The set Φ is updated by the UCCOR algorithm during the Inter-Iteration Coverability Check in Step 3 discussed below. In addition, Φ is also updated after the termination of the UCCOR Algorithm, i.e., $\Phi = \Phi \cup \mathcal{C}_u^{(2)}$, to include the coverings that are prevented in this iteration.

4.5.1 Unsafe Covering Construction Algorithm

From the input of the UCCOR Algorithm, we know the RIDM siphon S and an associated partial modified marking $\overline{M}_u(S)$. As discussed above, we want to find the RIDM-unsafe coverings that cover any possible RIDM-unsafe marking M , such that $\overline{M}(S) = \overline{M}_u(S)$. The desired RIDM-unsafe coverings are obtained in the Unsafe Covering Construction Algorithm, which is described as follows.

Firstly, for each generalized resource place in S , there is an associated P-semiflow equation. Denote the set of all such equations associated with $S \cap (P_R \cup P_C)$ as \mathcal{V} . Secondly, substitute the unknown variables in \mathcal{V} corresponding to places $S \cap \|\tilde{Y}_S\|$ using the values specified by $\overline{M}_u(S)$. The set of updated equations is denoted as \mathcal{V}' . Thirdly, solve \mathcal{V}' , together with the constraint that $M(p) \in \{0, 1\}, \forall p \in \|\tilde{Y}_S\| \setminus S$. The set of solutions of \mathcal{V}' are denoted as $\mathcal{M}_u(\|\tilde{Y}_S\|)$, which is a set of partial markings on $\|\tilde{Y}_S\|$. Finally, construct the RIDM-unsafe coverings based on the obtained $\mathcal{M}_u(\|\tilde{Y}_S\|)$ and the given $\overline{M}_u(S)$. For each $M \in \mathcal{M}_u(\|\tilde{Y}_S\|)$, define the corresponding covering C with a dimension of $|P| \times 1$ as follows: (i) $C(\|\tilde{Y}_S\| \cap P_S) = \overline{M}(\|\tilde{Y}_S\| \cap P_S)$; (ii) $C((S \setminus \|\tilde{Y}_S\|) \cap P_S) = \overline{M}_u((S \setminus \|\tilde{Y}_S\|) \cap P_S)$; and, (iii) $C(p) = \chi, \forall p \notin \Theta_S$. The resulting set of coverings is the output of this algorithm, denoted as \mathcal{C}_u .

Remark IV.5. Observe that for any $C \in \mathcal{C}_u$, C is a RIDM-unsafe covering with respect to S . Thus, for any P_S -marking \overline{M} that is covered by C , the corresponding original marking M is also RIDM-unsafe with respect to S . Moreover, C only specifies binary values for the places in Θ_S , and the other places not in Θ_S are irrelevant to the analysis of the RIDM siphon S under the notion of covering. \square

Example IV.3. Consider the net $\mathcal{N}_G^{c(1)}$ in Figure 4.1. We use $\mathcal{N}_G^{c(1)}$ as the initial condition of ICOG. The first iteration of ICOG detects a RIDM siphon:

$$S_1 = \{r_A, r_B, r_C, p_{12}, p_{13}, p_{14}, p_{15}, p_{21}, p_{23}, p_{24}, p_{25}\} \quad (4.2)$$

at the marking M_{u1} , where the places p_{01} , p_{02} , p_{11} , and p_{22} each have one token, and all the other places are empty. For this example, Step 1 of UCCOR outputs the set \mathcal{C}_u that contains one RIDM-unsafe covering C , where $C(p_{11}) = C(p_{22}) = 1$, $C(p_{1i}) = C(p_{2j}) = 0$, for $i = 2, 3, 4, 5$ and $j = 1, 3, 4, 5$, and $C(p_{01}) = C(p_{02}) = C(r_A) = C(r_B) = C(r_C) = \chi$. \square

4.5.2 Unsafe Covering Generalization

Given the set of possible RIDM-unsafe coverings \mathcal{C}_u with respect to S , the Unsafe Covering Generalization *generalizes* \mathcal{C}_u and outputs a modified set of coverings $\mathcal{C}_u^{(1)}$.

Given two markings M_1 and M_2 , we say that “ M_1 dominates M_2 ”, denoted by $M_1 >_d M_2$, if the following two conditions are satisfied: (i) $M_1(p) \geq M_2(p)$, for all $p \in P$, and (ii) $M_1(q) > M_2(q)$, for at least some $q \in P$. The dominance relationship between two coverings C_1 and C_2 can be defined in a similar way by substituting “ M ” above by “ C ”. Note that “ χ ”, as a covering component, stands for “0 or 1”. So, we have: $1 \geq \chi \geq 0$. Moreover, if $C_1 >_d C_2$, then Condition (ii) above can only be satisfied by the case when $C_1(q) = 1$ and $C_2(q) = 0$.

The following theorem is closely related to the *monotonicity property* of state safety in resource allocation systems [89].

Theorem IV.2. *Consider a Gadara net \mathcal{N}_G^c , and a marking M of it that satisfies the net semiflow equations (2.2) and (2.3) but cannot reach M_0^c . Then, any marking M' that satisfies all the semiflow equations (2.2) and (2.3) and $\overline{\overline{M'}} >_d \overline{\overline{M}}$, cannot reach M_0^c either.*

Proof. We prove the contra-positive proposition, i.e., we prove that if M' can reach M_0^c and satisfies all the semiflow equations (2.2) and (2.3), then any marking M that satisfies all the semiflow equations (2.2) and (2.3) and $\overline{\overline{M'}} >_d \overline{\overline{M}}$, can also reach M_0^c .

By assumption, starting from M' , there exists a feasible firing transition sequence σ' , which will lead the net from M' to M_0^c . Furthermore, since both markings M and

M' satisfy all the semiflow equations (2.2) and (2.3) and $\overline{M'} >_d \overline{M}$, Properties II.1 and II.2 imply that $M(r) \geq M'(r), \forall r \in P_R \cup P_C$. That is, the net under M contains only a subset of the processes that are active in M' , and it is “resource richer”. As a result, starting from M , there also exists a feasible firing transition sequence σ , which will lead the net from M to M_0^c ; such a sequence σ can be obtained from σ' by “erasing” the set of transitions that are fired by the extra tokens in P_S under M' as compared to M , and the feasibility of σ under M can be formally established by an induction on the length of the sequence. \square

An immediate corollary of Theorem IV.2 is as follows:

Corollary IV.2. *Consider a Gadara net \mathcal{N}_G^c , and a marking M that is RIDM-unsafe and satisfies all the semiflow equations (2.2) and (2.3). Then, any marking M' that satisfies all the semiflow equations (2.2) and (2.3) and $\overline{M'} >_d \overline{M}$, cannot reach M_0^c .*

Remark IV.6. From Proposition IV.2 and its associated discussion, we know that only the set of places $S \cup \|\tilde{Y}_S\|$ is relevant to the analysis of siphon S (or equivalently, under the notion of P_S -marking, only the set of places Θ_S is relevant). Note that $(S \cup \|\tilde{Y}_S\|) \cap (P_R \cup P_C) = S \cap (P_R \cup P_C)$. This implies that Corollary IV.2 still holds if we replace the condition “satisfies all the semiflow equations (2.2) and (2.3)” on M and M' , by the condition “satisfies all the semiflow equations associated with $S \cap (P_R \cup P_C)$.” \square

In Step 1 of UCCOR, we obtain the set of RIDM-unsafe coverings \mathcal{C}_u with respect to S . According to Remark IV.5, for *any* $C_1 \in \mathcal{C}_u$, and *any* M_1 , such that $C_1 \succeq \overline{M}_1$, M_1 is RIDM-unsafe with respect to S . Due to the construction of \mathcal{C}_u in Step 1 of UCCOR, M_1 satisfies all the semiflow equations associated with $S \cap (P_R \cup P_C)$. Consider the partial marking $M_1(\Theta_S)$. If there exists at least one “0” component in $M_1(\Theta_S)$, we replace *any* subset of the “0” components in $M_1(\Theta_S)$ by “1”, and leave the other components in M_1 unchanged. The resulting marking is denoted as M_2 ,

and it is obvious that $\overline{\overline{M}}_2 >_d \overline{\overline{M}}_1$. Therefore, M_2 either does not satisfy the semiflow equations associated with $S \cap (P_R \cup P_C)$ (and hence is not reachable), or satisfies the semiflow equations associated with $S \cap (P_R \cup P_C)$ and cannot reach M_0^c (based on Corollary IV.2 and Remark IV.6).

As a consequence, for a given covering $C \in \mathcal{C}_u$ that needs to be prevented, any covering C' , such that $C' >_d C$, satisfies the following: for any P_S -marking $\overline{\overline{M}}$ covered by C' , the corresponding marking M is either reachable and cannot reach M_0^c , or not reachable. Therefore, all the 0 components in C can be replaced by χ , and the resulting covering is denoted as C' , where $C' \succeq C$. In the control synthesis, we can prevent C' instead of C .

In the Unsafe Covering Generalization, we “generalize” each $C \in \mathcal{C}_u$ by replacing all the 0 components in C by χ , and obtain a corresponding modified covering $C^{(1)}$. The resulting set of modified coverings is denoted as $\mathcal{C}_u^{(1)'}$. Consequently, the elements in \mathcal{C}_u and those in $\mathcal{C}_u^{(1)'}$ are in one-to-one correspondence. Observe that any corresponding pair $(C, C^{(1)})$, where $C \in \mathcal{C}_u$ and $C^{(1)} \in \mathcal{C}_u^{(1)'}$, satisfies: $C^{(1)} \succeq C$. Therefore, by considering the set of modified coverings $\mathcal{C}_u^{(1)'}$ afterwards in the UCCOR Algorithm, we will not “miss” preventing any element in \mathcal{C}_u due to this coverability relationship. Moreover, the property of maximal permissiveness is still preserved, i.e., we only prevent reachable markings that cannot reach M_0^c , or markings that are not reachable, due to the above discussion.

Furthermore, we determine if there exists a pair of coverings (C_1, C_2) , such that $C_1, C_2 \in \mathcal{C}_u^{(1)'}$ and $C_1 \succeq C_2$. (i) If such a pair is detected, then we perform $\mathcal{C}_u^{(1)'}$ = $\mathcal{C}_u^{(1)'}$ \setminus $\{C_2\}$, and repeat the process in the updated $\mathcal{C}_u^{(1)'}$. (ii) If no pair is detected, then we output the set $\mathcal{C}_u^{(1)} := \mathcal{C}_u^{(1)'}$. Note that $\mathcal{C}_u^{(1)}$ and $\mathcal{C}_u^{(1)'}$ have the same power of coverability, because the operations performed above simply remove the “redundant” coverings in the set $\mathcal{C}_u^{(1)'}$.

Example IV.4. Let us continue the example of applying UCCOR to the net $\mathcal{N}_G^{c(1)}$

as shown in Figure 4.1. In Step 2 of the UCCOR algorithm, for this example, the set $\mathcal{C}_u^{(1)}$ contains one covering C_1 , where $C_1(p_{11}) = C_1(p_{22}) = 1$ and $C_1(p) = \chi$, for any $p \in P \setminus \{p_{11}, p_{22}\}$. \square

Clearly, $\mathcal{C}_u^{(1)}$ will cover, in general, a larger set of markings than \mathcal{C}_u does. Thus, by considering $\mathcal{C}_u^{(1)}$ in the UCCOR Algorithm, the synthesized monitor places are more efficient, in terms of the number of markings that they can prevent. As we mentioned, some markings covered by $\mathcal{C}_u^{(1)}$ may not be reachable, however, the property of maximal permissiveness is not compromised because of this.

4.5.3 Inter-Iteration Coverability Check

In the step of Inter-Iteration Coverability Check, each pair of coverings $(C_1, C_2) \in \{(C_1, C_2) : C_1 \in \mathcal{C}_u^{(1)} \text{ and } C_2 \in \Phi\}$ is tested. (i) If $C_1 \preceq C_2$, then the existing monitor place associated with $C_2 \in \Phi$ already prevents C_1 , and we perform: $\mathcal{C}_u^{(1)} = \mathcal{C}_u^{(1)} \setminus C_1$. (ii) If $C_1 \succeq C_2$ and $C_1 \neq C_2$, then by synthesizing a new monitor place in the current iteration that prevents C_1 , this monitor place will also prevent $C_2 \in \Phi$. That is, the existing monitor place associated with C_2 will become redundant after the current iteration. In this case, we perform: $\Phi = \Phi \setminus C_2$, and remove the existing monitor place (and its ingoing and outgoing arcs) associated with C_2 from the net. (iii) If C_1 and C_2 are incomparable, then no action is performed. The algorithm finally outputs a modified set of coverings corresponding to $\mathcal{C}_u^{(1)}$, denoted as $\mathcal{C}_u^{(2)}$, and updates Φ .

Example IV.5. We continue the discussion on the running example. The set Φ is initialized as an empty set before the first iteration of ICOG. Thus, in the first iteration of ICOG, no action is needed in Step 3 of UCCOR. After this step of UCCOR, we have: $\mathcal{C}_u^{(2)} = \{C_1\}$ and $\Phi = \emptyset$. \square

4.5.4 Monitor Place Synthesis Algorithm

In Step 4 of UCCOR, if the set $\mathcal{C}_u^{(2)}$ is empty, then we terminate the algorithm and start the next iteration of ICOG. If the set $\mathcal{C}_u^{(2)}$ is not empty, then for each covering in $\mathcal{C}_u^{(2)}$, a monitor place is synthesized. The key of the Monitor Place Synthesis Algorithm is to find an appropriate linear inequality constraint in the form of (2.1) for each element $C_u \in \mathcal{C}_u^{(2)}$, so that we can employ SBPI to synthesize a monitor place to prevent C_u , and finally obtain an *admissible* controlled Gadara net. In general, for any given $C_u \in \mathcal{C}_u^{(2)}$, we can find an associated linear inequality constraint in two stages.

In Stage 1, we specify a linear inequality constraint in the form of (2.1) for C_u , according to the discussion following Theorem IV.1. From the above discussion of UCCOR, we know that C_u contains only “1” or “ χ ” components. So the parameters of the constraint associated with C_u are:

$$l_{C_u}(p) = \begin{cases} 1, & \text{if } C_u(p) = 1; \\ 0, & \text{otherwise.} \end{cases} \quad (4.3)$$

$$b_{C_u} = \sum_{p:p \in \Theta_S \text{ and } C_u(p)=1} C_u(p) - 1 \quad (4.4)$$

Note that this constraint *only* prevents C_u according to Theorem IV.1. SBPI can be employed to synthesize a monitor place based on this constraint. If the resulting \mathcal{N}_G^c is admissible, then Stage 2 is not necessary for this C_u and we can continue with the next element (if any) in $\mathcal{C}_u^{(2)}$; otherwise, we need to proceed to Stage 2, where constraint transformation is carried out to deal with the partial controllability and ensure the admissibility of \mathcal{N}_G^c .

Example IV.6. Before moving on to Stage 2, let us first illustrate Stage 1 by the running example. T_{uc} is chosen to be the lower bound specified in Assumption II.2, which is \emptyset in this example. From Step 3 of UCCOR, we know that $\mathcal{C}_u^{(2)}$ contains one

covering C_1 . According to (4.3) and (4.4), we specify the following linear inequality constraint in the form of (2.1) to prevent C_1 :

$$M(p_{11}) + M(p_{22}) \leq 1 \quad (4.5)$$

The monitor place p_{c2} , which enforces (4.5), is synthesized by SBPI and shown in Figure 4.1. The controlled net obtained in the first iteration of ICOG, which consists of \mathcal{N}_G , p_{c1} , p_{c2} , and their associated arcs, is denoted as $\mathcal{N}_G^{c(2)}$. At the end of the first iteration, we update the global bookkeeping set as: $\Phi = \Phi \cup \mathcal{C}_u^{(2)} = \{C_1\}$. \square

The constraint transformation technique in Stage 2 is presented as follows. For the sake of discussion, the constraint obtained in Stage 1 can be rewritten as:

$$M(p_1) + M(p_2) + \dots + M(p_n) \leq n - 1 \quad (4.6)$$

We apply constraint transformation to (4.6) to handle partial controllability, adapted and much simplified from the corresponding procedure in [68], due to the special structure of Gadara nets. The core idea is the following. If place p_i in (4.6) can gain tokens through a sequence of uncontrollable transitions, places along the sequence of uncontrollable transitions must be included to the left-hand-side of (4.6) as we cannot prevent these transitions from firing and populating tokens into p_i . We make two remarks for the above statement: (i) The set of places corresponding to a given sequence of uncontrollable transitions is unique due to the state-machine structure of the process subnet. (ii) The uncontrollable transitions in this sequence are not blocked by any generalized resource place, otherwise they would be controllable. The pseudo-code that implements the constraint transformation for (4.6) is given in Figure 4.4. Based on the set of places C obtained above, the new, transformed constraint is:

<p>Algorithm: Constraint Transformation Input: A linear inequality constraint, e.g., (4.6) Output: A set of places C Method:</p> <ol style="list-style-type: none"> 1. add p_1, \dots, p_n in (4.6) to stack S, and to set C 2. while S is not empty 3. $p = S.pop()$ 4. for each uncontrollable t in $\bullet p_i$, if $\bullet t$ is not in C, add $\bullet t$ to S and C 5. end while

Figure 4.4: The constraint transformation technique used in Stage 2 of the Monitor Place Synthesis Algorithm

$$\sum_{p \in C} M(p) \leq n - 1 \quad (4.7)$$

Without any confusion, in the following discussion we will refer to (4.6) as the original constraint, and refer to (4.7) as the new constraint.

Proposition IV.3. *Using SBPI, all the outgoing arcs of the monitor place synthesized for the new constraint do not connect to any uncontrollable transition, i.e., the resulting \mathcal{N}_G^c is admissible.*

Proof. Proof by contradiction. It can be shown that by applying SBPI to a constraint of the form (4.6) or (4.7), the outgoing arcs of the synthesized monitor place connect to “entry” transitions only, i.e., transitions whose input places (in the process subnet) are not in the constraint, and whose output places (in the process subnet) are in the constraint. This follows from the fact that SBPI enforces a P-invariant based on the constraint via a monitor place. If an “entry” transition is uncontrollable, the constraint transformation technique must have included its input place into the new constraint. Therefore, it is not an “entry” transition anymore. \square

Proposition IV.4. *(a) Any marking prevented by the original constraint is also prevented by the new constraint. (b) Any reachable marking that is prevented by the new constraint but not by the original constraint, can reach a marking prevented by the original constraint via a sequence of uncontrollable transitions.*

Proof. (a) This is a direct result of the construction of the new constraint. Any marking that violates the original constraint will also violate the new one.

(b) The new constraint simply adds more places to the left-hand-side of the original constraint. By construction, any token in these new places may reach one of the places in the original constraint through a sequence of uncontrollable transitions. If a reachable marking M satisfies the original constraint but not the new one, then at M there must be extra tokens in the set of places added. These tokens can “leak” into the set of places in the original constraint through a sequence of uncontrollable transitions. Thus, in the reachability graph, there must be a sequence of uncontrollable transitions connecting from M to a marking that violates the original constraint. \square

Example IV.7. The Gadara net model of a deadlock case in the OpenLDAP software is shown in Figure 4.5. In this example, T_{uc} is chosen to be the upper bound as specified in Assumption II.2; thus, only t_1, t_2 and t_8 are controllable transitions. When we apply UCCOR to this example, both stages in Step 4b are required. In Stage 1 of Step 4b, the original constraint is $M(p_1) + M(p_5) \leq 1$; in Stage 2 of Step 4b, the new, transformed constraint is $\sum_{i=1}^6 M(p_i) \leq 1$, where the synthesized monitor place p_c is shown in dashed lines in Figure 4.5. The resulting controlled Gadara net is admissible. \square

Example IV.8. Let us return to the running example of Figure 4.1. In the second iteration of ICOG, we further input $\mathcal{N}_G^{c(2)}$ to ICOG, and detect a new RIDM siphon:

$$S_2 = \{p_{c1}, p_{c2}, p_{12}, p_{13}, p_{14}, p_{15}, p_{22}, p_{23}, p_{24}, p_{25}\} \quad (4.8)$$

at the marking M_{u2} , where the places p_{01}, p_{02}, p_{11} , and p_{21} each have one token, and all the other places are empty. We apply UCCOR to this RIDM siphon in the second iteration of ICOG. After Step 3 of UCCOR, the set $\mathcal{C}_u^{(2)}$ contains one covering C_2 , where $C_2(p_{11}) = C_2(p_{21}) = 1$ and $C_2(p) = \chi$, for any $p \in P \setminus \{p_{11}, p_{21}\}$. In Stage 1

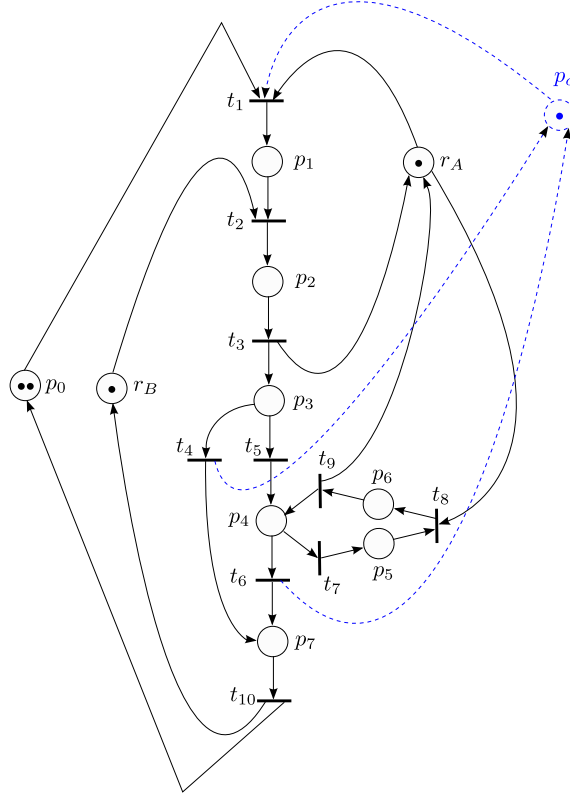


Figure 4.5: Gadara net model of a deadlock example in the OpenLDAP software

of Step 4b, the monitor place p_{c3} shown in Figure 4.1 is synthesized to prevent C_2 . The resulting controlled net is denoted as $\mathcal{N}_G^{c(3)}$, and it is admissible. Thus, Stage 2 of Step 4b is not necessary. At the end of the second iteration, we update the global bookkeeping set as: $\Phi = \Phi \cup \mathcal{C}_u^{(2)} = \{C_1, C_2\}$.

Next, we input $\mathcal{N}_G^{c(3)}$ to ICOG, and no new RIDM siphon is detected. Therefore, ICOG converges after the second iteration. \square

Two important observations can be made from the above example. (i) In the second iteration of ICOG, we notice that the new RIDM siphon S_2 is induced by the monitor places p_{c1} and p_{c2} . This is an example of the scenario we discussed in Section 4.3, where monitor places can introduce new potential deadlocks and thus force further iterations. (ii) As discussed in Section 4.4.1, in the initial net $\mathcal{N}_G^{c(1)}$, the marking M_{u2} is not RIDM-unsafe but cannot reach the initial marking. However, in the controlled net $\mathcal{N}_G^{c(3)}$, M_{u2} is RIDM-unsafe. More specifically, it is RIDM-unsafe

4.6 Properties

4.6.1 Correctness and maximal permissiveness

In Section 4.3, we presented the global flowchart of the ICOG Methodology. Here, we present its main properties. In this section, when we say that ICOG is “correct with respect to the goal of liveness enforcement”, it will mean that the resulting controlled net is admissible and live. We will carry out the proofs in two steps: we first prove the properties of UCCOR (employed in each iteration of ICOG), then we prove the properties maintained by ICOG throughout the entire set of the performed iterations.

Theorem IV.3. *In \mathcal{N}_G^c , the control logic synthesized for any RIDM siphon S based on the UCCOR Algorithm is correct and maximally permissive with respect to the goal of preventing S from becoming a RIDM siphon and the given set of uncontrollable transitions.*

Proof. First, we prove the correctness. We are going to show that the UCCOR Algorithm does not miss preventing any RIDM-unsafe marking with respect to S .

For any RIDM siphon S with its associated $\overline{M}_u(S)$, which needs to be prevented, Step 1 of the UCCOR Algorithm finds the set of RIDM-unsafe coverings \mathcal{C}_u that covers all the possible RIDM-unsafe markings M , such that $\overline{M}(S) = \overline{M}_u(S)$. This set of RIDM-unsafe markings is denoted as $\mathcal{M}_u(S)$. According to the Unsafe Covering Generalization algorithm and the property of “covering”, the set $\mathcal{C}_u^{(1)}$ obtained in Step 2 covers \mathcal{C}_u , which covers $\mathcal{M}_u(S)$. Moreover, Step 3 only removes the coverings that are already prevented in previous control synthesis iterations. Thus, $\mathcal{C}_u^{(2)}$, together with the prevented coverings Φ , covers $\mathcal{M}_u(S)$. From Step 4 as well as Propositions IV.2 and IV.4(a), we know that any marking in the set $\mathcal{M}_u(S)$ will be prevented in this step, or this marking has already been prevented in previous iterations.

The above discussion applies to any RIDM siphon S in the net. Thus, UCCOR does not miss preventing any RIDM-unsafe marking with respect to any RIDM siphon S . This, together with Assumption II.1 and Proposition IV.3, implies that UCCOR is correct with respect to the goal of preventing S from becoming a RIDM siphon and the given set of uncontrollable transitions.

Next, we prove the maximal permissiveness. Recall from Theorem III.3 that \mathcal{N}_G^c is live *iff* it is reversible. Thus, we are going to show that the UCCOR Algorithm *only* prevents markings that cannot reach the initial marking M_0^c , or markings that can reach the aforementioned type of markings via a sequence of uncontrollable transitions.

According to Proposition IV.2, it follows from the Unsafe Covering Construction Algorithm that the set \mathcal{C}_u obtained in Step 1 of the the UCCOR Algorithm *only* covers RIDM-unsafe markings with respect to S . Moreover, Corollary IV.2 and Remark IV.6 imply that any marking, covered by the refined set $\mathcal{C}_u^{(1)}$ obtained in Step 2, cannot reach M_0^c . In Step 3, the obtained set $\mathcal{C}_u^{(2)}$ is a subset of $\mathcal{C}_u^{(1)}$. Hence, any marking covered by $\mathcal{C}_u^{(2)}$ cannot reach M_0^c either. Moreover, Stage 1 of Step 4 only prevents the coverings in $\mathcal{C}_u^{(2)}$; Stage 2 of Step 4 only prevents the coverings in $\mathcal{C}_u^{(2)}$, and the markings that can reach some marking covered by $\mathcal{C}_u^{(2)}$, through a sequence of uncontrollable transitions (see Proposition IV.4(b)). Such coverings and markings must be removed. Therefore, UCCOR is maximally permissive with respect to the goal of preventing S from becoming a RIDM siphon and the given set of uncontrollable transitions. \square

From Definition III.9, we know that any marking in a Gadara net can be uniquely characterized by the corresponding P_S -marking without any ambiguity. That is, $M_1 = M_2$ if and only if $\overline{\overline{M}}_1 = \overline{\overline{M}}_2$. The set of reachable P_S -markings induced by the set of reachable markings is defined as $\overline{\overline{R}}(\mathcal{N}_G^c, M_0^c) = \{\overline{\overline{M}} \mid M \in R(\mathcal{N}_G^c, M_0^c)\}$, which is denoted as $\overline{\overline{R}}$ for simplicity. We immediately have the following result.

Lemma IV.1. *The reachability graph associated with $R(\mathcal{N}_G^c, M_0^c)$ and the reachability graph associated with $\overline{\overline{R}}(\mathcal{N}_G^c, M_0^c)$ are isomorphic.*

Lemma IV.1 subsequently enables us to prove the following theorem.

Theorem IV.4. *ICOG terminates in a finite number of iterations.*

Proof. Due to Lemma IV.1, in the following proof, we can restrict our attention to $\overline{\overline{R}}$. By Definition II.6, the number of operation places in a Gadara net is finite. Further, for any $p \in P_S$, $M(p)$ is always binary. As a result, the set of reachable P_S -markings $\overline{\overline{R}}$ has finite cardinality. The set of reachable P_S -markings that need to be prevented, which is a subset of $\overline{\overline{R}}$, also has finite cardinality.

For the sake of discussion, we use $\overline{\overline{N}}$ to denote the set of non-reachable P_S -markings, each of which is a binary vector. According to the above discussion, the cardinality of $\overline{\overline{R}} \cup \overline{\overline{N}}$ is at most $2^{|P_S|}$. Note that the aforementioned $\overline{\overline{R}}$ and $\overline{\overline{N}}$ are associated with the input Gadara net before the first iteration of ICOG is applied.

In each iteration of ICOG, we only expand the set P_C by adding monitor places while leaving P_S unchanged. So, ICOG does not expand $\overline{\overline{R}}$. In other words, the set of reachable P_S -markings that need to be prevented has a finite upper bound $\overline{\overline{R}}$; another looser but also finite upper bound for this set is $\overline{\overline{R}} \cup \overline{\overline{N}}$, whose cardinality is $2^{|P_S|}$ at most. In every iteration of ICOG, the synthesized monitor place eliminates at least one marking from $\overline{\overline{R}} \cup \overline{\overline{N}}$, which is not prevented in the previous iterations of ICOG. Therefore, the proposed ICOG will terminate in a finite number of iterations. \square

Theorem IV.5. *ICOG is correct and maximally permissive with respect to the goal of liveness enforcement and the given set of uncontrollable transitions.*

Proof. First, we prove the correctness of ICOG.

In each iteration of ICOG, a new RIDM siphon in the net is detected. According to Theorem IV.3, for any detected RIDM siphon S with its associated $\overline{M}_u(S)$, the UCCOR Algorithm ensures that *any* possible RIDM-unsafe marking M , such that

$\overline{M}(S) = \overline{M}_u(S)$, will be prevented. And the detected RIDM siphon S will not become reachable under the synthesized control logic. ICOG terminates when no further new RIDM siphons can be detected. By using the UCCOR Algorithm for all detected RIDM siphons in all the iterations, any RIDM-unsafe marking associated with any RIDM siphon will be prevented, and no siphon will become a RIDM siphon. Furthermore, in each iteration of ICOG, UCCOR always synthesizes an admissible Gadara net, according to Assumption II.1 and Proposition IV.3. This, together with Theorems III.1 and IV.4, implies that the proposed ICOG ensures admissibility and liveness of the final controlled Gadara net, i.e., it is correct with respect to the goal of liveness-enforcement and the given set of uncontrollable transitions.

Next, we prove the maximal permissiveness of ICOG. This is an immediate consequence of the maximal permissiveness of UCCOR on a single iteration basis as established in Theorem IV.3. In each iteration of ICOG, UCCOR is employed to prevent markings in the net. Since UCCOR only prevents markings that cannot reach the initial marking, or markings that can reach the aforementioned type of markings via a sequence of uncontrollable transitions, so does ICOG. Therefore, ICOG is maximally permissive with respect to the goal of liveness-enforcement and the given set of uncontrollable transitions. \square

Remark IV.7. We interpret the effect of ICOG and UCCOR from the viewpoint of the Supervisory Control Theory. Let $\mathcal{N}_G^{c,\text{final}}$ be the final controlled Gadara net when ICOG terminates. Let G and G_{final} be the automata models of the reachability graphs associated with \mathcal{N}_G and $\mathcal{N}_G^{c,\text{final}}$, respectively. The language generated by G is denoted as $\mathcal{L}(G)$. In G and G_{final} , only the initial states are marked. The languages marked by G and G_{final} are denoted as $\mathcal{L}_m(G)$ and $\mathcal{L}_m(G_{\text{final}})$, respectively. The live (equivalently, reversible) part of \mathcal{N}_G corresponds to the trim of automaton G and is captured by the marked language $\mathcal{L}_m(G)$. However, this language need not be *controllable* (as defined in [86]) with respect to $\mathcal{L}(G)$ and E_{uc} , where E_{uc} is the set of uncontrollable

events corresponding to the set T_{uc} in the Gadara net. ICOG and UCCOR control \mathcal{N}_G and finally obtain $\mathcal{N}_G^{c,\text{final}}$, so that $\mathcal{L}_m(G_{\text{final}})$ is equal to the *supremal controllable sublanguage* [86] of $\mathcal{L}_m(G)$ with respect to $\mathcal{L}(G)$ and E_{uc} . Throughout the iterations of ICOG, the cumulative effect of the constraint transformation in Stage 2 of Step 4b of UCCOR corresponds to the elimination of the states that violate the controllability condition in the supremal controllable sublanguage algorithm; the cumulative effect of the remaining operations in UCCOR corresponds to the removal of the blocking states in that algorithm. \square

4.6.2 Ordinariness of monitor places synthesized by UCCOR

Our last result is the following interesting property of the UCCOR Algorithm.

Theorem IV.6. *In \mathcal{N}_G^c , for any monitor place synthesized by the UCCOR Algorithm, all its incoming and outgoing arcs have unit arc weights.*

Proof. From Step 4b of the UCCOR Algorithm, we know that for any synthesized monitor place p_c , the arc weights of its associated incoming and outgoing arcs are determined by the nonzero components in the row vector D_{p_c} , which is calculated by the following equation:

$$D_{p_c} = -l_{C_u}^T D \quad (4.9)$$

In (4.9)

$$l_{C_u}(p) = \begin{cases} 1, & \text{if } C_u(p) = 1; \\ 0, & \text{otherwise.} \end{cases} \quad (4.10)$$

is a column vector that has the same dimension with C_u , and D is the incidence matrix of the net.

For the sake of discussion and without loss of generality, we can always rearrange the order of rows in a marking, covering, and incidence matrix such that row 1 to row $|P_S|$ correspond to the set of all operation places P_S , row $|P_S| + 1$ to row $|P_S| + |P_0|$

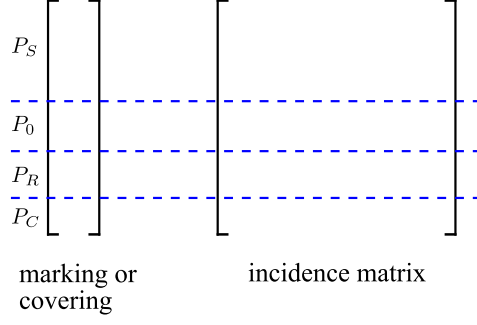


Figure 4.7: Illustration of the rearranged order of rows in a marking, covering, and incidence matrix

correspond to the set of all idle places P_0 , row $|P_S| + |P_0| + 1$ to row $|P_S| + |P_0| + |P_R|$ correspond to the set of all resource places P_R , and row $|P_S| + |P_0| + |P_R| + 1$ to $|P_S| + |P_0| + |P_R| + |P_C|$ correspond to the set of all monitor places P_C . The rearranged order is shown in Figure 4.7. In this way, any covering can be logically divided into four blocks corresponding to the four types of places. Then, any covering C_u can be rewritten as

$$C_u = (C_{u,S}^T, C_{u,0}^T, C_{u,R}^T, C_{u,C}^T)^T \quad (4.11)$$

where $C_{u,S}$, $C_{u,0}$, $C_{u,R}$ and $C_{u,C}$ are the partial coverings on P_S , P_0 , P_R , and P_C , respectively. Similarly, the aforementioned column vector l_{C_u} in (4.10) can be rewritten as

$$l_{C_u} = (l_{C_{u,S}}^T, l_{C_{u,0}}^T, l_{C_{u,R}}^T, l_{C_{u,C}}^T)^T \quad (4.12)$$

and the incidence matrix D can be rewritten as

$$D = (D_S^T, D_0^T, D_R^T, D_C^T)^T \quad (4.13)$$

The blocks are self-explanatory by their subscripts. From Definition IV.2 and its discussion thereafter, we know that for any covering C_u written as in (4.11), any component in $C_{u,0}$, $C_{u,R}$ and $C_{u,C}$ is always χ . As a result of this and (4.10), for any column vector l_{C_u} written as in (4.12), any component in $l_{C_{u,0}}$, $l_{C_{u,R}}$, and $l_{C_{u,C}}$ is

always 0. Therefore, (4.9) can be simplified as:

$$D_{p_c} = - \begin{pmatrix} l_{C_u,S} \\ l_{C_u,0} \\ l_{C_u,R} \\ l_{C_u,C} \end{pmatrix}^T \begin{pmatrix} D_S \\ D_0 \\ D_R \\ D_C \end{pmatrix} = - \begin{pmatrix} l_{C_u,S} \\ 0 \\ 0 \\ 0 \end{pmatrix}^T \begin{pmatrix} D_S \\ D_0 \\ D_R \\ D_C \end{pmatrix} = -l_{C_u,S}^T D_S \quad (4.14)$$

Note that D_S is the part of the incidence matrix of \mathcal{N}_G^c that corresponds to P_S , which describes the connectivity between operation places and transitions. Since D_S is also a part of the incidence matrix of \mathcal{N}_G and \mathcal{N}_G is ordinary, any component in D_S can only be -1 , 1 , or 0 . Moreover, according to Condition 3 of Definition II.6, we know that each transition in \mathcal{N}_G^c has at most one input operation place and at most one output operation place. That is, any column in D_S contains at most one “ -1 ” and at most one “ 1 ”, with all other components being zeros. On the other hand, we know from (4.10) that any component in $l_{C_u,S}$ is either 0 or 1 . Consequently, any component in the row vector D_{p_c} calculated in (4.14) can only be -1 , 1 , or 0 . \square

The implication of Theorem IV.6 will be exploited in the next chapter.

4.7 Discussion of related approaches

If the reachability graph of a Petri net is available, the problem of MPLE control can be solved by the Supervisory Control Theory for discrete event systems initiated by Ramadge and Wonham [85, 86, 8]. The theory of regions (see, e.g., [99, 26, 55]), which in some sense combines the modeling strength of Petri nets and the control strength of automata, synthesizes monitor places back into the Petri net to avoid unsafe states in the reachability graph. But employing an automaton model (of the reachability graph) in control synthesis suffers from the state explosion problem when modeling concurrent software, as it fails to capture the concurrency in the

target parallel program. Moreover, the associated control decisions are made based on a centralized controller, which needs to be updated at every transition execution, and thus introduces a global bottleneck in the concurrent program. For these two reasons, we are investigating *structural* control techniques for Petri net models in this dissertation.

Liveness-enforcing control is an important class of problems in the supervisory control of Petri nets. Many approaches have been proposed for the synthesis of liveness-enforcing control logic for Petri nets. These approaches are typically sub-optimal, i.e., they sacrifice maximal permissiveness due to the complexity of the problem and the inherent limitation of monitor-based control. As we discussed above, in general, our proposed MPLE control synthesis is an iterative process, because the synthesized control logic may introduce new potential deadlocks. Few works address such an iterative process and its implications for MPLE control synthesis. A siphon-based iterative control synthesis method is proposed in [97] for the class of S^4PR nets. But this method is sub-optimal in general, i.e., it does not guarantee maximal permissiveness. In [38], the role of iterations in liveness-enforcing control synthesis is discussed and a net transformation technique is employed to transform non-ordinary nets into PT-ordinary nets during the iterations. This approach, however, may not guarantee convergence within a finite number of iterations. In fact, as pointed out in [57], it is not easy to establish a formal and satisfactory proof of finite convergence for this type of problem; moreover, achieving optimal control logic is very difficult. The key reason is that the Petri net modeling framework might not be able to express the MPLE property for general process-resource nets; as a result, the problem of MPLE control synthesis based on siphon analysis in *non-ordinary* nets has not been well-resolved yet [53]. In [5], the “max-controlled-siphon-property” is proposed; however, siphon-based control synthesis by enforcing this property is not maximally permissive in general.

CHAPTER V

Control II: Optimal Control of Gadara Nets – Customization for Ordinary Case

5.1 Introduction

In Chapter IV, we developed a general methodology (called ICOG) of *optimal* control synthesis for controlled Gadara nets that need not be ordinary. The control synthesis algorithm (called UCCOR) presented in Chapter IV prevents a special type of siphons, termed RIDM siphons, from becoming reachable in the net. This algorithm possesses an interesting property that, for any monitor place synthesized by the algorithm, its associated arcs always have unit weights (cf. Theorem IV.6). In other words, the algorithm will never introduce additional non-ordinariness to a controlled Gadara net.

This property implies that if our control synthesis starts with a Gadara net model of a concurrent program, then the original net is ordinary, and the subsequent controlled nets will remain ordinary as well. Therefore, if the objective of our control synthesis is *strictly* liveness enforcement and the initial condition is an ordinary controlled Gadara net (including \mathcal{N}_G), then the general methodology of ICOG and UCCOR can be customized for this special case. This motivates us to investigate in this chapter the customization of the general algorithm in Chapter IV, and to

concentrate on the ordinary case of controlled Gadara nets, where only *resource-induced (RI) empty siphons* need to be considered. A resource-induced empty siphon is a special case of a RIDM siphon. Thus, all the properties of the general algorithm will be preserved in the customized algorithm. In addition, some steps in ICOG and UCCOR, such as bookkeeping, can also be simplified as a result of the customization.

This chapter is organized as follows. We first present some results in Section 5.2 that will serve as the foundation for the control synthesis. Then, in Section 5.3, we overview the proposed iterative control methodology, which customizes ICOG. In Section 5.4, we present an optimal control algorithm based on RI empty siphons, which customizes UCCOR. We investigate some important properties of the proposed methodology in Section 5.5, and we report on the results of its experimental evaluation in Section 5.6. We discuss the application of our results to real-world software in Section 5.7. Some of the results in this chapter also appear in [62, 61].

5.2 Foundation for control synthesis

As we discussed above, the control synthesis algorithm to be presented next guarantees that for any monitor place synthesized by this algorithm, its associated arcs always have unit weights. In the particular application of concurrent software, we always start with a Gadara net model \mathcal{N}_G of the software, which is ordinary. Thus, by applying this control synthesis algorithm, the resulting controlled Gadara nets will remain within the class of \mathcal{N}_{G1}^c . Consequently, we can restrict our attention to \mathcal{N}_G and \mathcal{N}_{G1}^c in the following development of the control synthesis algorithm.

Recall that we presented a deadlock example of the Linux kernel in Section 3.9. To facilitate our discussion, we will use it as a running example and demonstrate the relevant control synthesis throughout this chapter.

Example V.1. The Gadara net model \mathcal{N}_G of a deadlock bug in version 2.5.62 of

the Linux kernel is shown in Figure 3.6. This model, together with the source code involved in the deadlock, is presented in Section 3.9 (without control).

In this Gadara net model, let us consider the reachable marking M_{u1} , where there is one token in p_{14} , one in p_{22} , and one in p_{03} , while all other places are empty. At marking M_{u1} , all the transitions in the net are disabled, i.e., the net is in a total-deadlock. Therefore, this Gadara net model is not live, and its underlying program is deadlock-prone (cf. Proposition III.1 and Theorem III.3). \square

Based on the definition of siphon (Definition III.5), we further introduce the notion of resource-induced siphon as follows.

Definition V.1. In Gadara nets, a siphon S is said to be a *resource-induced (RI) siphon*, if S contains at least one generalized resource place, i.e., $S \cap (P_R \cup P_C) \neq \emptyset$.

The following theorem relates the liveness property of a Gadara net to its structural properties in terms of siphons. This theorem is a direct result of Theorem III.1.¹ According to Remark II.1, this theorem also holds for \mathcal{N}_G .

Theorem V.1. $\mathcal{N}_{G_1}^c$ is live iff there does not exist a modified marking $\bar{M} \in \bar{R}(\mathcal{N}_{G_1}^c, M_0^c)$ and a siphon S such that S is an RI empty siphon at \bar{M} .

Example V.2. We know from Example V.1 that the net \mathcal{N}_G shown in Figure 3.6 is not live. Let \bar{M}_{u1} be the modified marking that is induced by the marking M_{u1} defined in Example V.1. At \bar{M}_{u1} , there is one token in p_{14} and one in p_{22} , while all other places are empty. Let S_1 be the set of all empty places in the net at \bar{M}_{u1} . Then, S_1 is an RI empty siphon at \bar{M}_{u1} . \square

Remark V.1. Proposition III.1, Remark III.1, Theorem III.3, and Theorem V.1 together imply that the goal of deadlock-avoidance of a program can be achieved

¹Liveness of $\mathcal{N}_{G_1}^c$ is also equivalent to the absence of any empty siphon in the original reachable markings of the net. But we have opted to use the result of Theorem V.1 in order to stay close to the developments of the results in Chapter IV.

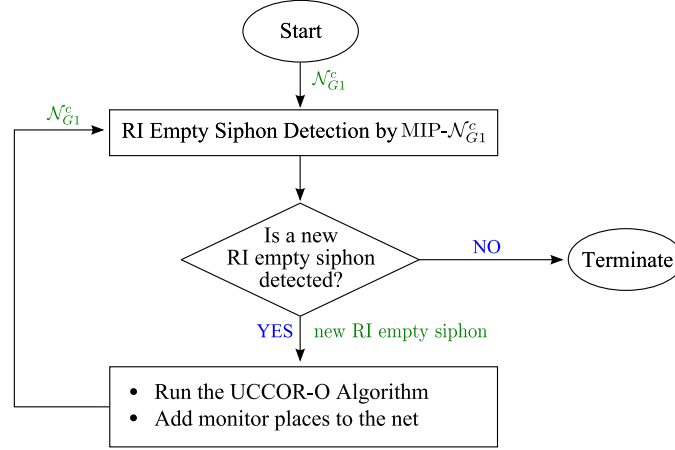


Figure 5.1: Iterative control of Gadara nets: Ordinary case (ICOG-O)

by preventing RI empty siphons from becoming reachable in its associated Gadara net model. They serve as a foundation for the control synthesis to be carried out next. \square

5.3 Overall strategy: Iterative control of ordinary Gadara nets

Our overall strategy for control synthesis is shown in Figure 5.1 and described as follows. Given a multithreaded program and its associated Gadara net model \mathcal{N}_G , we first detect if there is a potential RI empty siphon that can be reached under the modified markings of \mathcal{N}_G . For the detected RI empty siphon, we synthesize control logic to prevent it from becoming reachable, and obtain a controlled Gadara net \mathcal{N}_{G1}^c . Then, we detect again, over the modified markings of \mathcal{N}_{G1}^c , if there is a new RI empty siphon; and synthesize control logic to prevent it, if any. The above process continues, until there is no new RI empty siphon being detected. According to Remark V.1, upon termination, the resulting Gadara net is live, and its corresponding program is deadlock-free.

Similar to ICOG presented in Chapter IV, we see that the proposed methodology

is an iterative process, because (i) there may be some RI empty siphons that have not been identified in the previous iterations and need further consideration, and (ii) the synthesized monitor places are generalized resource places, so that they may introduce new potential RI empty siphons in the controlled net. We refer to the above process as the ICOG-O Methodology, which stands for “Iterative Control Of (controlled) Gadara nets: Ordinary case”. While ICOG in Chapter IV is based on exploiting RIDM siphons [88, 64] (which can be considered as a generalization of the notion of RI empty siphons for non-ordinary nets), ICOG-O presented in this chapter customizes ICOG and only considers RI empty siphons, resulting in lower analytical complexity and some interesting properties. In particular, bookkeeping of prevented states, which is required in ICOG, is no longer necessary in ICOG-O.

The main features of the proposed ICOG-O Methodology to be presented are summarized as follows. (i) ICOG-O is based on structural analysis (using RI empty siphons), and does not require the construction of the reachability space of the net. (ii) ICOG-O is correct and maximally permissive with respect to the goal of liveness enforcement. (iii) ICOG-O is guaranteed to terminate in a finite number of iterations.

There are two major tasks in ICOG-O: detecting RI empty siphons and rendering them unreachable. For the first task, the potential RI empty siphon is detected in each iteration by the MIP formulation, $\text{MIP-}\mathcal{N}_{G_1}^c$, we presented in Section 3.8. For the second task, the detected RI empty siphon is prevented by the UCCOR-O Algorithm, which will be presented in Section 5.4.

We mentioned in Section 3.8 that the objective function of $\text{MIP-}\mathcal{N}_{G_1}^c$ seeks to minimize the number of marked operation places in the detected total-deadlock modified-marking. The selection of such an objective function will produce siphons that are efficient for control synthesis using ICOG-O. Some resulting interesting properties will be presented in Section 5.5.

5.4 Optimal control algorithm based on RI empty siphons

Once an RI empty siphon is detected by $\text{MIP-}\mathcal{N}_{G_1}^c$, we input it to the control synthesis algorithm, called UCCOR-O, which customizes the general algorithm UCCOR presented in Chapter IV. The abbreviation UCCOR-O stands for “Unsafe-Covering-based Control Of RIDM siphons: Ordinary case”. In UCCOR-O, we focus on a special type of RIDM siphons in ordinary nets, namely RI empty siphons. UCCOR-O synthesizes control logic based on the notion of unsafe covering induced by an RI empty siphon, which is introduced next.

Definition V.2. In $\mathcal{N}_{G_1}^c$, a marking M is said to be an *RIE-unsafe marking*, if at its associated modified marking \overline{M} , there exists at least one RI-empty siphon.

Definition V.3. A covering C is said to be an *RIE-unsafe covering*, if for all P_S -markings \overline{M} it covers, the corresponding M is an RIE-unsafe marking.

5.4.1 UCCOR-O Algorithm: Overview

We are now ready to present the UCCOR-O Algorithm. We organize our presentation in a top-down manner. We first overview the procedure of UCCOR-O as illustrated in Figure 5.2, and then explain the three steps of UCCOR-O in subsequent sections. We will apply UCCOR-O to the running example throughout our discussion.

The input to UCCOR-O is $\mathcal{N}_{G_1}^c$, an RI empty siphon S , and the associated total-deadlock modified-marking \overline{M} obtained from $\text{MIP-}\mathcal{N}_{G_1}^c$. The output of UCCOR-O is a monitor place that prevents the RI empty siphon S from becoming reachable. The UCCOR-O Algorithm contains three steps. In Step 1, an RIE-unsafe covering is generated based on the input to the algorithm. This covering captures the RI empty siphon we want to prevent. In Step 2, the obtained RIE-unsafe covering is generalized into a new covering, by exploiting a monotonicity property of Gadara

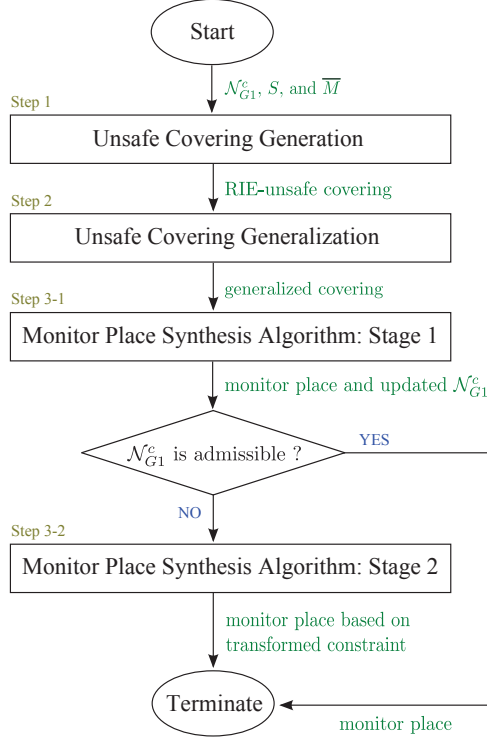


Figure 5.2: Flowchart of the UCCOR-O Algorithm

nets. This generalization step enhances the efficiency of the algorithm, in terms of the number of undesirable markings that can be prevented by the final monitor place. In Step 3, a monitor place is synthesized to prevent the covering obtained in Step 2. Step 3 contains two stages in general. Stage 2 is necessary only when the controlled Gadara net obtained in Stage 1 is not admissible. We discuss these three steps in further details below.

5.4.2 Unsafe Covering Generation

Step 1 of UCCOR-O generates an RIE-unsafe covering, denoted as C_{u1} , based on the input to the algorithm. We consider the following set of places:

$$\Lambda_S = \bigcup_{p \in S \cap (P_R \cup P_C)} \|Y_p\| \cup S \quad (5.1)$$

Intuitively, Λ_S contains the set of *all* places that are relevant to the siphon S . In particular, Λ_S complements S with all those operation places that utilize the generalized resources appearing in S .

Therefore, we can specify the values for the components of C_{u1} that are associated with Λ_S as: $C_{u1}(\Lambda_S) = \overline{M}(\Lambda_S)$; and set $C_{u1}(p) = \chi$, $\forall p \notin \Lambda_S$, since these places are irrelevant to the considered siphon. Moreover, we know from the definition of covering that we can further set $C_{u1}(p) = \chi$, $\forall p \in P_0 \cup P_R \cup P_C$. The resulting C_{u1} is input to Step 2 of UCCOR-O.

Example V.3. We continue our discussion on the example in Figure 3.6. Let \mathcal{N}_G , \overline{M}_{u1} , and S_1 , described in Example V.2, be the input to UCCOR-O. After Step 1 of UCCOR-O, the RIE-unsafe covering C_{u1} is specified as follows. $C_{u1}(p_{14}) = C_{u1}(p_{22}) = 1$; $C_{u1}(p) = 0$, $\forall p \in P_S \setminus \{p_{14}, p_{22}\}$; and $C_{u1}(p_{01}) = C_{u1}(p_{02}) = C_{u1}(p_{03}) = C_{u1}(r_A) = C_{u1}(r_B) = C_{u1}(r_C) = \chi$. \square

5.4.3 Unsafe Covering Generalization

Step 2 of UCCOR-O generalizes the RIE-unsafe covering obtained from Step 1, by exploiting a monotonicity property of Gadara nets, which is formally established in Theorem IV.2. The monotonicity property is explained as follows. Let M and M' be two markings of a Gadara net, which satisfy: $M(p) \geq M'(p)$, for all $p \in P_S$, and $M(p) > M'(p)$, for at least some $p \in P_S$. If M' is a marking that needs to be prevented, then M also needs to be prevented. The intuition is that loading a program, which is already in a deadlock or will unavoidably enter a deadlock, with even more active threads will only worsen the deadlock situation, but not cure it.

Based on the above property, for the RIE-unsafe covering C_{u1} obtained in Step 1, if we replace any of its 0 components (associated with operation places) by 1, the resulting covering will only cover reachable P_S -markings that need to be prevented, or non-reachable P_S -markings. Therefore, C_{u1} can be generalized by replacing all of

its 0 components by χ , and the resulting covering is denoted as C_{u2} , which is input to Step 3 of UCCOR-O.

By construction, the generalized covering C_{u2} will not “miss” covering any P_S -markings that are covered by C_{u1} . In general, C_{u2} will cover a larger set of P_S -markings than C_{u1} , because the former contains more χ components. So instead of preventing C_{u1} , a monitor place that prevents C_{u2} is more efficient, in the sense that it will prevent a larger set of markings in the controlled net. More importantly, the property of maximal permissiveness is still preserved, i.e., we only prevent reachable markings that need to be prevented, or markings that are not reachable, due to the above discussion.

Example V.4. Given the RIE-unsafe covering C_{u1} described in Example V.3, Step 2 of UCCOR-O generalizes C_{u1} and obtains C_{u2} , which is specified as follows. $C_{u2}(p_{14}) = C_{u2}(p_{22}) = 1$; and $C_{u2}(p) = \chi, \forall p \in P \setminus \{p_{14}, p_{22}\}$. \square

5.4.4 Monitor Place Synthesis Algorithm

Step 3 of UCCOR-O aims to find an appropriate linear inequality constraint in the form of (2.1), so that SBPI can be employed to synthesize a monitor place, to prevent C_{u2} that is obtained in Step 2; the constraint should also guarantee that the resulting controlled Gadara net is *admissible*. Generally, Step 3 consists of two stages. Stage 2 is necessary only when the controlled Gadara net obtained in Stage 1 is not admissible. For the sake of simplicity and without any confusion, we let $C_u \equiv C_{u2}$ and will use the notation C_u in the following discussion. (Step 3 of UCCOR-O in this chapter is similar to the corresponding step of UCCOR that is presented in Chapter IV, for which no customization is necessary; we include it here for the sake of completeness. Also note that in the general UCCOR Algorithm, there is a step called “Inter-Iteration Coverability Check”, which is eliminated in the customized UCCOR-O Algorithm. The reason of this customization will become clear when we

present Theorem V.3 in Section 5.5.)

In Stage 1, we specify a linear inequality constraint in the form of (2.1) for C_u . From the first two steps of UCCOR-O, we know that C_u contains only “1” or “ χ ” components. The parameters of the constraint associated with C_u are:

$$l_{C_u}(p) = \begin{cases} 1, & \text{if } C_u(p) = 1; \\ 0, & \text{otherwise.} \end{cases} \quad (5.2)$$

$$b_{C_u} = \left(\sum_{p:p \in \Lambda_S \text{ and } C_u(p)=1} C_u(p) \right) - 1 \quad (5.3)$$

According to Theorem IV.1, this constraint *only* prevents C_u (i.e., any P_S -marking or covering that is covered by C_u). Thus, the corresponding control logic synthesized based on this constraint is maximally permissive. The synthesis of a monitor place based on this constraint can be achieved by SBPI. If the resulting \mathcal{N}_{G1}^c is admissible, then Stage 2 is not necessary and we can continue with the next iteration of ICOG-O; otherwise, we need to proceed to Stage 2, where constraint transformation is carried out to deal with the partial controllability and ensure the admissibility of \mathcal{N}_{G1}^c .

Example V.5. We illustrate Stage 1 by continuing our discussion on the running example. Given the covering described in Example V.4, we specify the following linear inequality constraint according to (5.2) and (5.3):

$$M(p_{14}) + M(p_{22}) \leq 1 \quad (5.4)$$

The monitor place p_c , which enforces (5.4), is synthesized by SBPI and shown in Figure 5.3. We see that p_c has two out-going arcs, both of which connect to branching transitions. In this running example, we define that only the lock acquisition transitions are controllable; and all the other transitions (i.e., those corresponding to branching and lock releases) are uncontrollable. Thus, the controlled net that

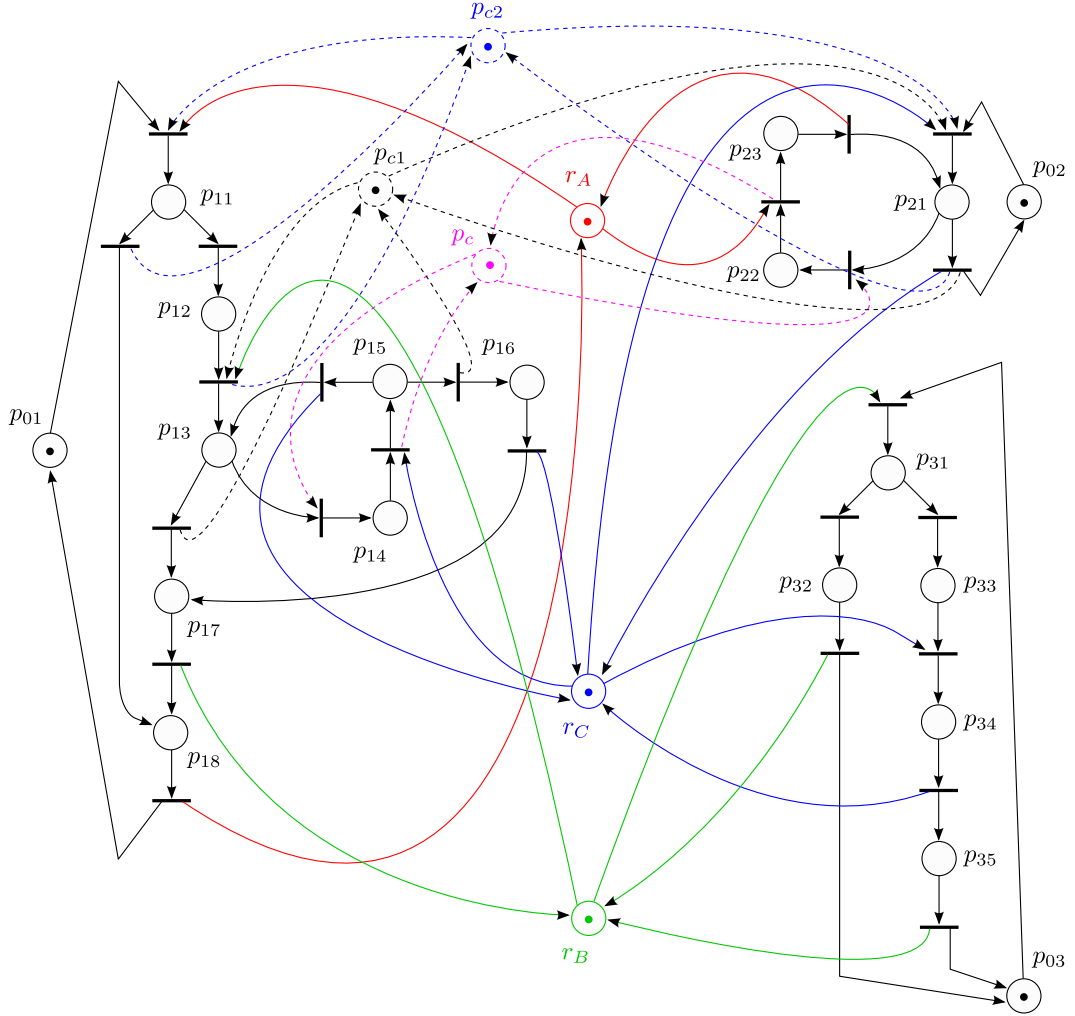


Figure 5.3: A deadlock example in the Linux kernel: Controlled Gadara net model

contains p_c is not admissible. We resolve this problem in Stage 2 of Step 3. \square

In Stage 2, the original constraint specified by (5.2) and (5.3) is transformed, so that the new constraint, when applied to SBPI, will render a monitor place that leads to an admissible controlled net. For the sake of discussion, the constraint obtained in Stage 1 can be rewritten as:

$$M(p_1) + M(p_2) + \dots + M(p_n) \leq n - 1 \quad (5.5)$$

The key idea of the proposed constraint transformation is the following. If place

<p>Algorithm: Constraint Transformation Input: A linear inequality constraint, e.g., (5.5) Output: A set of places C Method:</p> <ol style="list-style-type: none"> 1. add p_1, \dots, p_n in (5.5) to stack S, and to set C 2. while S is not empty 3. $p = S.pop()$ 4. for each uncontrollable t in $\bullet p_i$, if $\bullet t$ is not in C, add $\bullet t$ to S and C 5. end while

Figure 5.4: The constraint transformation technique used in Stage 2 of the Monitor Place Synthesis Algorithm

p_i in (5.5) can gain tokens through a sequence of uncontrollable transitions, places along the sequence of uncontrollable transitions must be included to the left-hand-side of (5.5) as we cannot prevent these transitions from firing and populating tokens into p_i . We make two remarks for the above statement: (i) The set of places corresponding to a given sequence of uncontrollable transitions is unique due to the state-machine structure of the process subnet. (ii) The uncontrollable transitions in this sequence are not blocked by any generalized resource place, otherwise they would be controllable. The pseudo-code that implements the constraint transformation for (5.5) is given in Figure 5.4. Based on the set of places C obtained above, the new, transformed constraint is:

$$\sum_{p \in C} M(p) \leq n - 1 \quad (5.6)$$

The important properties of the proposed constraint transformation technique are summarized as follows; see Chapter IV for a detailed discussion. (i) The constraint transformation technique guarantees that the resulting controlled Gadara net is admissible. (ii) Any marking prevented by the original constraint is also prevented by the new constraint. (iii) Any reachable marking that is prevented by the new constraint but not by the original constraint, can reach a marking prevented by the original constraint via a sequence of uncontrollable transitions.

Example V.6. We apply the proposed constraint transformation technique to (5.4), which is obtained from Step 1 in Example V.5. After Stage 2, the new, transformed constraint is:

$$[M(p_{14}) + M(p_{13}) + M(p_{15})] + [M(p_{22}) + M(p_{21}) + M(p_{23})] \leq 1 \quad (5.7)$$

The monitor place p_{c1} , which enforces (5.7), is synthesized by SBPI and shown in Figure 5.3. We see that p_{c1} has two out-going arcs, both of which connect to controllable transitions. Thus, the controlled net that contains p_{c1} is admissible. We denote the resulting controlled Gadara net as $\mathcal{N}_{G1}^{c(1)}$, which consists of \mathcal{N}_G and p_{c1} . \square

Example V.6 completes the first iteration of ICOG-O on the running example. We continue our discussion on the second iteration in Example V.7.

Example V.7. In the second iteration of ICOG-O, we first input the net $\mathcal{N}_{G1}^{c(1)}$ obtained from Example V.6 into MIP- \mathcal{N}_{G1}^c for the detection of RI empty siphons. MIP- \mathcal{N}_{G1}^c finds a total-deadlock modified-marking \bar{M}_{u2} , where there is one token in p_{12} and one in p_{22} , while all other places are empty. Note that this corresponds to a circular-wait deadlock induced by r_A and p_{c1} . Let S_2 be the set of all empty places in the net at \bar{M}_{u2} . Then, S_2 is an RI empty siphon at \bar{M}_{u2} .

We input $\mathcal{N}_{G1}^{c(1)}$, S_2 , and \bar{M}_{u2} to UCCOR-O. Step 1 of UCCOR-O generates the covering C_{u1} , which is specified as: $C_{u1}(p_{12}) = C_{u1}(p_{22}) = 1$; $C_{u1}(p) = 0, \forall p \in P_S \setminus \{p_{12}, p_{22}\}$; and $C_{u1}(p) = \chi, \forall p \in P_0 \cup P_R \cup P_C$. Step 2 of UCCOR-O further generalizes C_{u1} and obtains the covering C_{u2} , which is specified as: $C_{u2}(p_{12}) = C_{u2}(p_{22}) = 1$; and $C_{u2}(p) = \chi, \forall p \in P \setminus \{p_{12}, p_{22}\}$.

Based on C_{u2} , Stage 1 of Step 3 of UCCOR-O constructs the following constraint:

$$M(p_{12}) + M(p_{22}) \leq 1 \quad (5.8)$$

Similar to the situation encountered in Example V.5, the monitor place that is synthesized by SBPI and enforces (5.8), will attempt to disable uncontrollable transitions. Thus, the resulting controlled net would not be admissible, which necessitates Stage 2 of Step 3.

In Stage 2, the original constraint in (5.8) is transformed into:

$$[M(p_{12}) + M(p_{11})] + [M(p_{22}) + M(p_{21}) + M(p_{23})] \leq 1 \quad (5.9)$$

The monitor place p_{c2} , which enforces (5.9), is synthesized by SBPI and shown in Figure 5.3. We denote the resulting controlled net as $\mathcal{N}_{G_1}^{c(2)}$, which consists of \mathcal{N}_G , p_{c1} , and p_{c2} . The controlled Gadara net $\mathcal{N}_{G_1}^{c(2)}$ is admissible.

In the third iteration of ICOG-O, we input $\mathcal{N}_{G_1}^{c(2)}$ into MIP- $\mathcal{N}_{G_1}^c$, and no solution is found. Therefore, no new RI empty siphon can be detected in $\mathcal{N}_{G_1}^{c(2)}$, and ICOG-O terminates. \square

5.5 Properties

The general ICOG Methodology and UCCOR Algorithm proposed in Chapter IV are shown to be both correct and maximally permissive, with respect to the goal of liveness enforcement of Gadara nets via siphon-based control. Moreover, ICOG is guaranteed to terminate in a finite number of iterations. The general ICOG Methodology is developed independent of the method used to detect siphons. Therefore, ICOG-O and UCCOR-O presented in this chapter, which are customized versions of ICOG and UCCOR respectively, still preserve the aforementioned properties. Moreover, the customization possesses some new properties that are formally established below.

5.5.1 Properties of the UCCOR-O Algorithm

Theorem V.2. *In $\mathcal{N}_{G_1}^c$, for any monitor place $p_c \in P_C$ synthesized by UCCOR-O, any process subnet will never have two consecutive resource acquisitions from p_c without a resource release to p_c in between. Also, any process subnet will never have two consecutive resource releases to p_c without a resource acquisition from p_c in between.²*

Proof. Since any covering C_u considered in UCCOR-O is a generalized P_S -marking, the linear constraint generated in Step 3 of UCCOR-O will only involve operation places. That is, for any p such that $l_{C_u}(p) = 1$, p must be an operation place; further, $l_{C_u}(p) = 0, \forall p \in P_0 \cup P_R \cup P_C$. Given C_u , let p_c be the corresponding monitor place synthesized by UCCOR-O using SBPI. Also, let Q be the set of places that are involved in the linear constraint, i.e., $Q = \{p \in P_S : l_{C_u}(p) = 1\}$.

Consider an arbitrary transition $t \in T$. We discuss the connectivity of the monitor place p_c to t in four cases, as shown in Figure 5.5, where the places that belong to Q are highlighted. Due to the aforementioned property of l_{C_u} , we can focus on process subnets (since the generalized resource places will not affect the connectivity of p_c to t in terms of l_{C_u}). Recall Condition 3 of Definition 1 that, in the process subnet, t has only one input place, denoted as p_{11} , and one output place, denoted as p_{12} .

Case 1: $p_{11} \in Q$ and $p_{12} \notin Q$, as shown in Figure 5.5(a). In this case, we have: $l_{C_u}(p_{11}) = 1$ and $l_{C_u}(p_{12}) = 0$. The state machine structure of the process subnets leads to the following feature of the incidence matrix D of $\mathcal{N}_{G_1}^c$: if we only consider the rows associated with the places in all the process subnets, then in the column corresponding to t , there are *only* two nonzero entries, i.e., $D_{p_{11},t} = -1$ and $D_{p_{12},t} = 1$. Therefore, the algebraic calculation of SBPI will result in one arc connecting t to p_c , whose weight equals to 1.

Case 2: $p_{11} \notin Q$ and $p_{12} \in Q$, as shown in Figure 5.5(b). In this case, we have:

²This theorem also applies to UCCOR developed for the control synthesis for \mathcal{N}_G^c .

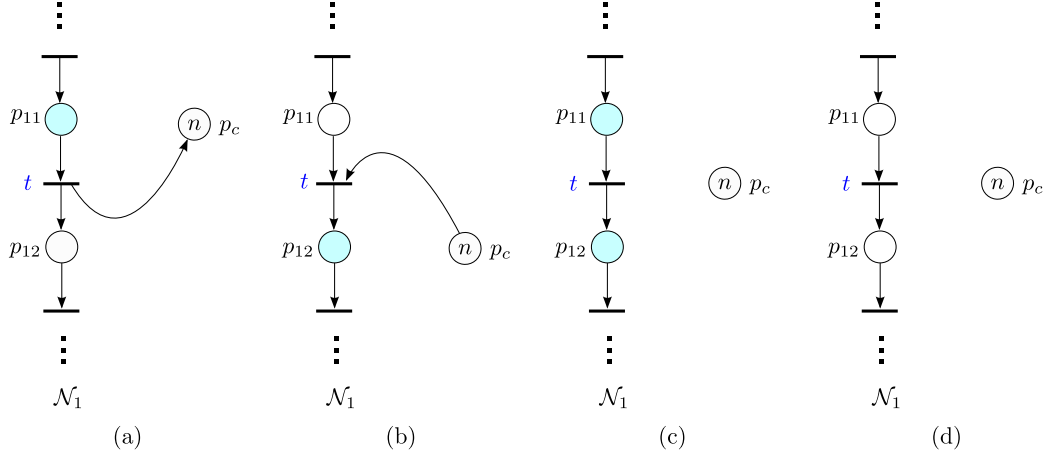


Figure 5.5: Cases considered in the proof: (a) Case 1; (b) Case 2; (c) Case 3; (d) Case 4

$l_{C_u}(p_{11}) = 0$ and $l_{C_u}(p_{12}) = 1$. Similar to the analysis in Case 1, the calculation results in one arc connecting p_c to t , whose weight equals to 1.

Case 3: $p_{11} \in Q$ and $p_{12} \in Q$, as shown in Figure 5.5(c). In this case, we have: $l_{C_u}(p_{11}) = l_{C_u}(p_{12}) = 1$. According to the calculation of SBPI, no arc will be synthesized between p_c and t .

Case 4: $p_{11} \notin Q$ and $p_{12} \notin Q$, as shown in Figure 5.5(d). In this case, we have: $l_{C_u}(p_{11}) = l_{C_u}(p_{12}) = 0$. Similar to Case 3, no arc will be synthesized between p_c and t .

Note that Cases 1 and 4 also apply to the situation when t is a terminating transition of the process subnet and p_{12} is an idle place. Similarly, Cases 2 and 4 also apply to the situation when t is an initiating transition of the process subnet and p_{11} is an idle place. Thus, the above four cases cover all the possibilities of the connectivity of p_c to an arbitrary transition t .

As a result, if we traverse from the upstream to the downstream of a process subnet, it is impossible for the subnet to have two consecutive resource acquisitions from (or resource releases to) p_c . □

As a consequence of Theorem V.2, we have the following corollary, which can be considered as a special case of Condition 8 of Definition II.8 when UCCOR-O is employed to synthesize monitor places.

Corollary V.1. *In Gadara nets, for each $p_c \in P_C$ synthesized by UCCOR-O, there exists a unique minimal-support P -semiflow, Y_{p_c} , such that $\{p_c\} = \|Y_{p_c}\| \cap P_C$, $(\forall p \in \|Y_{p_c}\|)(Y_{p_c}(p) = 1)$, $P_0 \cap \|Y_{p_c}\| = \emptyset$, $P_R \cap \|Y_{p_c}\| = \emptyset$, and $P_S \cap \|Y_{p_c}\| \neq \emptyset$.*

5.5.2 Properties of the ICOG-O Methodology

Define $C_u^{(i)}$ to be the covering input to Step 3 of UCCOR-O in the i -th iteration of ICOG-O; and define

$$K^{(i)} = \sum_{p:p \in \Lambda_S \text{ and } C_u^{(i)}(p)=1} C_u^{(i)}(p) \quad (5.10)$$

namely, $K^{(i)}$ is the total number of 1's in $C_u^{(i)}$ that is induced by the siphon S under consideration.

Lemma V.1. *In ICOG-O, $K^{(i)}$ is non-decreasing with respect to i . That is, the total number of 1's in the covering considered in Step 3 of UCCOR-O is non-decreasing, throughout the iterations of ICOG-O.*

Proof. Consider an arbitrary $i \geq 1$, and let p_c be the monitor place synthesized in the i -th iteration of ICOG-O that prevents $C_u^{(i)}$. According to Step 3 of UCCOR-O, the initial marking of p_c is $M_0(p_c) = K^{(i)} - 1$.

We mentioned above that a monitor place is essentially a generalized resource place and may introduce new potential deadlocks in the controlled net. More specifically, the monitor place p_c can *directly induce* a new circular-wait deadlock, if in the controlled net, (i) there exists a total-deadlock modified-marking \bar{M} ($M \neq M_0^c$), such that p_c is empty at \bar{M} , and (ii) p_c blocks at least one thread that is involved in a

circular-wait deadlock at \overline{M} , i.e., the thread is waiting for the resource from p_c while holding some other resources involved in the deadlock.

Let $C_u^{(i+1)}$ be the covering that corresponds to the optimal solution of $\text{MIP-}\mathcal{N}_{G_1}^c$ in the $(i+1)$ -st iteration of ICOG-O. We consider the following two cases.

Case 1: p_c does not directly induce the deadlock involved in $C_u^{(i+1)}$, i.e., p_c is not part of the deadlock. In this case, the optimal solution of $\text{MIP-}\mathcal{N}_{G_1}^c$ in the $(i+1)$ -st iteration of ICOG-O must also be a feasible solution in the i -th iteration, because, by the assumption of Case 1, this optimal solution is not a new feasible solution induced by p_c . Therefore, $\text{MIP-}\mathcal{N}_{G_1}^c$ guarantees that the number of 1's contained in $C_u^{(i+1)}$ will be greater than or equal to that in $C_u^{(i)}$; otherwise, $C_u^{(i+1)}$ would have been exploited in earlier iterations.

Case 2: p_c directly induces the deadlock involved in $C_u^{(i+1)}$, i.e., p_c is part of the deadlock. In this case, we show that at least $K^{(i)}$ operation places must be marked at $C_u^{(i+1)}$. Since p_c directly induces the deadlock, p_c is empty at $C_u^{(i+1)}$ (Condition (i) mentioned above). Thus, according to Theorem V.2, there must be $M_0(p_c) = K^{(i)} - 1$ different operation places in $\|Y_{p_c}\|$ that are marked at $C_u^{(i+1)}$ in order to empty p_c . Moreover, we know that p_c blocks at least one thread that is involved in the deadlock at $C_u^{(i+1)}$ (Condition (ii) mentioned above). Then, there exists an output transition t of p_c , such that the (unique) input operation place of t (denoted as q_1) is marked at $C_u^{(i+1)}$, which corresponds to a thread blocked by p_c . We argue that $q_1 \notin \|Y_{p_c}\|$. If $q_1 \in \|Y_{p_c}\|$, then the (unique) output operation place of t (denoted as q_2), which belongs to $\|Y_{p_c}\|$ by definition, must satisfy $Y_{p_c}(q_2) > 1$. This contradicts Corollary V.1. Thus, the marked operation place q_1 is different from the aforementioned $K^{(i)} - 1$ marked operation places in $\|Y_{p_c}\|$. As a result, at least $K^{(i)}$ operation places are marked at $C_u^{(i+1)}$, and the number of 1's contained in $C_u^{(i+1)}$, $K^{(i+1)}$, is at least $K^{(i)}$. \square

We conclude this section with an important property of ICOG-O that need not be true for ICOG.

Theorem V.3. *ICOG-O will not synthesize redundant monitor places. That is, there does not exist a pair of monitor places p_{ci} and p_{cj} synthesized by ICOG-O, such that the covering prevented by p_{ci} covers the covering prevented by p_{cj} .*

Proof. For the sake of discussion, let p_{ci} and p_{cj} be the monitor places synthesized in the i -th and j -th iterations of ICOG-O, respectively. Correspondingly, let $C_u^{(i)}$ and $C_u^{(j)}$ be the coverings considered in Step 3 of UCCOR-O in the i -th and j -th iterations of ICOG-O, respectively. That is, p_{ci} is synthesized to prevent $C_u^{(i)}$ and p_{cj} is synthesized to prevent $C_u^{(j)}$.

If $i > j$, then according to Lemma V.1 and the fact that $C_u^{(i)} \neq C_u^{(j)}$, we know that $C_u^{(i)}$ cannot cover $C_u^{(j)}$.

If $i < j$, we want to show that $C_u^{(i)}$ cannot cover $C_u^{(j)}$ either. In the i -th iteration of ICOG-O, p_{ci} is synthesized to prevent $C_u^{(i)}$; hence, any marking covered by $C_u^{(i)}$ will not be reachable in the net considered in the j -th iteration of ICOG-O. As a result, in the j -th iteration, any marking covered by $C_u^{(i)}$ will not be a feasible solution to the state equation of the net, and hence will not be a feasible solution to $\text{MIP-}\mathcal{N}_{G_1}^c$. In other words, in the j -th iteration, the solution of $\text{MIP-}\mathcal{N}_{G_1}^c$ and the corresponding $C_u^{(j)}$ cannot be covered by $C_u^{(i)}$. \square

Theorem V.3 implies that the step “Inter-Iteration Coverability Check” in UCCOR is not necessary in the customized UCCOR-O Algorithm, and the “global bookkeeping set” in ICOG is not necessary in the customized ICOG-O Methodology.

5.6 Experimental evaluation

We discussed above that the development of the control synthesis methodology and the validity of the associated properties are independent of the method used to detect RI empty siphons. However, we observe that the RI empty siphon detection algorithm does play an important role in the efficiency of control synthesis; it is

in fact the computational bottleneck of ICOG-O. This motivated us to develop the customized formulation, $\text{MIP-}\mathcal{N}_{G_1}^c$, for efficient siphon detection in Gadara nets, which we presented in Section 3.8.

While $\text{MIP-}\mathcal{N}_{G_1}^c$ is specifically designed for Gadara nets, siphon detection algorithms for more general classes of Petri nets have been extensively studied in the literature. As discussed in Section 3.8, a generic MIP formulation, MIP-ES, is presented in [11] for the detection of maximal empty siphons in ordinary, structurally bounded Petri nets, and it is one of the most widely used empty siphon detection algorithms in the literature. Our customized algorithm, $\text{MIP-}\mathcal{N}_{G_1}^c$, is inspired by MIP-ES, and it further incorporates the special properties of Gadara nets.

5.6.1 Objective and setup of the experiments

In this section, we investigate the performance of two versions of ICOG-O: (i) the original ICOG-O that uses $\text{MIP-}\mathcal{N}_{G_1}^c$ for siphon detection, and (ii) a modified version of ICOG-O, denoted as ICOG-O-ES, that uses MIP-ES for siphon detection. Since $\text{MIP-}\mathcal{N}_{G_1}^c$ is customized for Gadara nets, while MIP-ES is formulated for general, ordinary bounded Petri nets, we of course expect ICOG-O to be more efficient than ICOG-O-ES in the context of the Gadara nets. Thus, in the following experiments, we use ICOG-O-ES as the baseline for assessing and concretizing this attained efficiency by ICOG-O. We also report a sample of experimental results that demonstrate the scalability of ICOG-O.

Our experiments were completed on a Mac OS X laptop with a 2.4 GHz Intel Core2Duo processor and 2 GB of RAM. Both ICOG-O and ICOG-O-ES are implemented in C++ and compiled under the GNU gcc compiler. The MIP formulations are solved using Gurobi 3.0.1 [30]. Random Gadara nets for these experiments are generated by the random Gadara net generator, as we discussed in Section 3.8. The input parameters of the generator are further explained in

Section 5.6.2 and Table 5.1.

In our experiments, for each set of parameters (each row in Table 5.1), 150 samples of random Gadara nets are generated. The generated nets with no unsafe states³ are removed from the samples. We set a time-out threshold of 10 seconds for the stage of RI empty siphon detection in ICOG-O and ICOG-O-ES. A net times out if it cannot be solved by either MIP- \mathcal{N}_{G1}^c or MIP-ES in less than 10 seconds. Unless otherwise specified, all statistical results reported below are calculated over the sample nets where both ICOG-O and ICOG-O-ES did not time out.

5.6.2 Comparative analysis of ICOG-O and ICOG-O-ES

Figure 5.6 shows the time to converge (TTC) of ICOG-O and ICOG-O-ES. Figure 5.6(a) shows the Normalized Cumulative Frequency (NCF, a.k.a. the empirical cumulative distribution function), as defined in (3.27). The x -axis is the TTC (in seconds), and the y -axis is the NCF, which is the cumulative number of samples normalized by the sample size. A point (x, y) on the graph means that a fraction of y samples have a TTC that is less than x seconds. From Figure 5.6(a), we observe that using ICOG-O, 64% of the samples can be completed within 0.1 second, while using ICOG-O-ES, 18% of the samples can be completed within 0.1 second. Moreover, using ICOG-O, 89% of the samples can be completed within 1 second, while using ICOG-O-ES, 43% of the samples can be completed within 1 second. Figure 5.6(b) is the empirical probability distribution function obtained by kernel density estimation. The x -axis is the TTC, and the y -axis is the probability. We see that using ICOG-O, the majority of the samples can be completed between 0.01 second and 0.1 second, while using ICOG-O-ES, the majority of the sample completion times span a wider range from 0.1 second to 100 seconds.

³A state is said to be *unsafe* if (i) at this state, there exists a deadlock in the corresponding program, or (ii) starting from this state the net will unavoidably or uncontrollably reach a state, where there exists a deadlock in the corresponding program; otherwise it is said to be *safe*.

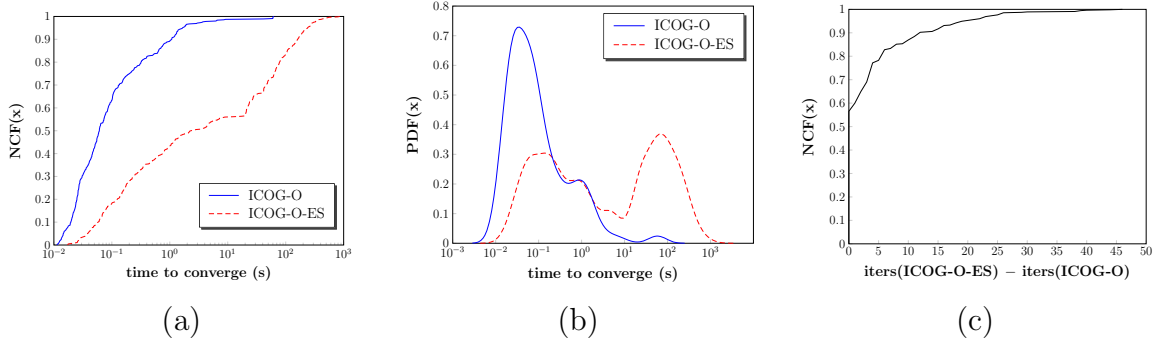


Figure 5.6: (a) TTC of ICOG-O and ICOG-O-ES: Normalized cumulative frequency; (b) TTC of ICOG-O and ICOG-O-ES: Estimated probability density function; (c) Difference of the number of iterations of ICOG-O-ES and ICOG-O

Figure 5.6(c) is the NCF graph for the difference of the number of iterations of ICOG-O-ES and ICOG-O. The x -axis is the extra number of iterations required by ICOG-O-ES as compared to ICOG-O. The y -axis is the NCF. Note that for *all* the samples we tested, ICOG-O always requires fewer or equal number of iterations than ICOG-O-ES; and correspondingly, ICOG-O always synthesizes fewer or equal number of monitor places than ICOG-O-ES. From Figure 5.6(c), we see that ICOG-O requires fewer iterations (and synthesizes fewer monitor places) than ICOG-O-ES for 43% of the samples.

Table 5.1 presents a summary of the experimental results of the comparative analysis between the performance of ICOG-O and that of ICOG-O-ES. For each row of the table, the sub-row with italics corresponds to the performance of ICOG-O-ES, and the counterpart without italics corresponds to the performance of ICOG-O.

The first two columns correspond to the parameters used to generate the random sample Gadara nets. The first (s) and second (a) columns are the number of process subnets and the number of resource acquisitions per subnet. In generating the random nets, the number of resources (locks) in the original Gadara net is set to be 11, the probability of acquiring a new resource before releasing one already held is 0.2, and the branching probability is 0.1.

The third column (TLE) shows the ratio of sample nets that timed out in any iteration of ICOG-O and ICOG-O-ES. The fourth (SS_1) and fifth (US_1) columns describe the state space complexity. The sub-row without italics (resp., with italics) shows the average number of safe and unsafe states that are reachable by the original nets, where ICOG-O (resp., ICOG-O-ES) did not ever time out. Note that ICOG-O and ICOG-O-ES do *not* construct the state space, since they exploit structural properties of Gadara nets; these numbers were generated separately for the sake of scalability assessment.

The sixth column (n) is the number of generated Gadara nets, where both ICOG-O and ICOG-O-ES did not ever time out throughout the iterations. The seventh (P) and eighth (T) columns correspond to the average number of places and transitions in the original Gadara nets. The ninth (SS_2) and tenth (US_2) columns shows the average number of safe and unsafe states that are reachable by the original nets, where both ICOG-O and ICOG-O-ES did not ever time out.

The eleventh column (time (s)) shows the average and standard deviation of the time (in seconds) the entire ICOG-O and ICOG-O-ES processes took until they converged. The twelfth column (iterations) shows the average and standard deviation of the number of iterations for ICOG-O and ICOG-O-ES to converge. Since for any sample net, the number of synthesized monitor places is always 1 less than the number of total iterations, we have not included the number of monitor places in the table. The last column (time/iterations) is the average time per iteration of ICOG-O and ICOG-O-ES.

In the experiments, we observed that the *majority* of time spent by ICOG-O or ICOG-O-ES is on the stage of RI empty siphon detection. This is precisely why we developed a customized MIP formulation for RI empty siphon detection in Gadara nets. Compared to the baseline performance of ICOG-O-ES, the data above show the efficiency attained by ICOG-O – the improvement in average time ranges from 17 to

404 times faster. In addition, the average number of iterations of ICOG-O is smaller than that of ICOG-O-ES for all the cases. From the second to fourth columns, we see that ICOG-O timed out on much fewer nets; and, on average, ICOG-O is able to handle much larger nets than ICOG-O-ES.

5.6.3 Scalability study of ICOG-O

Table 5.2 presents a sample of experimental results that highlight the scalability of ICOG-O. The first (SS) and second (US) columns are the number of safe and unsafe states. (Again, ICOG-O does not expand these states; these numbers were generated separately.) The third column (time (s)) is the total time (in seconds) for ICOG-O to converge. The fourth column (iters) is the number of iterations until convergence. We set a time-out threshold of 6000 seconds for these experiments. Table 5.2 shows that ICOG-O is very scalable even on a modest computer set up.

5.7 Discussion of applications

In the analysis of multithreaded programs, our approach fully exploits the structural properties of the proposed Petri net models, without explicitly constructing the reachability space of the programs [64]. Our choice of Petri nets is also supported by the implementation of control logic. The overhead of controlling software can be generally attributed to two aspects: (i) control logic runtime decisions, and (ii) transitions blocked as a result of the control decisions. With an automaton model, the control decision is based on the global state of the program. In contrast, the control logic in a Petri net model is expressed as a set of decentralized monitor places, which only locally intervene the critical regions that are involved in the

Table 5.1: Experimental results of comparative analysis between ICOG-O and ICOG-O-ES

s	a	TLE	SS ₁	US ₁	n	P	T	SS ₂	US ₂	time (s)		iterations		time	
										μ	σ	μ	σ	μ	σ
6	6	0.00	4,202	969	16	35.62	29.00	1,441	200	0.10	0.21	5.25	7.22	0.02	0.02
		<i>0.11</i>	<i>1,441</i>	<i>200</i>						<i>19.89</i>	<i>52.63</i>	<i>6.38</i>	<i>7.10</i>	<i>3.12</i>	
6	7	0.05	3,341	1,017	27	41.46	34.69	1,612	251	0.19	0.40	8.00	8.98	0.02	0.02
		<i>0.31</i>	<i>1,553</i>	<i>242</i>						<i>41.50</i>	<i>78.72</i>	<i>11.31</i>	<i>11.96</i>	<i>3.67</i>	
6	8	0.14	4,244	958	30	42.93	35.48	2,293	276	0.23	0.50	8.07	10.18	0.03	0.03
		<i>0.32</i>	<i>2,216</i>	<i>267</i>						<i>30.70</i>	<i>51.92</i>	<i>10.17</i>	<i>12.01</i>	<i>3.02</i>	
7	6	0.05	3,146	449	19	38.95	31.89	2,077	230	0.08	0.16	4.84	6.67	0.02	0.02
		<i>0.10</i>	<i>2,077</i>	<i>230</i>						<i>17.48</i>	<i>49.09</i>	<i>5.79</i>	<i>6.64</i>	<i>3.02</i>	
7	7	0.07	7,831	3,030	29	46.79	39.69	3,818	697	0.17	0.33	7.83	8.30	0.02	0.02
		<i>0.34</i>	<i>3,818</i>	<i>697</i>						<i>70.04</i>	<i>160.09</i>	<i>13.35</i>	<i>15.65</i>	<i>5.25</i>	
7	8	0.13	8,969	2,833	36	46.89	39.22	3,746	481	1.89	10.00	8.50	10.08	0.22	0.22
		<i>0.35</i>	<i>3,746</i>	<i>481</i>						<i>32.75</i>	<i>51.58</i>	<i>11.22</i>	<i>11.67</i>	<i>2.92</i>	
8	6	0.00	8,750	1,280	21	43.19	35.76	5,716	483	0.08	0.16	5.14	6.51	0.02	0.02
		<i>0.16</i>	<i>5,716</i>	<i>483</i>						<i>19.21</i>	<i>54.44</i>	<i>5.95</i>	<i>6.22</i>	<i>3.23</i>	
8	7	0.06	12,375	4,484	35	48.14	40.54	5,340	855	0.22	0.40	8.66	9.40	0.03	0.03
		<i>0.31</i>	<i>5,340</i>	<i>855</i>						<i>46.19</i>	<i>69.40</i>	<i>12.86</i>	<i>12.46</i>	<i>3.59</i>	
8	8	0.24	10,413	1,384	37	49.23	41.57	5,731	612	1.95	10.15	8.49	9.71	0.23	0.23
		<i>0.40</i>	<i>5,421</i>	<i>579</i>						<i>38.13</i>	<i>59.51</i>	<i>11.86</i>	<i>11.60</i>	<i>3.22</i>	
8	9	0.17	17,558	4,755	27	48.96	41.00	5,101	789	2.62	12.30	9.35	10.57	0.28	0.28
		<i>0.59</i>	<i>4,912</i>	<i>760</i>						<i>58.55</i>	<i>108.88</i>	<i>13.96</i>	<i>14.91</i>	<i>4.19</i>	
8	10	0.18	12,261	4,155	30	55.90	47.66	8,890	1,895	0.66	1.33	14.52	15.48	0.05	0.05
		<i>0.58</i>	<i>8,594</i>	<i>1,832</i>						<i>79.34</i>	<i>126.98</i>	<i>19.62</i>	<i>21.32</i>	<i>4.04</i>	
9	8	0.14	20,871	5,841	41	54.02	46.05	11,062	1,472	1.85	9.36	11.61	12.87	0.16	0.16
		<i>0.41</i>	<i>11,062</i>	<i>1,472</i>						<i>70.60</i>	<i>141.38</i>	<i>16.07</i>	<i>16.25</i>	<i>4.39</i>	
9	9	0.22	21,314	4,481	30	52.83	44.45	8,791	1,049	1.60	7.66	8.76	9.28	0.18	0.18
		<i>0.61</i>	<i>8,498</i>	<i>1,014</i>						<i>35.63</i>	<i>79.70</i>	<i>12.07</i>	<i>12.41</i>	<i>2.95</i>	
9	10	0.23	19,039	5,091	33	58.67	50.24	10,597	1,763	1.06	2.03	17.70	19.74	0.06	0.06
		<i>0.58</i>	<i>10,597</i>	<i>1,763</i>						<i>104.72</i>	<i>143.20</i>	<i>22.64</i>	<i>23.43</i>	<i>4.63</i>	
10	8	0.15	31,562	6,733	47	55.63	47.28	17,848	1,970	1.51	8.85	8.50	9.03	0.18	0.18
		<i>0.40</i>	<i>17,469</i>	<i>1,929</i>						<i>42.80</i>	<i>60.19</i>	<i>14.33</i>	<i>12.36</i>	<i>2.99</i>	
10	9	0.22	39,690	9,206	37	56.27	47.95	14,721	1,761	0.28	0.45	9.59	9.63	0.03	0.03
		<i>0.56</i>	<i>14,721</i>	<i>1,761</i>						<i>46.00</i>	<i>71.70</i>	<i>14.19</i>	<i>12.72</i>	<i>3.24</i>	
10	10	0.21	34,488	9,676	31	60.03	51.57	14,439	1,319	0.82	1.92	14.27	18.96	0.06	0.06
		<i>0.64</i>	<i>13,973</i>	<i>1,277</i>						<i>80.94</i>	<i>134.43</i>	<i>18.37</i>	<i>22.05</i>	<i>4.41</i>	

Table 5.2: Experimental results of scalability study of ICOG-O

SS	US	time (s)	iters
786,430	487,990	46.05	102
727,240	295,290	2.17	48
532,630	233,800	46.05	61
373,700	136,260	18.45	91
354,270	64,488	25.92	29
336,250	200,370	8.35	83
320,180	118,470	18.35	91
290,970	50,002	3.54	51
285,700	64,386	0.34	13
271,780	64,488	46.21	29
247,920	84,502	26.41	57
226,330	28,242	0.50	20
176,960	26,788	0.42	13
176,920	22,392	0.44	20

potential deadlocks, thus avoiding a global bottleneck for control decisions. A synthesized monitor place is essentially a generalized resource place, whose outgoing arc effectively delays the target lock acquisition action that will otherwise lead to a CMW-deadlock [105]. The similarity between the monitor places and resource places (that model locks) implies that the synthesized control logic can be implemented with primitives supplied by standard multithreading libraries, e.g., `libpthread`. The framework of Gadara nets enables the synthesis of correct and maximally permissive control logic that provably prevents all the potential CMW-deadlocks in the program and will delay a lock acquisition only when necessary [60]. The customized methodology developed in this chapter further guarantees that no redundant control logic is synthesized throughout the iteration process (Theorem V.3).

CHAPTER VI

Evaluation: Analysis of Program Models Using Discrete Event Simulation

6.1 Introduction

Our discussions so far have focused on the class of *untimed* Petri nets and mainly addressed *logical* level properties, e.g., deadlock-freeness. In this chapter, we extend our models to the class of *stochastic timed* Petri nets and use them to investigate the *quantitative* performance of programs, before and after control, via discrete event simulation.

Our simulation analysis principally investigates three aspects: the impact of the synthesized control logic on the program's performance; the effect of key parameters on the program before and after control; and the tradeoff between aggressive and conservative deadlock-avoidance control strategies. More importantly, our study provides a general simulation-based methodology to evaluate the performance of multithreaded program models when deadlock-avoidance control logic is applied. Therefore, our contributions are both in terms of modeling methodology and analysis methodology for the problem under consideration.

This chapter is organized as follows. We introduce relevant background in Section 6.2. The proposed discrete event simulation model is described in Section 6.3,

and the performance metrics are introduced in Section 6.4. We present the simulation results and analysis of two cases of deadlock-prone programs in Section 6.5. Finally, we discuss related work and applications in Section 6.6. Some of the results in this chapter also appear in [63].

6.2 Stochastic timed Gadara net model

Based on Definition II.2, we can further define a stochastic timed-place Petri net as follows [8, 102].

Definition VI.1. A stochastic timed-place Petri net is a six-tuple $\mathcal{N} = (P, T, A, W, M_0, \mathbf{V})$, where $\mathcal{N} = (P, T, A, W, M_0)$ is a Petri net, and, $\mathbf{V} : P \rightarrow \mathbb{R}^+$ is a timing structure that associates places with stochastic time delays.

From Chapter II, we know that the tokens in $P_0 \cup P_S$ represent the threads and drive the dynamics of the net, while the tokens in $P_R \cup P_C$ represent the availability of (generalized) resources. This implies that for the purpose of simulation of Gadara nets, we *only* need to consider delay times associated with idle or operation places, which represent thread waiting or execution times. More specifically, based on Definition VI.1, in a *stochastic timed-place Gadara net*, the timing structure is as follows.

$$\mathbf{V} : P_0 \cup P_S \rightarrow \mathbb{R}^+ \quad (6.1)$$

In general, timed Petri nets can have delays associated with transitions or places, which results in *timed-transition Petri nets* or *timed-place Petri nets*, respectively. From a theoretical viewpoint, these two subclasses of nets are expressively equivalent [95]. In timed-transition Petri net models of physical systems, transitions usually represent actions in the system that take time to complete, while places and tokens usually represent the pre-conditions of the execution of the actions, which are not directly related to time. In contrast, in the proposed timed-place

Gadara net models of multithreaded programs, we only need to assign time delays to idle and operation places, because these places and tokens therein are used to model thread executions, which take time to complete; transitions are used to model branches or lock allocations and releases, which can be completed in the program instantaneously (when enabled). In this chapter, we assume that all the delay times follow exponential distribution. However, our proposed simulation model can be applied to any general distribution.

6.3 The discrete event simulation model

We follow the simulation framework proposed in Section 1.3.2 of [52], with necessary extensions to incorporate the special features in Petri nets. The basic components of our simulation model are defined as follows.

The *system* being simulated is the Gadara net \mathcal{N}_G , which is obtained from a multithreaded program. The *system state* is the marking (or state) of \mathcal{N}_G . An *event* is the firing of a transition in \mathcal{N}_G . An event is denoted as a two-tuple (τ, t) , where τ is the scheduled event time, and t is the transition scheduled to fire at time τ .

We maintain an *enhanced event list* in our simulation. This is due to a special dynamic feature in Petri nets: a transition, which is scheduled to fire at some time, say τ , can be *disabled* in the net at τ due to lack of tokens in its input place. Moreover, since it corresponds to a pending action of the multithreaded program we study, this scheduled event cannot be discarded, but rather, it should be “backlogged” and fired whenever it becomes enabled after τ . Any element in the enhanced event list is an event and is denoted as a two-tuple (τ, t) as defined above. As shown in Figure 6.1, the proposed enhanced event list is divided into two parts: (i) *Future Event List (FEL)*, that records the scheduled events for future execution; (ii) *Backlogged Event List (BEL)*, that records the backlogged events to be executed once they become enabled under a “First-Come First-Served” discipline. Other relevant approaches

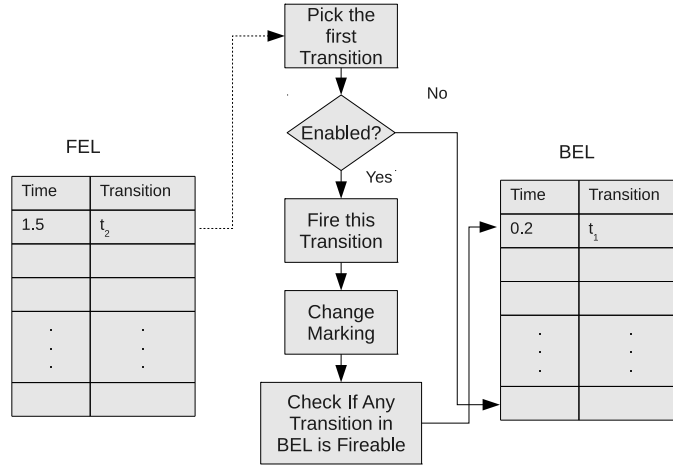


Figure 6.1: Enhanced event list

dealing with this situation include rescheduling a new time for the disabled transition once it becomes enabled [31], and maintaining different event chains as in General Purpose Simulation System (GPSS).

The *main function* invokes several routines throughout the simulation, including *initialization routine*, *timing routine*, *event routine*, and *report generator*. They follow the standard simulation framework as described in [52]. Here, we further describe the *event-scheduling* scheme that is customized for the special features of \mathcal{N}_G . At the beginning of the simulation, for each token in any idle place $p \in P_0$, the simulation program schedules a (future) time to fire the output transition of p . During the simulation, when a token enters an operation place $p \in P_S$, the simulation program immediately schedules a (future) time to fire the output transition of p . In both cases, the time is scheduled according to the delay time distribution associated with p . When p has more than one output transition (e.g., when the output transitions of p model *if/else*), the simulation program first selects one of the output transitions of p , according to some pre-specified probability distribution. Then, the simulation program schedules a time to fire the selected transition according to the delay time distribution associated with p .

Due to the nature of the problem, our simulation falls into the class of *terminating*

simulations. There are two alternative *terminating events*: (i) $E_1 = \{\text{a transition is fired so that the system goes back to the initial state}\}$; (ii) $E_2 = \{\text{a transition is fired so that the system goes into a deadlock state}\}$. The simulation terminates if either E_1 or E_2 occurs.

6.4 Performance metrics

We are interested in the following three performance metrics. These metrics are measured for program models before and after deadlock-avoidance control is applied. A comparison analysis between the original uncontrolled program model and the controlled program model is conducted based on these metrics.

6.4.1 Measure of safety

A program is *safe* if no deadlock ever occurs; otherwise, it is *unsafe*. Given a Gadara net model of a deadlock-prone program, we want to measure the *deadlock probability*, P_d , of this program. Assume we make n independent replications of the simulation. Let X_i be the random variable associated with the i -th replication, which is defined as follows.

$$X_i = \begin{cases} 0, & \text{if the } i\text{-th replication terminates with event } E_1; \\ 1, & \text{if the } i\text{-th replication terminates with event } E_2. \end{cases} \quad (6.2)$$

According to Section 9.4.2 of [52], we know that

$$\hat{P}_d = \frac{\sum_{i=1}^n X_i}{n} \quad (6.3)$$

is an unbiased point estimator for P_d .

6.4.2 Measure of efficiency

We use the average total time the threads take to complete their tasks to characterize the *efficiency* of the program. Thus, we measure the *Mean Time To Finish (MTTF)*, given that no deadlock occurs in the program. MTTF is estimated by mean termination times of the replications that terminate with event E_1 .

6.4.3 Measure of activity level

We use the average number of threads, which are simultaneously executing in the critical region, to characterize the *activity level* of the program, which also reflects the program's concurrency level. According to the definition of Gadara nets, the critical region is captured by the set of operation places. Therefore, the activity level, β , can be estimated as follows.

$$\hat{\beta} = \sum_{p \in P_0} M_0(p) - \sum_{p \in P_0} \hat{U}(p) \quad (6.4)$$

where $M_0(p)$ is the initial number of tokens in place p , and where $\hat{U}(p)$ is the expected time-average number of tokens in place p given that no deadlock occurs in the program. In (6.4), the first term represents, at the initial state, the total number of threads waiting in the idle places; the second term represents, throughout the simulation, the average number of threads waiting in the idle places. The difference of these two terms, $\hat{\beta}$, represents the average number of threads executing in the operation places throughout the simulation.

The measure $\hat{U}(p)$, also known as the *utilization* of place p , can be estimated as:

$$\hat{U}(p) = E \left[\frac{\int_0^T M_\tau(p) d\tau}{T} \right] \quad (6.5)$$

where $M_\tau(p)$ is the number of tokens in place p at time τ and T is the termination time of a replication that terminates with event E_1 . Note that T is a random variable, and

the expectation is with respect to T . $\hat{U}(p)$ can be measured by standard techniques employed in the simulation analysis of queueing systems for estimating average queue length or average server utilization.

6.5 Case studies

We present our simulation study for two deadlock-prone Gadara nets, both before and after control. The sensitivity analysis reports the performance metrics introduced in Section 6.4 for a range of values of key parameters. For each case, we carried out 20,000 replications. When comparing the before-control and after-control nets in each example, we employ the *Common Random Number (CRN)* technique to facilitate the comparison analysis.

6.5.1 Case study 1: A deadlock scenario in OpenLDAP

OpenLDAP is a popular open-source implementation of the Lightweight Directory Access Protocol (LDAP). In Example IV.7, we discussed the Gadara net model of a deadlock case in the OpenLDAP software, as shown in Figure 4.5. The Gadara net, shown in solid lines, is the program model before control. A deadlock will occur if one token (representing thread 1) is in place p_5 and another token (representing thread 2) is in place p_1 . In this scenario, thread 1 is holding lock B and waiting for lock A, while thread 2 is holding A and waiting for B. The program model after control is the entire net shown in Figure 4.5, where the synthesized monitor place is shown in dashed lines. In presence of the monitor place, the aforementioned deadlock will not be reachable in the controlled model.

Recall that each operation place models a code segment where a thread can execute. So the random delay time associated with each operation place should reflect the execution time of the involved thread. Methodologies for determining the accurate execution time of code segments have been developed by researchers in the

area of real-time embedded systems [32]. One conventional approach is to assume that the execution time of each instruction is a constant. However, factors such as machine status can also add randomness to the execution time. For the purpose of our present study, we will assume that the delay associated with each operation place is exponentially distributed with mean equal to 1. At the beginning of each replication, we schedule each token in p_0 to fire t_1 after a random delay time that is exponentially distributed with mean μ , which is chosen to be 0.5 in this study. Simulations for other values of μ can be carried out in a similar manner.

We employ sensitivity analysis to study the effect of the program parameter, namely branch selection probability distribution, on the program's performance. There are two branch selections in this example: t_4/t_5 and t_6/t_7 . If there is a thread in p_3 , we assume this thread will choose branch t_4 with probability π_4 and choose branch t_5 with probability $1 - \pi_4$. Similarly, if there is a thread in p_4 , we assume this thread will choose branch t_6 with probability π_6 and choose branch t_7 with probability $1 - \pi_6$.

The deadlock probability P_d of the uncontrolled model under various values of (π_4, π_6) is shown in Figure 6.2. We observe that the smaller the values of π_4 and π_6 are, the larger the value of P_d is. This observation agrees with our intuition: when π_4 and π_6 decrease, the thread holding lock B is more likely to enter the loop (p_4, p_5 , and p_6) to acquire lock A, and thus more likely to enter a CMW deadlock. The deadlock probability of the controlled model is always 0, which is also demonstrated by simulation.

The MTTF of the uncontrolled and controlled models, under various values of (π_4, π_6) , are shown in Figures 6.3(a) and (b), respectively, where the z -axis is on a log-scale. We observe that MTTF increases in controlled models. One reason leading to the increase is the imposition of the synthesized monitor place. Another important reason is that the calculation of the statistics of MTTF before control only

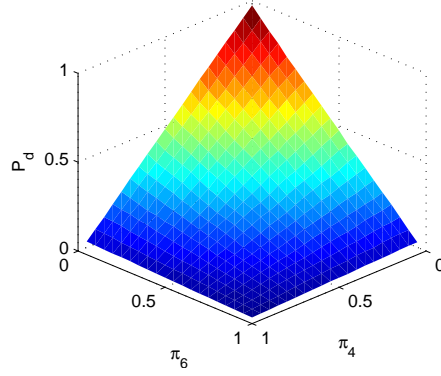


Figure 6.2: P_d of uncontrolled program model under various values of (π_4, π_6)

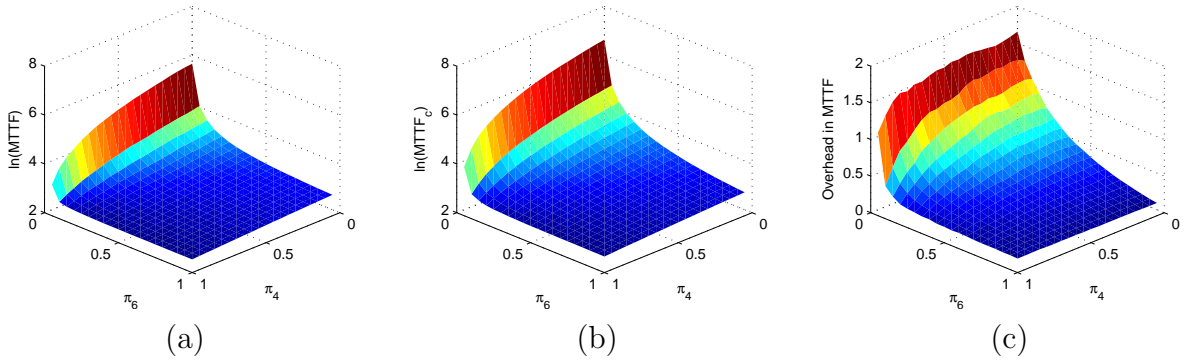


Figure 6.3: MTTF under various values of (π_4, π_6) : (a) Before control; (b) After control; (c) Overhead

takes into account those replications that did not deadlock, and ignores the ones that deadlocked. In other words, MTTF before control is “biased downwards” because it only considers deadlock-free replications. To quantify this comparison, we further compute the overhead in MTTF, which is defined as the ratio of the increase in MTTF after control and the original MTTF before control. The overhead in MTTF is shown in Figure 6.3(c). We see that π_6 , which directly affects the probability of entering the loop (p_4 , p_5 , and p_6), is the key factor in the MTTF performance of program models. There exists a threshold value for π_6 , denoted as TH_{π_6} . When π_6 is smaller than TH_{π_6} , MTTF in uncontrolled and controlled models as well as the overhead in MTTF dramatically increase.

The β of the uncontrolled and controlled models, under various values of $(\pi_4,$

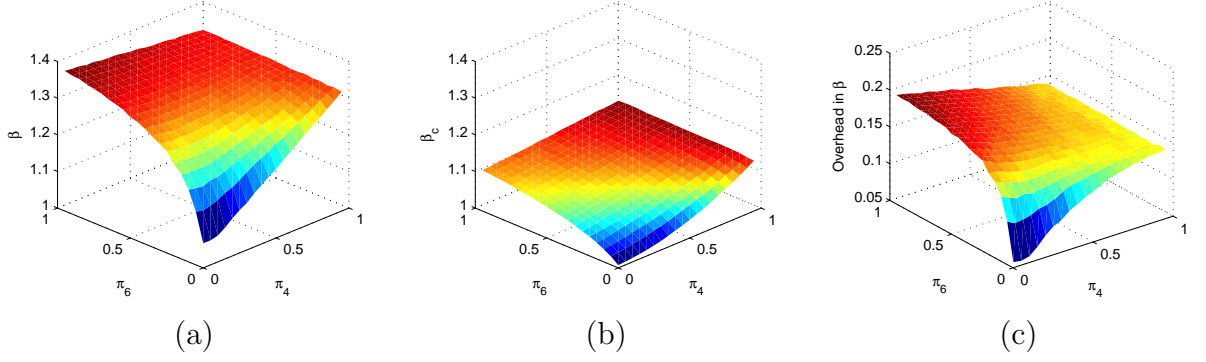


Figure 6.4: β under various values of (π_4, π_6) : (a) Before control; (b) After control; (c) Overhead

π_6), are shown in Figures 6.4(a) and (b), respectively. We see that β decreases in controlled models. Similarly, we compute the overhead in β , which is defined as the ratio of the decrease in β after control and the original β before control. The overhead in β is shown in Figure 6.4(c). We also see that β decreases when π_4 and π_6 decrease. This observation agrees with our analysis above. When π_4 and π_6 decrease, the uncontrolled model has a higher deadlock probability, and the effect of the monitor place in the controlled model is more prominent, thus the overall thread activity decreases. Note that in this situation, the overhead in β also decreases.

Remark VI.1. In practice, if the consequence of the potential deadlock is manageable, then we can operate the monitor place to balance P_d against MTTF and β . When π_4 and π_6 are large, we know from Figure 6.2 that P_d is small in the uncontrolled model, thus we can turn off the monitor place, and avoid the overhead in MTTF and β . As shown in Figure 6.4(c), the saved overhead in β in this case is relatively large. \square

6.5.2 Case study 2: Two threads sharing three resources

The second case we will study is the Gadara net model of a multithreaded simulator for a hypothetical concurrent healthcare system. As shown in Figure 6.5, the original Gadara net before control is shown in solid lines. The subnet \mathcal{N}_1 models the first patient flow, and the subnet \mathcal{N}_2 models the second patient flow. The resource

places r_A , r_B , and r_C model the nurse, physician, and medical equipment, respectively. The two patient flows represent two prototype procedures of medical treatment. Each flow consists of five treatment stages, as modeled by the operation places. The requirement of resources in each treatment stage is self-explanatory from the Gadara net.

The multithreaded simulator can use mutexes to prevent the above three resources from being accessed concurrently. Thus, the potential deadlocks of the system can manifest themselves in the multithreaded simulator at run time. There are two potential deadlock scenarios in this example: one deadlock occurs when $M(p_{11}) = M(p_{23}) = 1$; another deadlock occurs when $M(p_{13}) = M(p_{21}) = 1$. (The unspecified operation places are empty by default; the marking of resource and idle places can be uniquely determined based on the marking of operation places.) There are also three *deadlock-free unsafe states*: (i) $M(p_{11}) = M(p_{21}) = 1$, (ii) $M(p_{11}) = M(p_{22}) = 1$, and (iii) $M(p_{12}) = M(p_{21}) = 1$. When the net is in any of these states, even if it is not in a deadlock, it will unavoidably enter a deadlock in the future. Thus, we need to synthesize control logic to prevent all of the aforementioned states. The control synthesis constructs three monitor places, as shown in dashed lines in Figure 6.5.¹ The various combinations of ON/OFF of these monitor places lead to eight different control strategies, as defined in Table 6.1.

In the simulation, the delays associated with operation places are exponentially distributed. For the five operation places p_{11} to p_{15} in \mathcal{N}_1 , the mean parameters are 1, 2, 1, 5, and 12, respectively; for the five operation places p_{21} to p_{25} in \mathcal{N}_2 , the mean parameters are 3, 5, 1, 2, and 1, respectively. In addition, the delays associated with p_{01} and p_{02} are exponentially distributed with means μ_1 and μ_2 , respectively.

For the eight control strategies shown in Table 6.1, one can think of Strategy 1

¹The original Gadara net before control in Figure 6.5 is the same as that in Figure 4.1, while we have used different control synthesis algorithms in these two cases. More specifically, the monitor places in Figure 6.5 are synthesized by the algorithm presented in Section IV.A.1 of [59].

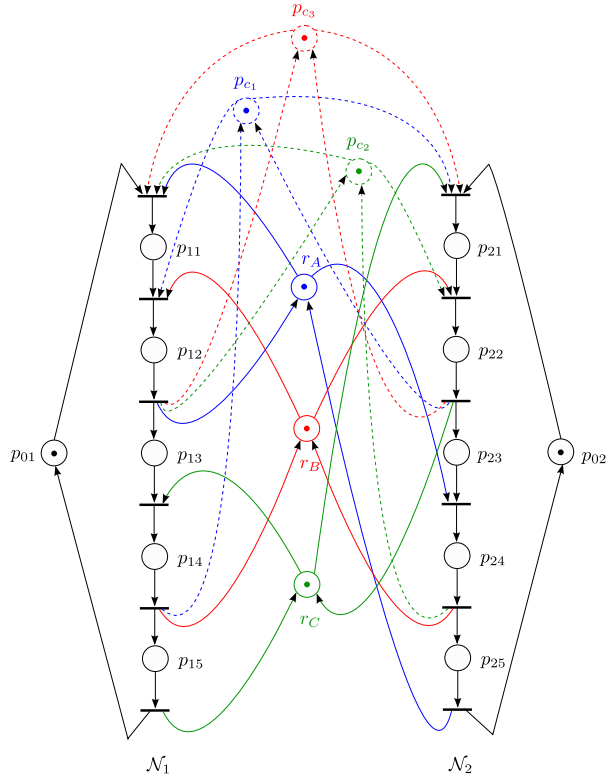


Figure 6.5: A Gadara net model of two threads sharing three resources

as the most “aggressive” control, since it turns off all three monitor places for better performance in terms of MTTF and β ; on the other hand, Strategy 8 can be considered as the most “conservative” control, since it turns on all three monitor places, which *guarantees* deadlock-freeness in the controlled model at the price of degraded performance for MTTF and β . We have conducted sensitivity analysis to study the effect of μ_1 and μ_2 on the program’s performance under these eight control strategies. *Our goal is:* given a tradeoff criterion between P_d and MTTF (or β), find the best control strategy for any pair of (μ_1, μ_2) .

To illustrate, let us consider the sensitivity analysis results for Strategy 2 (i.e., p_{c3} only), which are shown in Figure 6.6. To measure the effectiveness of deadlock reduction of a certain control strategy, we introduce the *deadlock probability reduction rate*, ρ , which is defined as the ratio between the decrease in deadlock probability due to this strategy in the controlled model and P_d of the uncontrolled model. The metric

Table 6.1: Definition of control strategies

Strategy	Monitor p_{c_1}	Monitor p_{c_2}	Monitor p_{c_3}
1	OFF	OFF	OFF
2	OFF	OFF	ON
3	OFF	ON	OFF
4	ON	OFF	OFF
5	OFF	ON	ON
6	ON	OFF	ON
7	ON	ON	OFF
8	ON	ON	ON

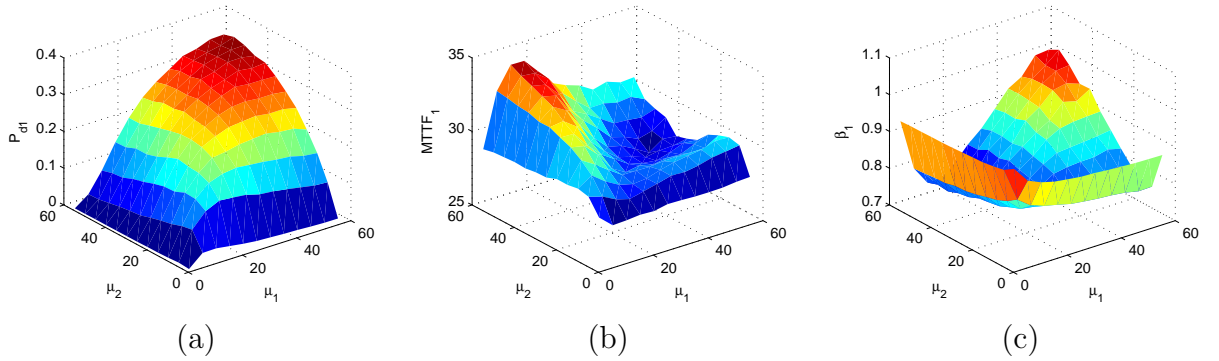


Figure 6.6: Sensitivity analysis results for Strategy 2: (a) P_d ; (b) $MTTF$; (c) β

ρ of Strategy 2, derived from the results in Figure 6.6(a) and the counterpart of the uncontrolled model, is shown in Figure 6.7. It is interesting to see that when μ_1 and μ_2 are small, by using Strategy 2, the monitor place p_{c_3} alone can prevent most of the potential deadlocks. Therefore, similar in spirit to the discussion in Remark VI.1, if the consequence of the potential deadlock is manageable (e.g., one of the patients in deadlock can be rescheduled without jeopardizing his/her health), then we can employ Strategy 2 (instead of the most conservative Strategy 8) to gain better $MTTF$ and β performance when μ_1 and μ_2 are small. Similar analysis can be carried out for all the other strategies.

If one can specify a minimum allowed value for ρ , say ρ_0 , based on the empirical analysis of system tolerance, then a possible tradeoff criterion (between P_d and $MTTF$) for selecting a control strategy is: given ρ_0 and (μ_1, μ_2) , find the best strategy

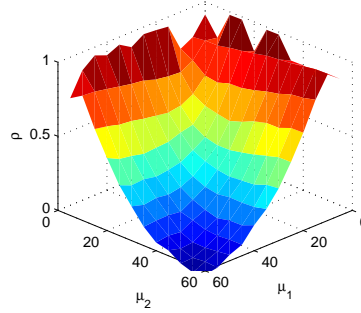


Figure 6.7: Deadlock probability reduction rate of Strategy 2

such that (i) its ρ is greater than ρ_0 , and (ii) its MTTF is as small as possible. Based on our sensitivity analysis results obtained above, the best strategy at (μ_1, μ_2) can be found by first searching for the set of strategies whose ρ is greater than ρ_0 , then selecting the one whose MTTF is the smallest in this set. After conducting this search process for all pairs of (μ_1, μ_2) of interest, we can construct a *Control Strategy Map*, under the tradeoff between P_d and MTTF, on the μ_1 - μ_2 plane as shown in Figure 6.8(a). Using the above sensitivity analysis results, we can construct various forms of Control Strategy Maps according to specific needs. For instance, if we substitute Condition (ii) above by “(ii’) its β is as large as possible”, then we can obtain a Control Strategy Map under the tradeoff between P_d and β , as shown in Figure 6.8(b). For both maps in Figure 6.8, we chose $\rho_0 = 0.75$. Further extensions are possible by using a requirement in terms of a maximum allowed value for P_d , instead of Condition (i) above.

6.6 Discussion of related work and applications

With the increasing complexity of simulation models driven by the demand for higher accuracy, and the prevalence of multicore architectures in computer hardware, parallel programming techniques are being deployed in the field of simulation to enhance computational capacity and efficiency [67, 33, 23, 73, 112, 51]. Similar to general purpose concurrent software, circular-wait deadlock is also an

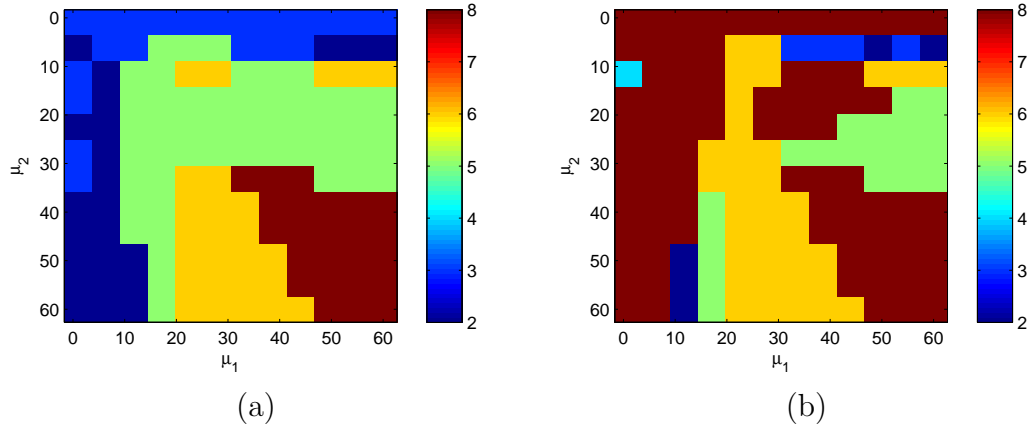


Figure 6.8: Control Strategy Maps: (a) Tradeoff between P_d and MTTF; (b) Tradeoff between P_d and β

important class of failure in parallel simulations, where a set of *tasks* are waiting for one another indefinitely and no progress can be made. The deadlock problem incurred by event message processing in parallel discrete event simulation has been investigated previously, and various conservative solutions were proposed; see, e.g., [21]. Conservative algorithms were further evaluated and compared in [4]. A circular-wait deadlock can also be induced by lack of *resources* due to contention among concurrent tasks. Reference [50] presented a deadlock detection algorithm in simulation models by using a linked list structure of resources and tasks. Various algorithms have been reported for deadlock analysis using graph theoretic models; see, e.g., [109, 100, 9]. An algorithm based on dependency graphs has also been reported for deadlock detection in system level design [9]. Recently, an object-oriented, bottom-up approach to simulation modeling using Petri nets has been presented [69], where the desired property of deadlock-freeness can be verified in small subsets, and is preserved in the synthesized large model.

We are interested in multithreaded programs that use shared data, a common paradigm for general-purpose concurrent software. This programming technique has also been employed in multithreaded simulators [36, 73, 112]. Case studies 1 and 2 presented in this chapter represent the two levels at which CMW deadlocks may arise

in applications: *the program source code* itself, and *the system being simulated* in the case of simulation analysis. Our investigations pertain to deadlocks that may arise at either of these two levels.

At the *program* level, the aforementioned tasks are the concurrent threads that are executing, and the resources are sections of shared data in memory. In this case, mutexes prevent threads from accessing the same data concurrently, thus allowing threads to update the shared data in an orderly manner. Misuse of mutexes by programmers can lead to CMW deadlocks. Case Study 1, presented in Section 6.5.1, addresses this type of program-level deadlock.

At the *system simulation* level, the aforementioned tasks and resources can model various entities in different contexts. For example, in flexible manufacturing system simulation, the tasks can be parallel assembly lines, and the resources can be machines processing the parts of a product; in healthcare system simulation, the tasks can be concurrent patient flows, and the resources can be physicians, nurses, or medical equipment. In multithreaded simulations, these shared resources are protected via mutexes by the tasks that first acquire them. If the system design is such that deadlocks due to shared resources can arise, and no proper efforts are made to avoid them, then these deadlocks can potentially manifest themselves as CMW deadlocks when the system is being simulated. Case Study 2, presented in Section 6.5.2, addresses the deadlock problem at this level.

A similar analytical approach has also been employed to study software contention in computer systems [91]. Our proposed methodology works for general-purpose multithreaded software; in particular, it can be applied to multithreaded simulators. In this latter context, the deadlock-avoidance control logic synthesized by our method applies to CMW deadlocks at both the aforementioned program and system levels.

In the context of discrete event simulation, in contrast to [69] where Petri nets have been used in the simulation modeling phase to prevent deadlocks, we focus on

existing simulation models and their associated multithreaded programs, which may be deadlock-prone. Also, in contrast to [109, 100], where graph theoretic models are used for deadlock detection and resolution, we not only detect deadlocks via formal methods in Petri nets, but also synthesize *optimal* control logic to *provably* prevent potential CMW deadlocks.

CHAPTER VII

Conclusion

7.1 Summary of main contributions

We have adopted a model-based approach and proposed a new class of Petri nets, called Gadara nets, to systematically model, analyze, and control concurrent software for the purpose of deadlock avoidance. We have established a set of important properties of Gadara nets. The liveness and reversibility properties provide a means to map the *behavioral* objective of the CMW-deadlock-freeness of a program to the *structural* requirement on its corresponding Gadara net model, which in turn lays the foundations for the structure-based optimal control synthesis of Gadara nets. The linear separability property further shows the feasibility of optimal control synthesis through monitor places.

In order to avoid CMW-deadlocks of a program, we require the *liveness* of its corresponding Petri net model. Thus, liveness is the key Petri net property under study in this dissertation. We have proposed a set of customized mathematical programming algorithms for the verification of liveness of Gadara nets and compared their performance with generic algorithms that are well-known in the literature. The proposed algorithms also yield some certain types of siphons that can be used in the control synthesis.

Based on the established properties of Gadara nets, we have proposed an optimal

control synthesis methodology for general Gadara nets that need not be ordinary. The method is an iterative process and converges in a finite number of iterations. It exploits the structural properties of Gadara nets via siphon analysis, without the need to construct the reachability space of the nets. The resulting control logic is optimal, i.e., it enforces liveness of Gadara nets in a maximally permissive manner. Our proposed method also takes into account the net uncontrollability and guarantees that the resulting controlled net is always admissible.

The above general control synthesis methodology possesses an interesting property that, for any monitor place synthesized by this method, all its incoming and outgoing arcs have *unit* arc weights. In the particular application of concurrent software, a Gadara net model of a program before control is always ordinary, and hence we always have an ordinary Gadara net as the initial condition in the control synthesis. This motivates us to investigate the customization of the general control synthesis methodology for ordinary Gadara nets. The customized methodology preserves all the properties of the general one, and it has the further property that it will never synthesize redundant control logic throughout the control iterations.

We have extended the class of untimed Gadara nets to the class of stochastic timed Gadara nets and proposed a customized discrete event simulation methodology for the extended class. We have conducted simulation analysis on the Gadara net models of programs to study a set of performance metrics, including safety, efficiency, and activity level. We have further conducted sensitivity analysis to investigate the effect of key parameters on the programs and the implication for deadlock-avoidance control.

The class of Gadara nets together with its associated analysis and control synthesis techniques provide a novel technology for the systematic, rigorous, principled control of multithreaded programs. The results developed in this dissertation make it possible to formalize and automate the procedure of modeling, analyzing, and controlling multithreaded programs. They also contribute new theoretical developments to the

control of Petri nets, which have a significant potential to be extended to a broader class of resource allocation systems and other application domains [58].

7.2 Future work

For large-scale resource allocation systems, such as concurrent software, scalability is a key property that must be possessed by the control synthesis algorithms. Our experiments on large-scale, randomly generated programs demonstrate the attained efficiency of our methods as compared to some existing approaches. However, our method did time out on some large, complex sample nets. We observe that the sole computational bottleneck in the proposed methodology is the MIP algorithms. Therefore, we are interested in developing even more efficient algorithms for the detection of unsafe states that correspond to program deadlocks. One potential direction is to formulate the above detection task as a Boolean satisfiability problem and leverage the existing SAT solvers to find feasible solutions [12, 29, 46, 66].

We have shown that our proposed methodology will not synthesize redundant control logic. Yet the number of monitor places synthesized is not minimal in general. Nazeem *et al.* [76] exploit the reachability space of the nets and use classification theory to find a minimum-size control solution in terms of the number of monitor places. We can further reduce the number of obtained monitor places by using some of the techniques in this paper.

In practice, a multithreaded program may not satisfy the semiflow condition (Condition 5 of Definition II.6) for every resource due to programming language complications and missing information in the CFG representation. For example, a thread may acquire a lock without releasing it. In this case, users may restore the semiflow manually, such as adding annotations to the program source code [104]. In future work, we are interested in automating this process by conducting systematic lock/unlock pairing analysis [10].

An important condition of Gadara nets is that every resource place contains only one initial token (Condition 6 of Definition II.6), which models the availability of a mutual exclusion lock. On the one hand, this condition is critical to our development of the optimal control synthesis algorithms. On the other hand, this condition also implies that Gadara nets may not be able to model other types of synchronization primitives, such as *semaphore*, which is essentially a resource with an arbitrary capacity. Another example is the *reader-writer lock*, which allows concurrent readers and hence requires a resource with a capacity larger than one. Both semaphores and reader-writer locks can be modeled by resource places with possibly more than one initial token. Therefore, the modeling of these synchronization primitives calls for an extension of the existing Gadara net models.

A consequence of relaxing the above condition is that the safe region in the hyperspace defined by reachable markings may no longer be linearly separable (i.e., Theorem III.5 no longer holds for the extended models). As a result, optimal control logic cannot in general be synthesized through monitor places by SBPI for these models. Optimal control in this case could be achieved using non-linear policy structures and representations, such as the generalized algebraic deadlock avoidance policies proposed previously [90] and the control policies based on classification theory [74]. We can customize these approaches for the extended Gadara net models.

The Gadara project has opened many new research directions for discrete event control, where we approach offline synthesis and online implementation in a formal and integrated framework. From a more general perspective, the results in this dissertation demonstrate that software failure avoidance is a fertile application area for discrete event control. Moreover, special features from this application area are motivating further theoretical developments on the control of discrete event systems.

BIBLIOGRAPHY

- [1] Allen, L. V. (2010), Verification and anomaly detection for event-based control of manufacturing systems, Ph.D. thesis, University of Michigan.
- [2] Allen, L. V., and D. M. Tilbury (2012), Anomaly detection using model generation for event-based systems without a preexisting formal model, *IEEE Transactions on Systems, Man and Cybernetics, Part A: Systems and Humans*, 42(3), 654–668.
- [3] Auer, A., J. Dingel, and K. Rudie (2009), Concurrency control generation for dynamic threads using discrete-event systems, in *Proc. Allerton Conference on Communication, Control and Computing*.
- [4] Bagrodia, R. L., and M. Takai (2000), Performance evaluation of conservative algorithms in parallel simulation languages, *IEEE Transactions on Parallel and Distributed Systems*, 11(4), 395–411.
- [5] Barkaoui, K., and J.-F. Pradat-Peyre (1996), On liveness and controlled siphons in Petri nets, in *Proc. the 17th International Conference on Applications and Theory of Petri Nets*, pp. 57–72.
- [6] Boer, E. R., and T. Murata (1994), Generating basis siphons and traps of Petri nets using the sign incidence matrix, *IEEE Transactions on Circuits and Systems—I*, 41(4), 266–271.
- [7] Cano, E. E., C. A. Rovetto, and J.-M. Colom (2010), An algorithm to compute the minimal siphons in S^4PR nets, in *Proc. International Workshop on Discrete Event Systems*, pp. 18–23.
- [8] Cassandras, C. G., and S. Lafortune (2008), *Introduction to Discrete Event Systems*, 2nd ed., Springer, Boston, MA.
- [9] Cheung, E., X. Chen, H. Hsieh, A. Davare, A. Sangiovanni-Vincentelli, and Y. Watanabe (2009), Runtime deadlock analysis for system level design, *Design Automation for Embedded Systems*, 13(4), 287–310.
- [10] Cho, H. K., Y. Wang, H. Liao, T. Kelly, S. Lafortune, and S. Mahlke (2012), Practical lock/unlock pairing for concurrent programs, *Tech. rep.*, University of Michigan.

- [11] Chu, F., and X.-L. Xie (1997), Deadlock analysis of Petri nets using siphons and mathematical programming, *IEEE Transactions on Robotics and Automation*, 13(6), 793–804.
- [12] Claessen, K., N. Een, M. Sheeran, N. Sorensson, A. Voronov, and K. Akesson (2009), SAT-solving in practice, with a tutorial example from supervisory control, *Discrete Event Dynamic Systems: Theory and Applications*, 19(4), 495–524.
- [13] Costa, M., M. Castro, L. Zhou, L. Zhang, and M. Peinado (2007), Bouncer: Securing software by blocking bad input, in *Proc. ACM SIGOPS symposium on Operating systems principles*, pp. 117–130.
- [14] Delaval, G., H. Marchand, and E. Rutten (2010), Contracts for modular discrete controller synthesis, in *Proc. ACM Conference on Languages, Compilers and Tools for Embedded Systems*.
- [15] Dijkstra, E. W. (1965), Solution of a problem in concurrent programming control, *Communications of the ACM*, 8(9).
- [16] Dijkstra, E. W. (1982), *Selected Writings on Computing: A Personal Perspective*, chap. The Mathematics Behind the Banker’s Algorithm, pp. 308–312, Springer-Verlag.
- [17] Dragert, C., J. Dingel, and K. Rudie (2008), Generation of concurrency control code using discrete-event systems theory, in *Proc. ACM International Symposium on Foundations of Software Engineering*.
- [18] Engler, D., and K. Ashcraft (2003), RacerX: Effective, static detection of race conditions and deadlocks, in *Proc. the 19th ACM Symposium on Operating Systems Principles*.
- [19] Ezpeleta, J., J. M. Colom, and J. Martínez (1995), A Petri net based deadlock prevention policy for flexible manufacturing systems, *IEEE Transactions on Robotics and Automation*, 11(2), 173–184.
- [20] Ezpeleta, J., F. García-Vallés, and J. M. Colom (2002), A banker’s solution for deadlock avoidance in FMS with flexible routing and multiresource states, *IEEE Transactions on Robotics and Automation*, 18(4), 621–625.
- [21] Fujimoto, R. M. (1990), Parallel discrete event simulation, *Communications of the ACM*, 33(10), 30–53.
- [22] Gamatie, A., H. Yu, G. Delaval, and E. Rutten (2009), A case study on controller synthesis for data-intensive embedded system, in *Proc. International Conference on Embedded Software and Systems*.

- [23] Geist, R., J. Hicks, M. Smotherman, and J. Westall (2005), Parallel simulation of Petri nets on desktop PC hardware, in *Proc. the 2005 Winter Simulation Conference*, pp. 374–383.
- [24] Gerakios, P., N. Papaspyrou, and K. Sagonas (2011), A type and effect system for deadlock avoidance in low-level languages, in *Proc. the 7th ACM SIGPLAN workshop on Types in language design and implementation*, pp. 15–28.
- [25] Gerakios, P., N. Papaspyrou, K. Sagonas, and P. Vekris (2011), Dynamic deadlock avoidance in systems code using statically inferred effects, in *Proc. the 6th Workshop on Programming Languages and Operating Systems*.
- [26] Ghaffari, A., N. Rezg, and X. Xie (2003), Design of a live and maximally permissive Petri net controller using the theory of regions, *IEEE Transactions on Robotics and Automation*, 19(1), 137–142.
- [27] Giua, A. (1992), Petri nets as discrete event models for supervisory control, Ph.D. thesis, Rensselaer Polytechnic Institute.
- [28] Giua, A., F. DiCesare, and M. Silva (1992), Generalized mutual exclusion constraints on nets with uncontrollable transitions, in *Proc. 1992 IEEE International Conference on Systems, Man, and Cybernetics*, pp. 974–979.
- [29] Gomes, C. P., H. Kautz, A. Sabharwal, and B. Selman (2008), *Handbook of Knowledge Representation*, chap. 2: Satisfiability Solvers, pp. 89–134, Elsevier.
- [30] Gurobi (2010), Gurobi Optimizer, <http://www.gurobi.com/>.
- [31] Haas, P. J. (2004), Stochastic Petri nets for modelling and simulation, in *Proc. the 2004 Winter Simulation Conference*.
- [32] Harmon, M. G., T. P. Baker, and D. B. Whalley (1994), A retargetable technique for predicting execution time of code segments, *Real-Time Systems*, 7(2), 159–182.
- [33] Heidelberger, P., and D. Nicol (1996), Building parallel simulations from serial simulators, in *Proc. the 4th Annual IEEE/ACM International Symposium on Modeling, Analysis and Simulation of Computer and Telecommunication Systems (MASCOTS)*, pp. 2–4.
- [34] Hellerstein, J. L., Y. Diao, S. Parekh, and D. M. Tilbury (2004), *Feedback Control of Computing Systems*, Wiley.
- [35] Hopcroft, J. E., R. Motwani, and J. D. Ullman (2006), *Introduction to Automata Theory, Languages, and Computation*, 3rd ed., Addison Wesley.
- [36] Hsu, C.-J., J. L. Pino, and S. S. Bhattacharyya (2008), Multithreaded simulation for synchronous dataflow graphs, in *Proc. the 45th Annual Design Automation Conference*, pp. 331–336.

- [37] Iordache, M., and P. Antsaklis (2005), A survey on the supervision of Petri nets, in *DES Workshop, Petri Nets 2005*.
- [38] Iordache, M. V., and P. J. Antsaklis (2006), *Supervisory Control of Concurrent Systems: A Petri Net Structural Approach*, Birkhäuser, Boston, MA.
- [39] Iordache, M. V., and P. J. Antsaklis (2009), Petri nets and programming: A survey, in *Proc. 2009 American Control Conference*, pp. 4994–4999.
- [40] Iordache, M. V., and P. J. Antsaklis (2010), Concurrent program synthesis based on supervisory control, in *Proc. 2010 American Control Conference*, pp. 3378–3383.
- [41] Jeng, M., and X. Xie (2001), Modeling and analysis of semiconductor manufacturing systems with degraded behaviors using Petri nets and siphons, *IEEE Transactions on Robotics and Automation*, 17(5), 576–588.
- [42] Jin, G., L. Song, W. Zhang, S. Lu, and B. Liblit (2011), Automated atomicity-violation fixing, in *Proc. the ACM SIGPLAN 2011 Conference on Programming Language Design and Implementation*.
- [43] Joshi, P., C.-S. Park, K. Sen, and M. Naik (2009), A randomized dynamic program analysis technique for detecting real deadlocks, in *Proc. ACM SIGPLAN conference on Programming language design and implementation*, pp. 110–120.
- [44] Jula, H., D. Tralamazza, C. Zamfir, and G. Candea (2008), Deadlock immunity: enabling systems to defend against deadlocks, in *Proc. the 8th USENIX Symposium on Operating Systems Design and Implementation*, pp. 295–308.
- [45] Jula, H., S. Andrica, and G. Candea (2012), Efficiency optimizations for implementations of deadlock immunity, in *Runtime Verification*, pp. 78–93.
- [46] Kautz, H., and B. Selman (2007), The state of SAT, *Discrete Applied Mathematics*, 155(12), 1514–1524.
- [47] Kavi, K. M., A. Moshtaghi, and D. Chen (2002), Modeling multithreaded applications using Petri nets, *International Journal of Parallel Programming*, 35(5), 353–371.
- [48] Kelly, T., Y. Wang, S. Lafortune, and S. Mahlke (2009), Eliminating concurrency bugs with control engineering, *IEEE Computer*, 42(12), 52–60.
- [49] Kleijn, J., and M. Koutny (2011), The mutex paradigm of concurrency, in *Petri Nets 2011, Lecture Notes in Computer Science*, pp. 228–247.
- [50] Krishnamurthi, M., A. Basavatia, and S. Thallikar (1994), Deadlock detection and resolution in simulation models, in *Proc. the 1994 Winter Simulation Conference*, pp. 708–715.

- [51] Kunz, G., O. Landsiedel, S. Gotz, K. Wehrle, J. Gross, and F. Naghibi (2010), Expanding the event horizon in parallelized network simulations, in *Proc. the 18th Annual IEEE/ACM International Symposium on Modeling, Analysis and Simulation of Computer and Telecommunication Systems (MASCOTS)*, pp. 172–181.
- [52] Law, A. M. (2007), *Simulation Modeling and Analysis*, 4th ed., McGraw-Hill Companies, Inc.
- [53] Li, Z., and M. Zhou (2009), *Modeling, Analysis, and Deadlock Control of Automated Manufacturing Systems*, Science Press, Beijing.
- [54] Li, Z., and M. Zhou (2009), *Deadlock Resolution in Automated Manufacturing Systems: A Novel Petri Net Approach*, Springer-Verlag, London.
- [55] Li, Z., M. Zhou, and M. Jeng (2008), A maximally permissive deadlock prevention policy for fms based on Petri net siphon control and the theory of regions, *IEEE Transactions on Automation Science and Engineering*, 5(1), 182–188.
- [56] Li, Z., M. Zhou, and N. Wu (2008), A survey and comparison of Petri net-based deadlock prevention policies for flexible manufacturing systems, *IEEE Transactions on Systems, Man, and Cybernetics—Part C*, 38(2), 173–188.
- [57] Li, Z., N. Wu, and M. Zhou (2010), Deadlock control of automated manufacturing systems based on Petri nets - A literature review, *Tech. rep.*, Xidian University, China.
- [58] Liao, H., and M. Lu (2011), A Petri net approach to resource allocation in brand management systems, in *Proc. IEEE International Conference on Industrial Engineering and Engineering Management*.
- [59] Liao, H., S. Lafortune, S. Reveliotis, Y. Wang, and S. Mahlke (2010), Synthesis of maximally-permissive liveness-enforcing control policies for Gadara Petri nets, in *Proc. the 49th IEEE Conference on Decision and Control*.
- [60] Liao, H., S. Lafortune, S. Reveliotis, Y. Wang, and S. Mahlke (2011), Optimal liveness-enforcing control of a class of Petri nets arising in multithreaded software, *conditionally accepted for publication in IEEE Transactions on Automatic Control*.
- [61] Liao, H., J. Stanley, Y. Wang, S. Lafortune, S. Reveliotis, and S. Mahlke (2011), Deadlock-avoidance control of multithreaded software: An efficient siphon-based algorithm for Gadara Petri nets, in *Proc. the 50th IEEE Conference on Decision and Control*.
- [62] Liao, H., Y. Wang, J. Stanley, S. Lafortune, S. Reveliotis, T. Kelly, and S. Mahlke (2011), Eliminating concurrency bugs in multithreaded software: A

new approach based-on discrete-event control, *submitted for journal publication, under review*.

- [63] Liao, H., H. Zhou, and S. Lafortune (2011), Simulation analysis of multithreaded programs under deadlock-avoidance control, in *Proc. 2011 Winter Simulation Conference*.
- [64] Liao, H., Y. Wang, H. K. Cho, J. Stanley, T. Kelly, S. Lafortune, S. Mahlke, and S. Reveliotis (2012), Concurrency bugs in multithreaded software: Modeling and analysis using Petri nets, *Journal of Discrete Event Dynamic Systems*.
- [65] Liu, C., A. Kondratyev, Y. Watanabe, J. Desel, and A. Sangiovanni-Vincentelli (2006), Schedulability analysis of Petri nets based on structural properties, in *Proc. International Conference on Application of Concurrency to System Design*.
- [66] Marques-Silva, J. P., and K. A. Sakallah (1999), Grasp: a search algorithm for propositional satisfiability, *IEEE Transactions on Computers*, 48(5), 506–521.
- [67] Mascarenhas, E., F. Knop, and V. Rego (1995), ParaSol: a multithreaded system for parallel simulation based on mobile threads, in *Proc. the 1995 Winter Simulation Conference*, pp. 690–697.
- [68] Moody, J. O., and P. J. Antsaklis (1998), *Supervisory Control of Discrete Event Systems Using Petri Nets*, Kluwer Academic Publishers, Boston, MA.
- [69] Mueller, R., C. Alexopoulos, and L. F. McGinnis (2007), Automatic generation of simulation models for semiconductor manufacturing, in *Proc. the 2007 Winter Simulation Conference*, pp. 648–657.
- [70] Murata, T. (1989), Petri nets: Properties, analysis and applications, *Proceedings of the IEEE*, 77(4), 541–580.
- [71] Murata, T., B. Shenker, and S. M. Shatz (1989), Detection of Ada static deadlocks using Petri net invariants, *IEEE Transactions on Software Engineering*, 15(3), 314–326.
- [72] Musuvathi, M., S. Qadeer, T. Ball, G. Basler, P. A. Nainar, and I. Neamtiu (2008), Finding and reproducing Heisenbugs in concurrent programs, in *Proc. the 8th USENIX Symposium on Operating Systems Design and Implementation*.
- [73] Mutschler, D. W. (2006), Enhancement of memory pools toward a multi-threaded implementation of the Joint Integrated Mission Model (JIMM), in *Proc. the 2006 Winter Simulation Conference*, pp. 856–862.
- [74] Nazeem, A., and S. Reveliotis (to appear), Designing compact and maximally permissive deadlock avoidance policies for complex resource allocation systems through classification theory: the non-linear case, *IEEE Transactions on Automatic Control*.

- [75] Nazeem, A., S. Reveliotis, Y. Wang, and S. Lafortune (2010), Optimal deadlock avoidance for complex resource allocation systems through classification theory, in *Proc. the 10th International Workshop on Discrete Event Systems*.
- [76] Nazeem, A., S. Reveliotis, Y. Wang, and S. Lafortune (2011), Designing compact and maximally permissive deadlock avoidance policies for complex resource allocation systems through classification theory: the linear case, *IEEE Transactions on Automatic Control*, 56(8), 1818–1833.
- [77] Nir-Buchbinder, Y., R. Tzoref, and S. Ur (2008), Deadlocks: From exhibiting to healing, in *Proc. Workshop on Runtime Verification*.
- [78] Novark, G., E. D. Berger, and B. G. Zorn (2007), Exterminator: Automatically correcting memory errors with high probability, in *Proc. Programming Language Design and Implementation*.
- [79] Novark, G., E. D. Berger, and B. G. Zorn (2008), Exterminator: Automatically correcting memory errors with high probability, *Communications of the ACM*, 51(12), 87–95.
- [80] Park, J., and S. A. Reveliotis (2001), Deadlock avoidance in sequential resource allocation systems with multiple resource acquisitions and flexible routings, *IEEE Transactions on Automatic Control*, 46(10), 1572–1583.
- [81] Park, J., and S. A. Reveliotis (2002), Liveness-enforcing supervision for resource allocation systems with uncontrollable behavior and forbidden states, *IEEE Transactions on Robotics and Automation*, 18(2), 234–240.
- [82] Park, S., S. Lu, and Y. Zhou (2009), Ctrigger: Exposing atomicity violation bugs from their hiding places, in *Proc. 14th International Conference on Architecture Support for Programming Languages and Operating Systems*.
- [83] Phoha, V. V., A. U. Nadgar, A. Ray, and S. Phoha (2004), Supervisory control of software systems, *IEEE Transactions on Computers*, 53(9), 1187–1199.
- [84] Qin, F., J. Tucek, J. Sundaesan, and Y. Zhou (2005), Rx: Treating bugs as allergies—a safe method to survive software failures, in *Proc. the 20th ACM Symposium on Operating Systems Principles*, pp. 235–248.
- [85] Ramadge, P., and W. M. Wonham (1987), Supervisory control of a class of discrete event processes, *SIAM Journal on Control and Optimization*, 25(1), 206–230.
- [86] Ramadge, P., and W. M. Wonham (1989), The control of discrete event systems, *Proceedings of the IEEE*, 77(1), 81–98.
- [87] Reisig, W. (1985), *Petri Nets: An Introduction*, Springer-Verlag.

- [88] Reveliotis, S. A. (2005), *Real-Time Management of Resource Allocation Systems: A Discrete-Event Systems Approach*, Springer, New York, NY.
- [89] Reveliotis, S. A., and P. M. Ferreira (1996), Deadlock avoidance policies for automated manufacturing cells, *IEEE Transactions on Robotics and Automation*, 12, 845–857.
- [90] Reveliotis, S. A., E. Roszkowska, and J. Y. Choi (2007), Generalized algebraic deadlock avoidance policies for sequential resource allocation systems, *IEEE Transactions on Automatic Control*, 52(12), 2345–2350.
- [91] Roy, N., A. Dabholkar, N. Hamm, L. Dowdy, and D. Schmidt (2008), Modeling software contention using colored Petri nets, in *Proc. the 16th Annual IEEE/ACM International Symposium on Modeling, Analysis and Simulation of Computer and Telecommunication Systems (MASCOTS)*, pp. 1–8.
- [92] Shatz, S. M., and W. K. Cheng (1988), A Petri net framework for automated static analysis of Ada tasking behavior, *The Journal of Systems and Software*, 8, 343–359.
- [93] Shatz, S. M., S. Tu, T. Murata, and S. Duri (1996), An application of Petri net reduction for Ada tasking deadlock analysis, *IEEE Transactions on Parallel and Distributed Systems*, 7(12), 1307–1322.
- [94] Sidiroglou, S., O. Laadan, C. R. Perez, N. Viennot, J. Nieh, and A. D. Keromytis (2009), ASSURE: Automatic software self-healing using rescue points, in *Proc. International conference on architectural support for programming languages and operating systems*, pp. 37–48.
- [95] Sifakis, J. (1980), Performance evaluation of systems using nets, *Net Theory and Applications, Lecture Notes in Computer Science*, 84, 307–319.
- [96] Silberschatz, A., P. B. Galvin, and G. Gagne (2008), *Operating System Concepts*, 8th ed., Wiley.
- [97] Tricas, F., F. Garcia-Valles, J. Colom, and J. Ezpeleta (2005), A Petri net structure-based deadlock prevention solution for sequential resource allocation systems, in *Proc. IEEE International Conference on Robotics and Automation*, pp. 271 – 277.
- [98] URL (Access on April 11, 2012), The Gadara Project, University of Michigan, <http://gadara.eecs.umich.edu/>.
- [99] Uzam, M. (2002), An optimal deadlock prevention policy for flexible manufacturing systems using Petri net models with resources and the theory of regions, *International Journal of Advanced Manufacturing Technology*, 19(3), 192–208.

- [100] Venkatesh, S., J. Smith, B. Deurmeyer, and G. Curry (1998), Deadlock detection and resolution for discrete-event simulation: multiple-unit seizures, *IIE Transactions*, 30(3), 201–216.
- [101] Wallace, C., P. Jensen, and N. Soparkar (1996), Supervisory control of workflow scheduling, in *Proc. International Workshop on Advanced Transaction Models and Architectures*.
- [102] Wang, J. (1998), *Timed Petri Nets: Theory and Application*, Kluwer Academic Publishers.
- [103] Wang, Y. (2009), Software failure avoidance using discrete control theory, Ph.D. thesis, University of Michigan.
- [104] Wang, Y., T. Kelly, M. Kudlur, S. Lafortune, and S. A. Mahlke (2008), Gadara: Dynamic deadlock avoidance for multithreaded programs, in *Proc. the 8th USENIX Symposium on Operating Systems Design and Implementation*, pp. 281–294.
- [105] Wang, Y., S. Lafortune, T. Kelly, M. Kudlur, and S. Mahlke (2009), The theory of deadlock avoidance via discrete control, in *Proc. the 36th Annual ACM SIGPLAN-SIGACT Symposium on Principles of Programming Languages*, pp. 252–263.
- [106] Wang, Y., H. Liao, A. Nazeem, S. Reveliotis, T. Kelly, S. Mahlke, and S. Lafortune (2009), Maximally permissive deadlock avoidance for multithreaded computer programs (extended abstract), in *Proc. the 5th Annual IEEE Conference on Automation Science and Engineering*, pp. 37–41.
- [107] Wang, Y., H. Liao, S. Reveliotis, T. Kelly, S. Mahlke, and S. Lafortune (2009), Gadara nets: Modeling and analyzing lock allocation for deadlock avoidance in multithreaded software, in *Proc. the 48th IEEE Conference on Decision and Control*, pp. 4971–4976.
- [108] Wang, Y., H. K. Cho, H. Liao, A. Nazeem, T. P. Kelly, S. Lafortune, S. Mahlke, and S. Reveliotis (2010), Supervisory control of software execution for failure avoidance: Experience from the Gadara project, in *Proc. International Workshop on Discrete Event Systems*.
- [109] Woodward, E. E., and G. T. Mackulak (1997), Detecting logic errors in discrete-event simulation: reverse engineering through event graphs, *Simulation Practice and Theory*, 5(4), 357–376.
- [110] Yamalidou, K., J. Moody, M. Lemmon, and P. Antsaklis (1996), Feedback control of Petri nets based on place invariants, *Automatica*, 32(1), 15–28.
- [111] Zeng, F. (2009), Pattern-driven deadlock avoidance, in *Proc. the 7th Workshop on Parallel and Distributed Systems: Testing, Analysis, and Debugging*.

- [112] Zuberek, W. M. (2009), Performance limitations of block-multithreaded distributed-memory systems, in *Proc. the 2009 Winter Simulation Conference*, pp. 899–907.